Study on species-specific pollen tube guidance mechanism and molecular evolution of pollen tube attractants by identification of attractants in *Arabidopsis thaliana*

シロイヌナズナの花粉管誘引物質の同定を基盤とした種特異的なガイダンス機構と誘引物質の分子進化に関する研究

Hidenori Takeuchi

2013

Division of Biological Science

Graduate School of Science

Nagoya University

Contents

Preface	**1**
Summary	**3**
Introduction	**5**
Results	**11**
Discussion	**31**
Materials and Methods	**41**
Figures and Tables	**55**
Conclusion and Perspectives	**90**
References	**93**
Acknowledgements	**105**

Preface

Successful reproduction is indispensable for seed production and colonization in higher plants. Healthy seeds and fruits result from appropriate fertilization between male and female gametes of the same species. Fertilization between two strains of the same species or very close relatives occasionally occurs, but rarely produces a new species that is more adaptive to the environment or more favorable to human beings (Rieseberg and Willis, 2007). Since ancient times, human beings have been aware that dusting pollen on the stigma of a flower assures seed production (Boavida et al., 2005). Only recently did we elucidate what occurs inside the pistil to produce seeds. In the late nineteenth century, pollen tubes (haploid male gametophytes), which are germinated from pollen grains, were observed to grow toward excised pistil tissues on a medium. For longer than a century, plant biologists have conducted studies to reveal the mechanisms of pollen tube growth and guidance (Higashiyama and Hamamura, 2008). At the beginning of the twenty-first century, several studies using a unique dicot, *Torenia fournieri*, achieved breakthroughs and eventually identified attractant molecules (Higashiyama et al., 2001; Higashiyama et al., 2006; Okuda et al., 2009). However, universal molecular mechanisms involving this attraction in a species-specific manner are still unclear.

Biologists now have access to the genomic information of many organisms. This provides much insight into the molecular evolution of particular genes involving species-specific traits. Nevertheless, the molecular evolution of reproductive genes, which frequently show characteristic evolution, is still largely unknown in both animals and plants. Crossbreeding is an important way to generate organisms with desirable traits, but interspecific incompatibility can interrupt the fertilization process. The

breakdown of these reproductive isolation barriers has become biologically and agriculturally significant and is a major goal in plant reproductive biology (Márton et al., 2012). Therefore, elucidation of the relationship between reproductive genes and their molecular evolution should be addressed to understand how successful reproduction is achieved in a species-specific manner and to overcome reproductive isolation barriers.

Arabidopsis thaliana is thought to be the best model organism for plant reproductive biology studies as well as the genome-wide study of the molecular evolution of reproductive genes. Nearly complete genomic sequence data for *A. thaliana* (Arabidopsis Genome Initiative, 2000) and high-quality genome sequence data for a close relative, *Arabidopsis lyrata* (Hu et al., 2011), have been disclosed. In addition, abundant information on its strains (accessions) is available (Aranzana et al., 2005), and the entire process of pollen tube growth and guidance *in vivo* can be easily examined due to the simple pistil structure. Furthermore, the development of *in vitro* systems has enabled observations of pollen tube attraction toward the ovule (Palanivelu and Preuss, 2006) and the double fertilization process (Hamamura et al., 2011) as well as investigation of the reactivity of growing pollen tubes by micromanipulation (Takeuchi and Higashiyama, 2011).

In the present study, I identified attractant molecules of *A. thaliana*, with convincing evidence from *in vivo* and *in vitro* physiological experiments and with insight into their molecular evolution. I demonstrate overcoming the reproductive isolation barriers presented by species-specific attraction and penetration of the female gametophyte. Also, I discuss universal mechanisms of species-specific pollen tube guidance from the perspective of attractant molecules derived from the female gametophyte in flowering plants.

Summary

To accomplish fertilization in flowering plants, a pollen tube grows to an embryo sac inside the pistil and delivers immotile sperm cells to an egg cell and a central cell. In the fertilization process, pollen tube guidance is a crucial mechanism that precisely guides only one pollen tube of own species to the embryo sac. Many genes controlling pollen tube guidance to the ovule have been identified in the model plant *Arabidopsis thaliana*; however, the molecules that attract pollen tubes of own species directly to the ovule have not been identified. Here, I report the identification of pollen tube attractants in *A. thaliana*, named AtLURE1 peptides, by a genome wide survey from more than 300 defensin-like (*DEFL*) genes of *A. thaliana*. AtLURE1 peptides are encoded by multiple *DEFL* genes forming a species-specific tandem array in the *A. thaliana* genome. The *AtLURE1* genes formed the sole species-specific cluster among *DEFL* genes compared to its close relative, *Arabidopsis lyrata*. No evidence for positive selection was detected in *AtLURE1* genes and their orthologs, implying neutral evolution of *AtLURE1* genes. AtLURE1 peptides were specifically expressed in egg-accompanying synergid cells and secreted toward the funicular surface through the micropyle. Genetic analyses showed that known gametophytic mutants defective in micropylar guidance do not express AtLURE1 peptides. Downregulation of the expression of these peptides impaired precise pollen tube attraction to the micropylar opening of some populations of ovules. Recombinant AtLURE1 peptides attracted *A. thaliana* pollen tubes at a higher frequency compared to *A. lyrata* pollen tubes, suggesting that these peptides are species-preferential attractants in micropylar guidance. In support of this idea, the heterologous expression of a single AtLURE1 peptide in the synergid cell of *Torenia fournieri* was sufficient to guide *A. thaliana* pollen tubes to the

T. fournieri embryo sac and to permit entry into it. I also imply a universal mechanism of expression of species-specific LURE peptides to attract pollen tubes of own species. My results suggest the unique evolution of *AtLURE1* genes, which are directly involved in male-female interaction among the *DEFL* multigene family, and furthermore suggest that these peptides are sufficient to overcome interspecific barriers in gametophytic attraction and penetration.

Introduction

Pollen tube guidance is a crucial mechanism underlying fertilization in flowering plants. Pistil tissue precisely controls the directional growth of the pollen tube (male gametophyte) to the embryo sac (female gametophyte) for the delivery of immotile sperm cells (Ge et al., 2011; Hamamura et al., 2011). The process of pollen tube guidance is divided into two phases; namely, sporophytic guidance and gametophytic guidance (Johnson and Preuss, 2002; Higashiyama and Hamamura, 2008; Figure 1). In many plant species, pollen tube guidance from the stigma to the ovary is likely governed by female sporophytic tissues. Various mechanisms such as chemoattraction and mechanical guidance have been proposed to explain the sporophytic guidance of bundles of pollen tubes into the ovary (Cheung et al., 1995; Wu et al., 1995; Kim et al., 2003; Crawford et al., 2007). In the ovary, individual pollen tubes are precisely guided to an ovule. Precise guidance to the ovule is controlled by the target female gametophyte of the ovule (Hulskamp et al., 1995). Sporophytic cells of the ovule coordinately support pollen tube guidance in the ovary by supporting the development of the female gametophyte (Wang et al., 2008) and by providing amino acids to the pollen tube (Palanivelu et al., 2003; Michard et al., 2011).

In the model plant *Arabidopsis thaliana*, the female gametophyte likely to controls at least two steps in guidance to the ovule, from the septum to the funiculus of the ovule (funicular guidance), and from the funiculus to the micropyle (micropylar guidance) (Higashiyama et al., 2003; Figure 1B). Ovules lacking the female gametophyte do not attract pollen tubes (Ray et al., 1997), and mutants defective in micropylar pollen tube guidance associate with pollen tubes at the funiculus (Shimizu and Okada, 2000; Kasahara et al., 2005; Chen et al., 2007). Pollen tubes lose their way

at the entrance of the micropyle in the micropylar guidance mutants. Several gametophytic mutants defective in micropylar guidance and their responsible genes have been identified. For example, *MYB98* was first identified as a gametophytic gene that controls pollen tube guidance to the ovule (Kasahara et al., 2005). *MYB98* encodes a transcription factor expressed specifically in synergid cells (egg-accompanying haploid cells) and is necessary for the formation of an ingrowth called the filiform apparatus and micropylar pollen tube guidance (Kasahara et al., 2005). Mutants of *magatama* (*maa*) showed impaired micropylar guidance (Shimizu and Okada, 2000). One responsible gene, *MAA3*, is probably ubiquitously involved in RNA metabolism in various cell types as a housekeeping gene (Shimizu et al., 2008). *CENTRAL CELL GUIDANCE* (*CCG*) plays an essential role in micropylar guidance (Chen et al., 2007). CCG is a nuclear protein expressed predominantly in the central cell of the ovule. GEX3, a plasma membrane protein, is expressed in both the sperm cells and egg cell and is likely involved in micropylar guidance (Alandete-Saez et al., 2008). The relationship of these genes with ovular attractant molecules is unknown.

The synergid cell is the most plausible cell responsible for micropylar guidance as well as reception and induction of pollen tube rupture for the release of the sperm cells (Figure 2). Higashiyama et al. clearly showed by the laser-mediated ablation of mature embryo sacs in the unique dicot *Torenia fournieri*, which has a protruding embryo sac, that the mature synergid cell autonomously attracted pollen tubes (Higashiyama et al., 2001). In *A. thaliana*, *MYB98* expressed in the synergid cell is involved in pollen tube attraction, although additional gametophytic cells are involved in pollen tube attraction possibly by controlling the production and/or secretion of attractant molecules in the synergid cells. To our knowledge, an attractant(s) responsible

for micropylar guidance in *A. thaliana* has not been identified. However, some diffusible chemoattractant must be derived from the micropyle. Pollen tubes growing through a cut style (semi-*in vivo* or -*in vitro* conditions) are directly attracted to the micropyle on medium in a species-specific manner (Palanivelu and Preuss, 2006). This attraction was much clearer when an excised ovule was put in front of a pollen tube growing semi-*in vitro*; the tube changed its growth direction toward the micropyle within several minutes (Takeuchi and Higashiyama, 2011; Figure 3). Mathematical estimation consistently showed that the pollen tubes were sensing a concentration gradient of an attractant 100-150 μm from the micropyle (Stewman et al., 2010). In *T. fournieri*, the synergid cell is the source of the pollen tube attraction signal and is likely to be effective within approximately 200 μm (Higashiyama et al., 1998, 2001). Attractant molecules derived from the synergid cell of *T. fournieri* were identified as defensin-like LURE peptides, belonging to the cysteine-rich peptides (CRPs), using a semi-*in vitro* system (Okuda et al., 2009). On the other hand, in the monocot *Zea mays*, EGG APPARATUS 1 (ZmEA1) peptide, which is not a CRP, has been reported to be an attractant molecule (Márton et al., 2005; Dresselhaus and Márton, 2009; Márton et al., 2012). These peptides are predominantly expressed in synergid cells.

The pollen tube guidance mechanism also ensures that a pollen tube of own species is preferentially guided to an embryo sac. It has been suggested that interspecific cross-pollination with *A. thaliana* pistils caused mis-targeting or growth arrest of pollen tubes of other species at various guidance steps (reviewed in Shimizu, 2002). However, molecular basis of interspecific incompatibility in pollen tube guidance is largely unknown. Interestingly, in *T. fournieri* and the closely related species *T. concolor*, rapid molecular evolution of *T. fournieri LURE1* (*TfLURE1*) and *TcLURE1* was likely directly

involved in the species preferentiality of pollen tube attraction at the micropyle (Higashiyama et al., 2006; Kanaoka et al., 2011). It is difficult to search for LURE peptides in *A. thaliana* based on homology with primary sequences of LURE peptides of *Torenia* because *A. thaliana* has at least 825 *CRP* genes, including more than 300 *defensin-like* (*DEFL*) genes, and *CRP* genes are highly variable between species (Silverstein et al., 2005, 2007). Therefore, molecular evolution and generality of LURE-like peptides in various plant species remain unclear.

The relationship between evolutionary patterns and functions of reproductive genes still remains unclear. However, sexual reproduction as well as disease is believed to have profound effects on molecular evolution because male–female and host–parasite interactions exert selection pressures (Haldane, 1949; Swanson and Vacquier, 2002). Genes involved in these interactions tend to show characteristic molecular evolution under positive Darwinian selection (Swanson and Vacquier, 2002; Nielsen et al., 2005; Clark et al, 2007a, 2007b; Lazzaro, 2008) and rapid gene turnover (gain/loss) (Rast et al., 2006; Sackton et al., 2007; Yoshida et al., 2009). A superfamily of *DEFL* genes in flowering plants is a good model to study the relationship between the evolutionary patterns and their functions because *DEFL* genes form a large multigene family, with 317 *DEFL* genes in *Arabidopsis thaliana* (accession Col-0) (Silverstein et al., 2005) and 93 *DEFL* genes in *Oryza sativa* (rice) (Silverstein et al., 2007). Genome-wide analysis of the 317 *DEFL* genes of *A. thaliana* suggested rapid molecular evolution, including tandem and segmental duplication events, and multiple gene duplication (Silverstein et al., 2005). Some of the plant *DEFL* genes are likely to be directly involved in both defense and sexual reproduction.

Defensins are antimicrobial peptides involved in innate immunity that are

generally found in eukaryotes, including mammals, insects, and plants (Ganz, 2003). Several plant DEFL peptides have been reported to be involved in the innate immune system (Thomma et al., 2002; Clauss and Mitchell-Olds, 2004). In addition to *TfLURE* peptides, other DEFL peptides are involved in various steps in male–female interactions in plant sexual reproduction (Higashiyama, 2010). For example, the SCR/SP11 peptide in Brassicaceae is the male determinant of self/nonself-recognition during pollination (Schopfer et al., 1999; Takayama et al., 2000). The ZmES4 peptide of *Zea mays*, predominantly expressed in the synergid cell, induces pollen tube rupture for the release of the sperm cell (Amien et al., 2010). However, whether any characteristically evolving *DEFL* genes exist among the *DEFL* genes of *A. thaliana,* and whether such genes are actually involved in disease or sexual reproduction, are not known.

In this study, I surveyed the *DEFL* genes of *A. thaliana* showing unique molecular evolution (in the form of rapid gene turnover) using whole-genome data of a closely related species, *Arabidopsis lyrata* (Hu et al., 2011). I especially focused on paralogous genes because rapid gene turnover has sometimes been suggested in multigene families, including the antimicrobial peptides of *Drosophila* (Sackton et al., 2007). I discovered a sole species-specific *DEFL* gene cluster that was demonstrated to encode attractant peptides, named *A. thaliana* LURE1 (AtLURE1) peptides, for pollen tubes in *A. thaliana*. I demonstrated *in vivo* evidence that the AtLURE1 peptides diffuse from the synergid cell toward the funicular surface and play an important role in micropylar guidance. Genetic data suggest that AtLURE1 peptides are generated via intercellular communication between the synergid cell and central cell. In addition, the heterologous expression of the LURE peptide was sufficient to overcome reproductive isolation barriers in the final steps of male-female interactions despite a large

evolutionary distance between organisms.

Results

Interspecific Cross-Pollination Experiments Demonstrate Abnormal Pollen Tube Guidance of *A. lyrata* Pollen Tubes inside *A. thaliana* Pistil

Abnormal growth and guidance of interspecific pollen tubes in the *A. thaliana* pistil suggested to be more severe when the genetic relationship between the pollen tube and the pistil is more distant (Shimizu and Okada, 2000; Shimizu, 2002). Indeed, when crossed to the *A. thaliana* pistil, pollen tubes of a distant species *T. fournieri* (Linderniaceae, Lamiales) was not geminated on the *A. thaliana* stigma, and that of *Capsella rubella* (Brassicaceae, Brassicales) and *Arabidopsis griffithiana* (or *Olimarabidopsis pumila*) arrested their growth in the style, the transmitting tract, or on the funiculus after germination (data not shown). It has been reported that pollen tubes from one of the closest relatives, *A. lyrata*, show abnormal pollen tube reception after reaching *A. thaliana* synergid cells, which is associated with overgrowth of the tube in the embryo sac (Escobar-Restrepo et al., 2007). To investigate whether the *A. lyrata* pollen tubes show any incompatibility in their growth and/or guidance, I performed aniline blue staining of pollen tubes in the *A. thaliana* pistil. First, I examined growth rates of apical-to-basal movement of pollen tubes from the stigma to the bottom of the ovary. Six hours after hand-pollination to *A. thaliana* pistils at 22°C, the longest pollen tubes of *A. thaliana* and *A. lyrata*, and, did not fully reach to the bottom of the ovary (Figure 4A and 4B). The lengths of them were 1845 ± 234 μm in *A. thaliana*, 2460 ± 146 μm in *A. lyrata* (Figure 4C). Thus, the pollen tube length of *A. lyrata* in the *A. thaliana* pistil was slightly longer than that of conspecific *A. thaliana*, suggesting that pollen tube growth of the close relatives were not so incompatible in the *A. thaliana*

pistil. Twelve hours after hand-pollination, the longest pollen tubes of both *A. thaliana* and the related species were near or reached to the bottom of the ovary (data not shown). However, abnormal pollen tube attraction toward the *A. thaliana* ovules was observed in *A. lyrata* pollen tubes (Figure 5A). Pollen tubes of *A. thaliana* grew to about 70% of the ovules, while that of *A. lyrata* grew to about 20% of the ovules. Conversely, ovules without *A. thaliana* pollen tube were about only 20% twelve hours after pollination, while *A. lyrata* pollen tubes were not attracted to about 70% of the ovules. This result suggested that *A. thaliana* ovules preferentially attracted pollen tubes of own species, consistent with observations in *Torenia* (Higashiyama et al., 2006; Kanaoka et al., 2011). Even though not many wandering *A. lyrata* pollen tubes around the micropyle after attraction to the funiculus were found in the *A. thaliana* pistil (Figure 5A), some disordered patterns in pollen tube growth of *A. lyrata* were observed around the micropyle (Figure 5B and 5C). Especially, aberrant pollen tubes on the funiculus, including branching of the pollen tube, were frequently observed (Figure 5C). These results support that interspecific *A. lyrata* pollen tubes show incompatible growth as well as delayed attraction in the *A. thaliana* pistil. Slightly longer growth toward the basal side observed in *A. lyrata* pollen tubes compared to *A. thaliana* (Figure 4) could be due to a reduced frequency of attraction to the *A. thaliana* ovules and thus due to increased growth to the basal side in the transmitting tract.

To investigate biological implications of the preferential attraction and growth, I performed hand-pollination experiments with *A. thaliana* and *A. lyrata* pollens. *A. thaliana* pistils pollinated with *A. thaliana* pollen produced normal developing seeds at a rate of 96 ± 3%, while pistils pollinated with *A. lyrata* pollen decreased them to about one-third (34 ± 15%) (Figure 6A and 6B). Since *A. lyrata* pollen tubes reached to almost

all ovules 18 hours after pollination (data not shown), the low rate of normal seeds was probably reflected by failures of fertilization or embryogenesis. When pistils were pollinated with both *A. thaliana* and *A. lyrata* pollens at the same time, the rate of normal seeds was 90 ± 3% (Figure 6A and 6B), suggesting preferential attraction of *A. thaliana* pollen tubes and, therefore, normal development of seeds. These results indicate that pollen tube attractants of *A. thaliana* are species-preferential or -specific molecules and may have evolved in a species-specific manner.

Identification of a Species-Specific Cluster of *DEFL* Genes in *A. thaliana*

To identify pollen tube attractants involved in species-specific attraction in *A. thaliana*, I tried to find candidate genes showing species-specific evolution. I first focused on *DEFL* genes as the candidates because they frequently show rapid molecular evolution, including lineage-specific gene expansion (Silverstein et al., 2005), and because attractant molecules found in *Torenia*, TfLURE1, -2, and TcLURE1, are DEFL peptides (Okuda et al., 2009; Kanaoka et al., 2011). In *A. thaliana*, there are 317 *DEFL* genes which are subdivided into 46 subgroups by the number and alignment of cysteine residues (Silverstein et al., 2005). They have evolved by tandem and segmental duplication events, and some individual subgroups include paralogous, multiply duplicated genes (Silverstein et al., 2005). To survey *DEFL* genes showing species-specific evolution and/or expansion, I identified paralogous genes among the 317 *DEFL* genes of *A. thaliana* by a phylogenetic tree analysis using 317 putative DEFL peptide sequences (Figure 7). I focused on four or more paralogous genes supported by high bootstrap values (≥ 90%) that could have evolved by recent multiple gene duplication, and found 13 groups of the multiple paralogous genes (Table 1). To

investigate interspecific variation and the origin of these genes, I searched for orthologs in *A. lyrata* using available genomic data (Hu et al., 2011). Multiple orthologs for the 13 groups of the *A. thaliana* genes were found in the *A. lyrata* genome by BLAST searches (Table 1). Notably, a phylogenetic tree analysis for the *A. thaliana* genes of the 13 groups and the *A. lyrata* orthologous genes showed that a single subtree, which includes six *DEFL* (*Cysteine-Rich Peptide 810*; *CRP810*) genes of *A. thaliana* and 10 orthologs of *A. lyrata*, branched into species-specific gene clades for *A. thaliana* and *A. lyrata* (Figure 8). No other clades, including *CRP90* (true plant defensin *PDF1* genes (Thomma et al., 2002)) and *CRP700* (tandemly duplicated genes encoding trypsin inhibitor (Clauss and Mitchell-Olds, 2004)), showed such a phylogenetic relationship between *A. thaliana* and *A. lyrata* (Figure 8). This result suggested that these *CRP810* genes diverged after the split between *A. thaliana* and *A. lyrata* (Koch et al., 2000; Hu et al., 2011). I decided to further analyze these *CRP810* genes, *CRP810_1.1* to *_1.6* and *AlCRP810_1.1* to *_1.10*, numbered according to their chromosomal locations (Table 1).

To elucidate how these genes evolved, I performed phylogenetic and synteny analyses of the *CRP810_1* and *AlCRP810_1* genes. Consistent with the phylogenetic analysis showing that the *CRP810_1* and *AlCRP810_1* genes clustered independently to form phylogenetically distinct groups (Figures 8 and 9A), the synteny analysis indicated that a single gene (*CRP810_1.1*) only showed synteny with the *AlCRP810_1* gene (Figure 10A, top). No *AlCRP810_1* gene was present on the contig of *A. lyrata* showing synteny with the *CRP810_1.2–1.6* region (Figure 10A, bottom). In summary, in *A. thaliana*, an ancestral gene (*CRP810_1.1*) likely was copied to one of the loci of *CRP810_1.2–1.6* on the same chromosome and then duplicated locally (within 15 kb). In contrast to this, the other 12 groups of paralogous *DEFL* genes of *A. thaliana* and *A.*

lyrata are not phylogenetically distinct groups (Figures 8 and 9B-9D) and showed synteny with multiple genes (Figure 10B-10D). I have thus identified the *CRP810_1* genes as the sole species-specific gene cluster among the 317 *DEFL* genes of *A. thaliana*.

Characterization of CRP810_1 Peptides

CRP810_1 consists of six paralogous genes, of which five are full-length genes (*CRP810_1.1* to *_1.5*) and one is a pseudogene containing a premature stop codon (*CRP810_1.6*), as a subset of the 16 *CRP810* genes (Silverstein et al., 2005). They encode ~90 amino acids with N-terminal secretory signal sequence, containing six cysteines in their putative mature peptides, with a CxC motif at the C-terminus (Figure 11A). *CRP810_1.1* to *_1.5* had 80–95% amino acid sequence identity. *CRP810_1.6* had a 1-bp deletion at the 17th nucleotide compared to the sequences of other *CRP810_1* genes that induces a frameshift, resulting in a truncated, nonfunctional protein. The putative original amino acid sequence of CRP810_1.6 (Ψ), as deduced from nucleotides 18–275 of *CRP810_1.6*, also showed 80–95% identity with CRP810_1.1 to _1.5. CRP810_1 peptides had the same number and alignment of cysteines and showed ~70% amino acid sequence identity with the AlCRP810_1 peptides (Figure 11B). A conserved cysteine residue (amino acid 84) in CRP810_1.5 was changed to a tyrosine.

CRP810_1 Peptides Are Specifically Expressed in Synergid Cells and Secreted toward the Funicular Surface through the Micropyle

To determine the functions of CRP810_1 peptides, I investigated their expression patterns and localization. Quantitative reverse transcription (qRT)-PCR with

vegetative and reproductive tissues revealed predominant *CRP810_1* expression in pistil tissue (Figure 12A). I also showed strong expression of *CRP810_1.1* to *_1.5* in the pistil (Figure 12B). Consistent with these results, previous data from a genome-wide analysis of *A. thaliana* ovules suggested that *CRP810_1* genes are expressed in the female gametophyte inside the pistil and downregulated in a *myb98* T-DNA insertion mutant (Higashiyama, 2002). The *MYB98* gene encodes a transcription factor predominantly expressed in the synergid cell and is necessary for pollen tube guidance at the micropyle of the ovule and development of the filiform apparatus of the synergid cell, a cell-wall ingrown structure (Kasahara et al., 2005; Punwani et al., 2008). In addition, I confirmed by custom array analysis that they were upregulated in mature ovules compared with seedlings (data not shown), suggesting that they might be specifically expressed in the female gametophyte. In ovules expressing green fluorescent protein (GFP) under the control of the promoters of *CRP810_1.1* to *_1.5*, GFP fluorescence was observed exclusively in the synergid cells (Figure 12D). I also generated transgenic plants that expressed GFP-fused CRP810_1 regulated by their own promoters. All GFP-fused CRP810_1 proteins were localized to the micropylar end of the female gametophyte (Figure 12E), possibly at the filiform apparatus of the synergid cell. This was consistent with the previous observation of GFP-fused CRP810_1.2 (DD2) (Punwani et al., 2007). These results indicate that CRP810_1 peptides are specifically expressed in the synergid cell and are likely secreted toward the micropylar end of the female gametophyte.

Immunostaining of the ovule using an anti-CRP810_1.2 antibody showed that the CRP810_1 peptides were secreted from the synergid cell toward the micropylar opening and then diffused to the funicular surface of the ovule (Figure 13A and 13B). The antibody recognized all of the CRP810_1 peptides in an immuno-dot blot analysis

(Figure 13C). The GFP-fused CRP810_1 proteins did not show this diffuse pattern, most likely due to the increased molecular weight of the fusion protein (~40 kDa), which is close to the transmission limit of the cell wall. Diffusion of the CRP810_1 peptides suggested the possibility that these peptides may be effective at a distance from the synergid cell. This raised the possibility that the CRP810_1 peptides may be involved in pollen tube guidance on the funiculus.

CRP810_1 Peptides Are Downregulated in Known Female Gametophytic Guidance Mutants

Accordingly, I next examined the relationship between the CRP810_1 peptides and known micropylar guidance mutants. *CRP810_1* genes have been suggested to be downregulated in a *myb98* mutant defective in micropylar guidance (Jones-Rhoades et al., 2007). In addition to *myb98*, *ccg*, a mutant defective in a nuclear protein expressed in the central cell (Chen et al., 2007), and *maa3*, a mutant possibly defective in RNA metabolism in ubiquitous cells (Shimizu et al., 2008), were investigated as female gametophytic mutants defective in micropylar guidance. I first performed a qRT-PCR analysis of *myb98/myb98* homozygous and *myb98*/*MYB98*, *ccg*/*CCG,* and *maa3*/*MAA3* heterozygous mutants (homozygous mutants for *ccg* and *maa3* were not obtained (Chen et al., 2007; Shimizu et al., 2008)) (Figure 14A). Note that the mean (n = 3) *CRP810_1* transcript level was 80% in *ccg/CCG* mutant pistils compared to wild-type pistils, although *CCG* is expressed specifically in the central cell among mature female gametophytic cells (Chen et al., 2007). The *CRP810_1* expression level was decreased in all examined mutants: 64% in *maa3/MAA3*, 58% in *myb98/MYB98*, and 1.4% in *myb98/myb98* pistils. Notably, the mean *MYB98* transcript level decreased to 72% in

ccg/CCG but increased to 135% in *maa3/MAA3*.

I also examined the downregulation of CRP810_1 peptides in these mutants using immunostaining. Secreted CRP810_1 peptides were detected in only half of the ovules in the pistils of *myb98*/*MYB98* (51.7%, *n* = 484), *ccg*/*CCG* (51.4%, *n* = 397), and *maa3*/*MAA3* (52.0%, *n* = 179) mutants, in contrast with wild-type (95.9%, *n* = 170) and *myb98*/*myb98* (4.4%, *n* = 499) ovules (Figure 14A and 14C). Therefore, ovules lacking fluorescence in the heterozygous mutants were implicated as mutant ovules because the expected segregation ratio of wild-type to mutant female gametophytes was 50% in the heterozygous mutants. These results indicate that the synergid cells of these micropylar guidance mutants produce less CRP810_1 peptide and support the notion that the CRP810_1 peptides are involved in pollen tube attraction around or toward the micropyle. Furthermore, the findings suggest that CCG expressed in the central cell and MAA3 expressed in possibly all female gametophytic cells are involved in expression and secretion of CRP810_1 peptides in the synergid cell.

Diffusible CRP810_1 Peptides Are Involved in Micropylar Guidance

To define the function of CRP810_1 peptides *in vivo*, I simultaneously downregulated the five paralogous genes (*CRP810_1.1* to *_1.5*) using RNA interference (RNAi) against the complete *CRP810_1.2* coding sequence (Figure 15A). I obtained 11 independent T_1 lines of *CRP810_1*-RNAi (RNAi), 14 lines of *MYB98*-RNAi as positive controls, and 13 lines of a linker for the RNAi construct (vector control). All 14 *MYB98*-RNAi T_1 lines showed reduced fertility (44 ± 15%, mean ± SD for the rate of developing seeds upon selfing) and a defect in micropylar guidance similar to the *myb98* mutant (data not shown); thus, my RNAi system appeared to work. I also

confirmed the specific downregulation of all *CRP810_1* genes in *CRP810_1*-RNAi lines by qRT-PCR (Figure 15B). To analyze the RNAi lines in greater detail, I selected three T_3 RNAi lines derived from three independent T_1 lines in which CRP810_1 peptides were barely observed in the micropylar opening by immunostaining (Figure 15C).

Some disordered patterns in pollen tube growth were observed around the micropylar opening in these RNAi lines after aniline blue staining. To evaluate abnormal pollen tube guidance around the micropylar opening, I classified defects in micropylar guidance into two groups. The first included those cases in which one or more pollen tubes wandered around the micropyle but finally entered the micropyle (class I abnormality; Figure 16B and 16C); the second was more severe, in which no pollen tube entered the micropyle after growing up the funiculus (class II abnormality; Figure 16D). Approximately 10% of the ovules in each RNAi line showed class I and class II abnormalities (Figure 16E). Of these, ~1% exhibited a class II abnormality, which was never observed in the ovules of the wild-type or vector control lines. The frequency of class I and class II abnormalities in all three RNAi lines was significant (Student's *t*-test; $P < 0.01$). Thus, I conclude that the downregulation of *CRP810_1* genes impaired micropylar pollen tube guidance, although it did not result in a complete loss of micropylar guidance. In the micropylar guidance mutants, the phenotype of abnormal pollen tube guidance was more severe and was observed at higher frequencies than in the RNAi lines; class I and class II abnormalities were 20 ± 14% and 65 ± 12% in *myb98/myb98*, 20 ± 12% and 14 ± 11% in *myb98/MYB98*, 22 ± 13% and 19 ± 10% in *ccg/CCG*, and 28 ± 15% and 17 ± 14% in *maa3/MAA3*, respectively.

To examine whether *CRP810_1* downregulation actually impaired the ability of

the ovules to attract pollen tubes, I performed a competitive assay semi-*in vitro* using wild-type and RNAi ovules simultaneously (Figure 17A). I placed a wild-type and an RNAi ovule together facing the micropylar opening so that a pollen tube could grow between the ovules. Ovules of *myb98* homozygous mutant were also examined. The pollen tubes were rarely attracted to the RNAi ovules (8.3%, n = 12) and never to *myb98* ovules (0%, n = 11) (Figure 17B). These results indicate that the loss of CRP810_1 peptides impaired pollen tube attraction to the micropylar opening *in vivo* and *in vitro*.

CRP810_1 Peptides Containing Six Cysteines Can Attract *A. thaliana* Pollen Tubes

CRP810_1 peptides expressed in the synergid cell were shown to diffuse toward the micropyle and were involved in pollen tube attraction at the micropyle. To examine whether CRP810_1 peptides can directly attract pollen tubes, I performed pollen tube attraction assay under an inverted microscope equipped with a micromanipulator (Figure 18). Recombinant His-tagged CRP810_1.1 to _1.5, following the putative cleavage site in the signal peptide, were individually expressed in *Escherichia coli*. These recombinant peptides were purified and refolded according to the procedures used for TfLUREs (Okuda et al., 2009). Pollen tubes were grown through a style on medium using an *in vitro* system (Palanivelu and Preuss, 2006; Hamamura et al., 2011) (Figure 19A). The purified peptides were embedded in gelatin beads 15-30 μm in diameter for micromanipulation (Figure 19B and 19C). First, I investigated the activity of CRP810_1.2 and its concentration dependency (Figure 20), since the expression level of *CRP810_1.2* was the highest among *CRP810_1* genes, except for *CRP810_1.5*, which lacks a conserved cysteine residue. When gelatin beads

containing 50 µM CRP810_1.2 were placed in front of the tip of a pollen tube, 100% (*n* = 15) of the tubes turned sharply toward the beads (Figure 20A). Some tubes formed narrow coils around the beads (Figure 20A). Beads containing 5 µM CRP810_1.2 also attracted all of the pollen tubes examined (*n* = 15). As the concentration of CRP810_1.2 in the beads decreased to 500 and 50 nM, the frequency of pollen tube attraction decreased (77%, *n* = 26 and 32%, *n* = 22, respectively). Beads containing buffer alone (0 M) could not attract pollen tubes (Figure 20B; 7%, *n* = 28). This low frequency (7%) was likely due to random directional change of the pollen tube growth, which was also observed without beads. These results suggest that CRP810_1.2 is sufficient to attract pollen tubes in a concentration-dependent manner.

Next, I examined each recombinant peptide of CRP810_1.1, _1.3, _1.4, and _1.5 at a concentration of 50 µM (Figure 21). Pollen tubes were attracted to CRP810_1.3 and _1.4 at a high frequency (83%, *n* = 29 and 100%, *n* = 20, respectively) and CRP810_1.1 at a lower frequency (35%, *n* = 20). In contrast, CRP810_1.5, lacking one of the conserved cysteines, did not attract pollen tubes (12%, *n* = 17). Note that mutated CRP810_1.5-Y84C, in which the 84th tyrosine reverted to a cysteine, showed significant activity (93%, *n* = 15). This suggests that a single amino acid substitution inhibited the pollen tube attraction activity of CRP810_1.5 and that cysteine residues and possibly the formation of disulfide bonds in CRP810_1 peptides are required for their activity. Furthermore, TfLURE1 and 2, which are attractants from *T. fournieri*, did not show significant attraction of *A. thaliana* pollen tubes (6%, *n* = 17 and 17%, *n* = 18, respectively) (Figure 21). In my pollen tube attraction assay, pollen tubes were frequently trapped or deviated by more than a 90° angle toward beads containing CRP810_1 peptides, but they never deviated by more than a 45° angle toward beads

containing buffer alone or TfLUREs, supporting the notion of specific attraction by CRP810_1 peptides. Since CRP810_1 peptides containing six cysteines, including CRP810_1.5-Y84C, had the ability to attract pollen tubes, I named the CRP810_1 peptides AtLURE1 peptides (e.g., CRP810_1.1 is AtLURE1.1). Together with the results from immunostaining the micropylar guidance mutants and the knockdown analysis, I concluded that AtLURE1 peptides are the micropylar pollen tube attractants in *A. thaliana*.

Various Mutations of *AtLURE1* Genes Have Occurred Independently in *A. thaliana* Accessions

I showed that *AtLURE1* (*CRP810_1*) genes encode pollen tube attractants for micropylar guidance in *A. thaliana*. However, I found two loss-of-function mutations (*AtLURE1.5* and *1.6*) among the six *AtLURE1* genes in the analysis of the Col-0 accession. To examine whether such loss-of-function mutations of the *AtLURE1* genes are frequently observed in other accessions, I attempted to determine the nucleotide sequences of *AtLURE1.1* to *1.6* using PCR-based direct sequencing from 12 different accessions (ecotypes) of *A. thaliana*. I obtained 60 genomic sequences of the *AtLURE1* genes (Figure 22). Each accession had at least 4 copies of *AtLURE1* genes although it was unknown whether a set of all paralogous *AtLURE1* genes was determined. I found many variations in nucleotide and amino acid sequences, some of which are likely to cause a loss of function, including a base substitution in a splicing acceptor site (Cvi-0 *AtLURE1.3*), the substitution of conserved cysteine residues (Kondara *AtLURE1.5*), and stop mutations (Ms-0 and Bur-0 *AtLURE1.5*). In contrast to the Col-0 accession, I also found putative functional *AtLURE1.5* and *AtLURE1.6* sequences which have no stop

mutation and no mutation in conserved cysteines (Figure 22). Furthermore, premature stop codons have been predicted in 2 accessions for *AtLURE1.3* and in 8 accessions for *AtLURE1.5* according to sequence information of 80 accessions from the 1001 Genome Project (Cao et al., 2012). These results suggest that a loss of function of some *AtLURE1* genes occurred independently in various accessions. *AtLURE1* genes without loss-of-function mutations must be sufficient to maintain each ecotype.

Evolutionary Characterization of LURE1 Peptides from *A. thaliana* and *A. lyrata*

The *AtLURE1* genes diverged after the split of *A. thaliana* and *A. lyrata* and formed a species-specific gene cluster (Figure 9A and 10A). To provide further insight into the evolutionary and physiological properties of the AtLURE1 peptides, and the AlCRP810_1 (AlLURE1) peptides in the orthologous clade, I performed the following two analyses: an evolutionary analysis to examine whether any significant positive selection was detected and a physiological pollen tube attraction assay to examine species specificity or preferentiality in pollen tube attraction.

The rates of nonsynonymous substitutions versus synonymous substitutions (dN/dS) were calculated for the *AtLURE1* and *AlLURE1* genes (Table 2), as well as other duplicated *DEFL* genes, using approximate methods (Nei and Gojobori, 1986) available in the PAML package (Yang, 2007). Although the dN/dS values of some of the duplicated *DEFL* genes were greater than 1, suggesting the occurrence of positive selection, I could detect no significant positive selection between the *AtLURE1* and *AlLURE1* genes. I also calculated the dN/dS values between a putative original copy *AtLURE1.1* and the other paralogous *AtLURE1* genes (*AtLURE1.2-1.5*) within *A. thaliana* (Table 3). The values were not greater than 1 in any comparisons (Table 3).

Next, I performed tests for positive selection on any of the individual codons and along any of the branches. A maximum likelihood tree of five *AtLURE1* and six *AlLURE1* genes which have no premature stop codon was used in these analyses. For the individual codons, there was no indication that the dN/dS values were significantly greater than 1 (the lowest probability of rejecting the null hypothesis of neutral evolution was > 0.19) using HyPhy implemented in MEGA (Tamura et al., 2011). For the branches, the test was conducted using the program codeml available in the PAML package (Yang, 2007). The program calculated the individual dN/dS values for each branch and a single average dN/dS value. By comparing the likelihood ratio for the two values with a chi-square test, the probability was not significant ($P > 0.41$). This suggested that there was not likely to be variation in the dN/dS values and thus the possibility of positive selection along any of specific branches. Consequently, I did not detect evidence for positive selection in pairwise comparisons of overall sequences, on specific codons, and along specific branches of *AtLURE1* and *AlLURE1* genes.

Since no evidence that the *AtLURE1* and *AlLURE1* genes are evolving under positive selection was observed, I conducted the McDonald-Kreitman test (McDonald and Kreitman, 1991) to test a hypothesis that *AtLURE1* genes have evolved under neutral evolution. According to the neutral theory, the dN/dS values between the two species should be equivalent to the rate of nonsynonymous to synonymous polymorphism within *A. thaliana*. Although one-to-one orthologous relationship between *AtLURE1* and *AlLURE1* genes could not be defined, I tried the test for coding sequences of each *AtLURE1* gene of the *A. thaliana* accessions (Figure 22) and *AlLURE1.5* gene as a representative from *AlLURE1* genes. The test was not significant for *AtLURE1.1*, *1.2*, *1.3*, *1.4*, and *1.6* ($P > 0.69$, 0.75, 1.0, 0.16, and 1.0, respectively;

Table 4) except for *AtLURE1.5* ($P < 0.05$; Table 4). I also observed similar results when compared to other *AlLURE1* genes as a representative (data not shown). These results implied that most *AtLURE1* genes have evolved by drifting neutrally.

I found that divergence of amino acid sequence between AtLURE1 and AlLURE1 peptides was higher among the subgroups of multiply duplicated DEFL peptides analyzed (Table 1). Since I did not detect evidence for positive selection for the LURE1 peptides of *A. thaliana* and *A. lyrata*, it is suggested that the AtLURE1 peptides have undergone relatively rapid sequence change under neutral evolution, resulting in higher divergence of the sequences, and gene duplication after the divergence of the two species.

AtLURE1 Has a Species-Preferential Pollen Tube Attraction Activity

Next, I investigated reciprocal pollen tube attraction activities of AtLURE1 and AlLURE1 peptides in *A. lyrata* and *A. thaliana*. I was able to prepare only one peptide from *A. lyrata*, being the predicted mature peptide of AlLURE1.3 (see Figure 11B), as a recombinant peptide. I confirmed the ability of AlLURE1.3 to attract *A. lyrata* pollen tubes (Figure 23A), suggesting that AlLURE1 peptides are also pollen tube attractants in *A. lyrata*. The attraction frequencies of a representative recombinant peptide from *A. thaliana*, AtLURE1.2, were 75% ($n = 24$) for *A. thaliana* pollen tubes and 44% ($n = 36$) for *A. lyrata* pollen tubes, whereas those of AlLURE1.3 were 75% ($n = 20$) and 77% ($n = 30$), respectively, under the same conditions (Figure 23B). These results suggested that the AtLURE1 peptide had species-preferentiality, whereas the AlLURE1 peptide did not. Additionally, I showed that the AtLURE1.2 peptide did not show significant attraction of *T. fournieri* pollen tubes when examined at 40 nM (13%, $n = 38$) and 50

μM (14%, *n* = 21), indicating specific attraction activity of the peptide depending on evolutionary distance.

Breakdown of Reproductive Isolation Barriers by Transforming the *AtLURE1* Gene into *Torenia*

If AtLURE1 peptides are in fact key molecules in the establishment of reproductive isolation, one may be able to break this barrier by introducing *AtLURE1* genes into other plant species. Thus, I produced transgenic *T. fournieri* plants expressing an AtLURE1 peptide and examined whether reproductive isolation can be overcome in this manner. Despite a large evolutionary distance between *A. thaliana* (Brassicaceae, Brassicales) and *T. fournieri* (Linderniaceae, Lamiales) (APG III, 2009), AtLURE1 peptides were partially similar to TfLUREs, including the alignment of conserved cysteines, the CxC motif at the C-terminus (Figure 24A), and specific expression in the synergid cell. The remaining amino acids, however, diverged considerably, demonstrating the loss of a conserved glycine residue for the gamma-core motif (Figure 24A), which is generally observed in antimicrobial CRPs. Consistent with this divergence, TfLUREs did not attract pollen tubes of *A. thaliana* (Figure 21). I then designed a transgenic plant co-expressing *AtLURE1.2* and cytosolic *GFP* specifically within the synergid cell of *T. fournieri*, under the control of the *TfLURE2* promoter (Figures 24B and 25A). In transgenic T_1 heterozygous *T. fournieri* plants, I confirmed the specific expression of GFP in the synergid cell (Figure 25B) and the secretion of AtLURE1.2 peptide to the micropylar end of GFP-expressing synergid cells via immunostaining (Figure 25C). Using the transgenic *T. fournieri*, I performed an interspecific pollen tube attraction assay, in which the transgenic *T. fournieri* ovules

manipulated by a glass needle were placed close to the tip of *A. thaliana* pollen tubes *in vitro* (Figure 25D). The ovule was applied twice to one pollen tube to determine whether the ovule consistently attracted the pollen tube. Strikingly, the GFP-labeled transgenic *T. fournieri* ovules strongly attracted *A. thaliana* pollen tubes in both trials (100%, n = 11) (Figure 25E), whereas non-labeled ovules did not (0%, n = 11). The attraction was also precise, in that pollen tubes were able to redirect themselves toward the micropylar end of embryo sacs that had been shifted to a slightly different position. Strikingly, all of the attracted pollen tubes that continued to grow (n = 9) penetrated the embryo sac of *T. fournieri* (Figure 26), through the region of the filiform apparatus (thickened cell wall) of the synergid cell, as reported in normal fertilization (Van der Pluijm, 1964). These results demonstrated that the heterologous expression of a single AtLURE1 attractant peptide alone is sufficient to overcome interspecific barriers in micropylar pollen tube guidance and penetration of the embryo sac, despite a large evolutionary distance between organisms.

Conserved Mechanisms for Expression of LURE Peptides

I showed that introduction of the *AtLURE1* gene driven by *TfLURE2* promoter of *T. fournieri* was sufficient to express a heterologous AtLURE1 peptide in *T. fournieri* synergid cell and to attract *A. thaliana* pollen tubes (Figures 25 and 26). In addition to *TfLURE2* promoter, I determined a *TfLURE1* promoter sequence from *T. fournieri* genomic DNA by thermal asymmetric interlaced (TAIL)-PCR (Figures 27A). It has been suggested that the consensus sequence AACGT is necessary and sufficient for *AtLURE1.2* (*DD2*) expression in the synergid cell and that the other consensus sequence GTAACNT is the *in vivo* MYB98-binding *cis*-element (Punwani et al., 2008). I found

that there are AACGT elements in *TfLURE2* promoter sequence within several hundred bp upstream from the transcription start site (Figures 24B and 27B), as well as all *AtLURE1* promoters (Punwani et al., 2008). On the other hand, *TfLURE1* promoter sequence contains GTAACNT element but not AACGT element in its promoter sequence (Figure 27A and 27B). These suggested the idea that promoters of *TfLURE1* and *2* could function in the synergid cell of *A. thaliana*. Thus, I introduced *pTfLURE1::GFP* and *pTfLURE2::GFP* sequences into *A. thaliana* plants, resulting in predominant GFP expression in synergid cells within *A. thaliana* ovules (Figure 28A and 28B). I also introduced *pTfLURE1::TfLURE1-GFP* and *pTfLURE2::TfLURE1-GFP* sequences, in which genomic sequences consisting of promoter and coding region without stop codon of each *TfLUREs* were connected to *GFP* sequence. While GFP signal was hardly-detectable in *pTfLURE1::TfLURE1-GFP* plants probably due to low expression in *A. thaliana*, localized TfLURE2-GFP signal was clearly observed in the micropylar end of the embryo sac of *pTfLURE2::TfLURE2-GFP* ovules (Figure 28C), comparable to or stronger than signals in *pAtLURE1::AtLURE1-GFP* ovules (Figure 12E). A magnified confocal image suggested that TfLURE2-GFP signal was mainly localized at the outside of the synergid cell membrane (Figure 28D). These analyses indicate that expression mechanism for species-specific *LURE* genes is conserved between *A. thaliana* and *T. fournieri*.

Next, I examined whether TfLURE peptides are secreted toward the micropyle in transgenic plants expressing *TfLURE* genes, and whether ovules of the transgenic plants can attract *T. fournieri* pollen tubes. *A. thaliana* plants were transformed with T-DNA constructs that contain *pMYB98::GFP*, which marks synergid cells only in the embryo sac possessing the T-DNA, and *TfLURE1* or *TfLURE2* genomic sequences from

promoter to 3′ untranslated regions (*pMYB98::GFP/pTfLURE1::TfLURE1* and *pMYB98::GFP/pTfLURE2::TfLURE2*, respectively). Immunostaining of ovules of the transgenic plants showed that TfLURE1 and TfLURE2 were observed around the micropyle as secreted peptides (Figure 29A and 29B). Note that despite GFP signal in the micropylar end of the embryo sac, GFP-fused TfLURE2 was unable to be detected in the micropyle by immunostaining for both GFP and TfLURE2 (Figure 29C). This result supported my previous view that the GFP-fused AtLURE1 did not diffuse from the filiform apparatus of the synergid cell due to the increased molecular weight of the fusion protein (see Figures 12E and 13). However, GFP-fused AtLURE1 and TfLURE2 might diffuse toward the outside at immunocytochemically undetectable level since GFP-fused ZmEA1, which is a possible attractant directly attracting the maize pollen tube, seemed to be effective on medium when expressed in the *A. thaliana* synergid cell (Márton et al., 2012). Nonetheless, I tried interspecific pollen tube attraction assay using the *A. thaliana* transgenic ovules expressing non-tagged TfLUREs and *T. fournieri* pollen tubes. The transgenic ovules were co-cultured with *T. fournieri* ovules and a cut style pollinated with *T. fournieri* pollen grains. 12-16 hours after co-cultivation, pollen tubes were grown on medium through the cut style and attracted to the embryo sacs of *T. fournieri* ovules, while none of them were clearly attracted to the transgenic *A. thaliana* ovules (data not shown). Since a sharp concentration gradient toward the synergid cell or the attractants is supposed to be important for precise attraction (Higashiyama et al., 2001; Okuda et al., 2009; Takeuchi and Higashiyama, 2011), detecting apparent attraction to the transgenic ovules might require me to perform pollen tube attraction assay with manipulated ovules, which has been previously conducted (Higashiyama and Hamamura, 2008; Figures 3 and 25). Consequently, my results suggest that the

heterologous expression of the LURE attractant peptides can be achieved by introducing a genomic sequence of the *LURE* gene with its upstream sequence and possibly overcome interspecific barriers in micropylar pollen tube guidance depending on assay system.

Discussion

Mechanistic Insights into Micropylar Pollen Tube Guidance Mediated by LURE Peptides

Pollen tube growth and guidance have been intensively studied in *A. thaliana*, but the key attractant molecule has not been identified (Takeuchi and Higashiyama, 2011). In this study, I identified paralogous *DEFL* genes forming the sole species-specific *DEFL* gene cluster in *A. thaliana*, compared to its close relative *A. lyrata*, and found evidence that these *DEFL* genes, designated the *AtLURE1* genes, encode pollen tube attractants in *A. thaliana*. AtLURE1 peptides are small, secreted DEFL peptides that are specifically expressed in synergid cells (Figure 12). *In vivo* data showed that AtLURE1 peptides diffused to the surface of the funiculus of the ovule through the micropyle (Figure 13) and that downregulation of these peptides impaired micropylar guidance (Figures 15-17). Moreover, recombinant AtLURE1 peptides expressed in *E. coli* attracted pollen tubes in a concentration-dependent and species-preferential manner *in vitro* (Figures 20, 21, and 23B). These results provide concrete evidence that AtLURE1 peptides are pollen tube attractants in *A. thaliana* necessary for micropylar guidance.

Specific and abundant attractant peptide expression in the synergid cell is suggested in *A. thaliana* (Figure 12; Jones-Rhoades et al., 2007), as in *T. fournieri* (Okuda et al., 2009). *AtLURE1* gene duplication appears to have contributed to the increased amount of *AtLURE1* mRNA (Figure 12B). I propose that highly homologous AtLURE1 peptides (80–95% amino acid sequence identity) are functionally redundant because each recombinant peptide showed attraction activity *in vitro* (Figure 21), I

could find no combination effect among them (data not shown), and heterologous expression of the AtLURE1.2 peptide in *T. fournieri* showed sufficient activity to attract *A. thaliana* pollen tubes into the embryo sac (Figure 25). Abundant expression might be a common characteristic of diffusible attractants derived from the synergid cell. The synergid cell is morphologically unique, showing characteristics typical of transfer cells, which are active in secretion and/or molecule uptake (Higashiyama, 2002). The synergid cell has been proposed to be a general source of pollen tube attractants in flowering plants due to its conserved morphology (Higashiyama, 2002; Higashiyama and Hamamura, 2008). As proposed after the laser-mediated ablation of synergid cells in *T. fournieri* (Higashiyama et al., 2001), the amount of attraction signal may be correlated with the effective range of the signal. The endogenous localization of AtLURE1 peptides, as revealed by the immunostaining, suggests that the peptides diffused to the surface of the ovular funiculus (~250 μm from the basal edge of the synergid cell). This is consistent with previous estimates of the effective range of pollen tube attraction in *A. thaliana,* based on the behavior of pollen tubes *in vivo* and *in vitro* (Takeuchi and Higashiyama, 2011; Stewman et al., 2010). The abundant expression and active secretion of AtLURE1 peptides might be important for retaining a sharp peptide concentration gradient toward the synergid cell at a sufficient distance.

Like TfLUREs, AtLURE1 peptides are DEFL peptides, although their amino acid sequences have diverged considerably (Figures 11 and 24A). The LURE peptides of *Torenia* (Okuda et al., 2009; Kanaoka et al., 2011) and *Arabidopsis* showed similar alignments of cysteines, which are typical of plant and insect defensins, including a CxC motif at the C-terminus (Thomma et al., 2002). A glycine in the gamma core of antimicrobial peptides is contained in *Torenia* LUREs (Okuda et al., 2009; Kanaoka et

al., 2011), but not in *Arabidopsis* LURE1 peptides (Figures 24A). Since *Arabidopsis* (Brassicaceae) and *Torenia* (Linderniaceae) are quite divergent dicots, DEFL peptides might function as general pollen tube attractants in dicotyledonous plants. Although searching for attractants in other plant species is difficult due to low homologies, my study suggests that LURE-type DEFL peptides, which are abundantly and specifically expressed in the synergid cell, are candidate attractants. In the monocot *Z. mays*, another type of small secreted peptide, ZmEA1, was recently reported to be an attractant molecule derived predominantly from the synergid cell (Márton et al., 2005; Dresselhaus and Márton, 2009; Márton et al., 2012). GFP-fused ZmEA1 appears to diffuse toward the micropylar opening as the ovule develops (Márton et al., 2005). EA1-like genes comprise a large family in monocots (Gray-Mitsumune and Matton, 2006). Monocots may use non-DEFL peptides as attractants, although EA1-like genes are not likely to be expressed in synergid cells in rice (Ohnishi et al., 2011).

Various CRPs, including DEFL peptides, are involved in the cell-cell communications underlying male-female interactions during plant reproduction (Higashiyama, 2011). The suggestion has been made that nearly 200 of 825 *CRP*s are expressed in the *A. thaliana* female gametophyte (Jones-Rhoades et al., 2007). Not only AtLURE1 peptides but also other DEFL peptides and CRPs could be involved in cell-cell communication among gametophytic cells. Since the downregulation of AtLURE1 peptides partly inhibited micropylar guidance (Figure 16), additional attractant peptides may be derived from the synergid cell. As I observed abnormal pollen tube guidance in the micropylar guidance mutants at higher frequencies than in the RNAi lines, such additional attractants may be downregulated in these mutants. In fact, I found that some additional genes belonging to the CRP810 subgroup, which

consists of 16 DEFL peptides in *A. thaliana* (Figure 30), were downregulated in the *myb98* mutant ovule (Jones-Rhoades et al., 2007). Therefore, I performed qRT-PCR analysis for all of the *CRP810* genes and confirmed that some of these were expressed in the pistil at high levels as *AtLURE1* genes (Figure 31). Two attractant DEFL peptides in *T. fournieri*, TfLURE1 and 2, share 47% similarity in amino acid sequence, while CRP810 peptides share >38% similarity, indicating the possibility that some other CRP810 peptides are pollen tube attractants in *A. thaliana*. Although whether they function as attractant peptides is unknown, my results suggest the possibility that many more pollen tube attractant peptides are expressed in the synergid cell, which may be required to efficiently attract pollen tubes to all female gametophytes. Nonetheless, my key finding will considerably accelerate the study of the directional control of tip-growing pollen tubes, the determination of precise spatiotemporal control of pollen tube attraction to the ovule, and identification of the receptor(s) of pollen tube attractants, which has not yet been identified (Takeuchi and Higashiyama, 2011).

The Sole Species-Specific Cluster of *DEFL* Genes in *A. thaliana* Encodes Micropylar Pollen Tube Attractants

Using phylogenetic and synteny analyses, the *AtLURE1* (*CRP810_1*) and *AlLURE1* (*AlCRP810_1*) genes were suggested to form species-specific tandem arrays after the divergence of the two species (Figures 9A and 10A), possibly via gene duplication and/or gene conversion (Leister, 2004; Nei and Rooney, 2005). Other clusters of paralogous *DEFL* genes in *A. thaliana* (≥ 4 genes with ≥ 90% bootstrap values) were suggested to be formed before speciation occurred (Figures 8 and 9B-D), and syntenic conservation was observed between these *DEFL* genes from *A. thaliana*

and *A. lyrata* (Figure 10B-D). Post-divergence, many genes have undergone lineage-specific duplication in *A. thaliana* (Hu et al., 2011); however, among the 317 *DEFL* genes, the *AtLURE1* attractant genes represent the only recently formed, species-specific cluster. Moreover, some subgroups of mammalian β-defensin gene lineages exist specifically in certain species and are preferentially expressed in the male reproductive tract (Patil et al., 2005). Clarifying whether these β-defensins play a role in fertility would be of interest.

Rapid gene turnover has been reported in multigene families involved in disease, including the effector genes of *Drosophila* (e.g., antimicrobial peptides (Sackton et al., 2007)), the recognition genes of the sea urchin *Strongylocentrotus purpuratus* (e.g., Toll-like receptors (Rast et al., 2006)), and the effector genes for avirulence activity of the rice blast fungal pathogen *Magnaporthe oryzae* (Yoshida et al., 2009), possibly due to a coevolutionary arms race. My work demonstrates that genes involved in direct male-female interactions in sexual reproduction can also increase rapidly in copy number during speciation. To my knowledge, such a species-specific gene cluster directly involved in male-female interactions has not been reported. The relationship between multicopy factors for sexual reproduction and their rapid molecular evolution is an important issue to be addressed. In addition to the indicated lineage-specific duplication, AtLURE1 peptides showed lower homology (~70%) among multiply duplicated DEFL peptides when compared to orthologous *A. lyrata* DEFL peptides. This suggests the rapid evolution of *AtLURE1* genes possibly by high mutation rate under neutral genetic drift because I was unable to detect any evidence of positive selection. Similarly no evidence for positive selection has been found in multicopy antimicrobial peptides in *Drosophila*, but they might not require functional

change between species due to a lack of coevolutionary arms race (Lazzaro, 2008; Sackton et al., 2007; Jiggins and Kim, 2005). This seems to be different from the case of *AtLURE1* genes which encode peptides showing species-preferential activity.

Various mutations, including cysteine substitutions and stop mutations, were observed in different ecotypes of *A. thaliana* (Figure 22). A cysteine substitution in AtLURE1.5 found in the Col-0 line was shown to impair attraction of the pollen tube (Figure 21). *AtLURE1* gene duplication is likely to confer a relaxation of functional constraints due to gene redundancy (Ohno, 1970). As long as some population of attractant peptides interacts with a receptor, functional changes such as specificity for a receptor of the other population of peptides could be permitted with normal pollen tube guidance. One may speculate that multiple attractant genes may be important for reinforcing species specificity by sequence divergence without loss of correct ligand–receptor pairing.

Non-Cell Autonomous Regulation of Pollen Tube Attraction

In addition to the mutant ovules of *myb98*, those of *ccg* and *maa3* could not secrete AtLURE1 peptides, as shown by immunostaining (Figure 14B and 14C), suggesting that attractant secretion occurs via CCG- and MAA3-related regulatory pathways. CCG is a transcriptional regulator in the central cell (but not the synergid cell) that functions in micropylar guidance. Regarding the phenotype of the *ccg* mutant, whether the central cell directly attracts pollen tubes by emitting a diffusible signal or indirectly controls pollen tube guidance via cell–cell communication between the central cell and synergid cell has been debated (Berger et al., 2008). My results are consistent with the latter model, in which CCG in the central cell indirectly controls the

expression of AtLURE1 peptides in the synergid cell. It was showed that *pMYB98::GFP* was expressed normally in the *ccg* mutant (Chen et al., 2007). However, I could not elucidate whether CCG controlled the expression of AtLURE1 independently of the MYB98 regulatory pathway, because *MYB98* and *AtLURE1* transcript levels seemed somewhat decreased in the *ccg* ovules (Figure 14A). Gametic cells (the egg cell and central cell) communicate with each other, and likely control cell specificity in the synergid and antipodal cells during female gametophyte development (Pagnussat et al., 2007; Gross-Hardt et al., 2007; Moll et al., 2008; Kägi et al., 2010). My results suggest that CCG in the central cell is required for full functioning of the synergid cell. The identification of additional downstream genes regulated by CCG and upstream genes regulating attractant production will clarify how the central cell controls attractants secreted from the synergid cell at the molecular level.

MAA3 helicase is essential for normal development of the female gametophyte and is likely generally involved in RNA metabolism in various cell types (Shimizu et al., 2008). Although the phenotype of the *maa3* ovule includes smaller nucleoli in two polar nuclei and failure of fusion of the polar nuclei in the central cell (Shimizu and Okada, 2000), whether the synergid cell and/or the central cell are responsible for abnormal pollen tube guidance in *maa3* remains unclear. AtLURE1 peptides were not secreted from the *maa3* ovule, as shown by immunostaining (Figure 14B and 14C). This finding implies that attractant production could be regulated by MAA3-mediated RNA metabolism. RNA metabolism, including rRNA biogenesis, is important for female gametophyte development (Shi et al., 2005; Li et al., 2009; Huang et al., 2010). Complex regulation via RNA metabolism and synergid cell-central cell interactions may

render female gametophytic cells fully mature, after which the expression of attractant peptides, including AtLURE1 peptide, is initiated.

AtLURE1 Peptides May Overcome Pre-zygotic Reproductive Barriers

Interspecific cross-pollination with *A. thaliana* pistils was shown to cause mis-targeting of some pollen tubes at the micropylar guidance step (Shimizu, 2002). Consistent with this idea, AtLURE1.2 peptide showed species-preferentiality in its attraction activity when pollen tubes from *A. thaliana* and *A. lyrata* were examined (Figure 23). Unexpectedly, AlLURE1.3 peptide showing low sequence identity (~70%) with AtLURE1 peptides attracted pollen tubes from both *A. thaliana* and *A. lyrata* in a similar frequency (Figure 23). This might be related to evolutionary pattern of receptor(s) for the LURE peptides between the two species. Elucidating coevolution of the LURE peptides and the receptors of both species would shed light on mechanism of formation of reproductive barriers in pollen tube guidance. In *T. fournieri* and its close relative *Torenia concolor*, rapid molecular evolution of *TfLURE1* and *TcLURE1* was likely directly involved in the species preferentiality of pollen tube attraction (Kanaoka et al., 2011; Higashiyama et al., 2006). The expression of LURE attractant peptides at the last step of pollen tube guidance is likely to be one of the more severe reproductive isolation barriers. This was supported by the fact that a single *AtLURE1* gene introduced into *T. fournieri* was sufficient to attract competent *A. thaliana* pollen tubes to the *T. fournieri* embryo sac. The degree of tracking precision shown by these pollen tubes was greater than expected: pollen tubes of *A. thaliana* followed the filiform apparatus (only 10 μm in surface diameter) of manipulated ovules of transgenic *T. fournieri*, as is normally observed when *T. fournieri* pollen tubes approach the embryo sac

(Higashiyama and Hamamura, 2008). Recently, synthetic ZmEA1 peptide was suggested to attract maize pollen tubes, and heterologous expression of ZmEA1-GFP in the synergid cell of *A. thaliana* resulted in the attraction of maize pollen tubes toward the micropyle (Márton et al., 2012). These results may open the way for new technologies to overcome reproductive barriers in flowering plants, although further research is required to identify other key factors preventing heterologous fertilization. My research into the AtLURE1 peptide further showed that heterologous pollen tubes can enter the embryo sac normally through the region of the filiform apparatus. This suggests that pollen tube entrance into the embryo sac does not involve any other severe species-recognition mechanism, at least when combining the *T. fournieri* embryo sac with an *A. thaliana* pollen tube. The succeeding steps in fertilization, being pollen tube recognition and triggered rupture by the synergid cell, may show severe species-specificity (Escobar-Restrepo et al., 2007; Amien et al., 2010). *FERONIA* (Escobar-Restrepo et al., 2007) and *ZmES4* (Amien et al., 2010) expressed in the synergid cell are good candidates for mediating species recognition during these steps.

Some post-zygotic isolation barriers (Coyne and Orr, 2004) involved in hybrid dysfunction have been identified in plants through genetic studies (Bikard et al., 2009; Mizuta et al., 2010; Yamagata et al., 2010). Rapidly changing reproductive genes, including *AtLURE1*, *TfLURE1*, *TcLURE1* (Kanaoka et al., 2011; Higashiyama et al., 2006), ZmEA1 (Márton et al., 2005; Gray-Mitsumune and Matton, 2006), *FERONIA* (Escobar-Restrepo et al., 2007), and *ZmES4* (Amien et al., 2010), represent potential pre-zygotic isolation barriers during the final steps of pollen-pistil interactions. In pollen-pistil interactions, the final steps show much greater species preferentiality (Higashiyama and Hamamura,2008). Identifying their partner molecules, including the

receptor of LURE, is important to understanding the mechanism of speciation and plant reproduction.

Materials and Methods

Plant Materials

For all experiments except the sequence analysis, accession Col-0 was used as wild-type *A. thaliana*. For the sequence analysis of 12 *A. thaliana* accessions, Cvi-0 (CS22614), Est-1 (CS22629), Mr-0 (CS22640), Tsu-1 (CS22641), Nok-3 (CS22643), Fei-0 (CS22645), Ts-1 (CS22647), Pro-0 (CS22649), Kondara (CS22651), Ms-0 (CS22655), Bur-0 (CS22656), and Ws-2 (CS22659), seeds were obtained from Sumie Ishiguro (Nagoya University). The *myb98* (SALK_020263) and *ccg* (SALK_077907) mutants are T-DNA insertion lines (Alonso et al., 2003). The T-DNA insertion mutant *maa3* was provided by Kentaro K. Shimizu (University of Zurich). *A. lyrata* (accession CS22696) was provided by Akira Kawabe (Kyoto Sangyo University). Seeds of *A. griffithiana* (accession CS22562) and *C. rubella* (accession CS22697) were provided from ABRC (Arabidopsis Biological Resource Center).

Plant Growth Conditions

Seeds of *Arabidopsis thaliana* and its relatives were sterilized and germinated on plates containing 0.5× Murashige and Skoog salts (Wako Pure Chemical Industries), 1% sucrose, 0.5× Gamborg's vitamin solution (Sigma), and 0.3% gelrite (Wako Pure Chemical Industries). Ten-day-old seedlings of *A. thaliana* and moderately grown seedlings of *Arabidopsis* relatives were transferred to soil and grown under continuous light at 22°C. To select *maa3/MAA3* heterozygous mutants, semi-sterility was checked. To select *myb98/MYB98* and *ccg/CCG* heterozygous mutants, T-DNA insertion was confirmed by PCR using the T-DNA-specific primer LBa1

(5’-TGGTTCACGTAGTGGGCCATCG-3’) and genomic sequence primer for *MYB98* (5’-TGGGTATAGTAAAAACACACATTAAATGTC-3’) or *CCG* (5’-ATTTGAGGGATCATCTCCTGACG-3’). Growth condition for *A. lyrata* and *C. rubella* was similar with the exception of a vernalizing cold treatment. For the treatment, *A. lyrata* or *C. rubella* plants in the rosette stage were grown in 8 h photoperiod at 4°C for at least 1 month.

Plant Transformation

T-DNA constructs were introduced into *Agrobacterium tumefaciens* strain GV3101 and then transformed into plants using the floral dip method for *A. thaliana* (Clough and Bent, 1998) or the leaf disc method for *T. fournieri* (Aida and Shibata, 1995), with some modifications. Transformed seeds or leaf discs were selected on medium containing antibiotics.

Sequence Determination of *AtLURE1* Genes and their Orthologs in *A. lyrata*

Arabidopsis thaliana (Col-0) nucleotide sequences were obtained from TAIR (http://www.arabidopsis.org/) and confirmed by sequencing. Predicted signal peptide cleavage sites in CRP810_1.1 to _1.5 (AtLURE1.1 to 1.5) were determined from their full-length amino acid sequences using SignalP (http://www.cbs.dtu.dk/services/SignalP/). Orthologous *DEFL* genes in *A. lyrata* were identified by BLAST search at the Department of Energy Joint Genome Institute (DOE JGI) (http://genome.jgi-psf.org/Araly1/Araly1.home.html). Four *CRP810_1* orthologs (*AlCRP810_1.4*, *1.7*, *1.9*, and *1.10*) were found by BLASTp (BLAST protein vs. protein). Additionally, six orthologs were found by BLASTn (BLAST nucleotide vs.

nucleotide); *AlCRP810_1.1*, *1.2*, *1.3*, *1.5*, and *1.6* were found in a region adjacent to *AlCRP810_1.4* and *1.7* on scaffold_8, while *AlCRP810_1.8* was found on scaffold_97, which showed no synteny to the *A. thaliana* genome. *AlCRP810_1.9* and *1.10* were tandemly duplicated genes within 2 kb on scaffold_1021, which also showed no synteny to the *A. thaliana* genome. These 10 genes were named according to their locations (Table 1). Other orthologous *DEFL* genes in *A. lyrata* were found by BLASTn (Table 1).

Synteny analysis of genomic regions containing *CRP810_1* genes, *CRP700* (*ATTI*) genes, *CRP580* (*LCR*) genes, and *CRP860* (*SCRL*) genes was performed using genomic data from the two species. For genomic regions containing *AlCRP810_1* genes, one gap on scaffold_8 (4535001-4570000) and two gaps on scaffold_8 (4222301-4251300) were sequenced using PCR-based direct sequencing. The reactions were performed using three pairs of primers: 5'-GTTTAAAAGAATTGATTAGGTCACC-3' and 5'-GGTATTGTAATCATTTTAAAAAAATTC-3', 5'-TCCGAAACCCGTAGACAGACAC-3' and 5'-GCGGTCACCATCTTTCATC-3', and 5'-AAGACTCTTATCACCTTCAAGGTC-3' and 5'-AACCGAAACATTGGCTTTAGAG-3', respectively. The products were sequenced using the same primers and sequencing primers for the latter two products, 5'-GGTTTTGTGAGAGTGCAGTTG-3' and 5'-CAGTTTGAGGAGATGTACCAGAG-3', and 5'-AAAGGATGTAGCATCTAAACACAG-3', 5'-CCAAAAAACACATTATTTAGGGAG-3', and 5'-CTTGGAGACGATCGACGATG-3', respectively. The gap-filled sequences

confirmed that no *AlCRP810_1* gene existed in these regions. The region containing *At5g43285* (*CRP810_1.1* or *AtLURE1.1*) showed synteny to the region including *AlLURE1.1* to *1.7*. On the other hand, no *AlLURE1* gene was found in a syntenic region containing *At5g43510* (*CRP810_1.2* or *AtLURE1.2*) to *At5g43525* (*CRP810_1.5* or *AtLURE1.5*). These two syntenic regions were drawn with reference to sequences from *A. thaliana* chromosome 5 (17360001–17386000) and *A. lyrata* scaffold_8 (4535001–4570000), and sequences from *A. thaliana* chromosome 5 (17469401–17495400) and *A. lyrata* scaffold_8 (4222301–4251300), respectively. The genes *CRP810_1.8*, *1.9*, and *1.10* were on a small scaffold (scaffold_97 and scaffold_1021) that showed no synteny with the *A. thaliana* genome. In a similar way, syntenic regions for *CRP700* (*ATTI*) genes, *CRP580* (*LCR*) genes, and *CRP860* (*SCRL*) genes were drawn with reference to sequences from *A. thaliana* chromosome 2 (18062001–18076000) and *A. lyrata* scaffold_4 (21267001–21289000), sequences from *A. thaliana* chromosome 4 (14423001–14440000) and *A. lyrata* scaffold_7 (5359000–5340001), and sequences from *A. thaliana* chromosome 1 (22448001–22466000) and *A. lyrata* scaffold_2 (2822000–2794001), respectively.

Phylogenetic Tree Analysis

Phylogenetic analyses were done as described previously (Higashiyama et al., 2006). Full-length amino acid or genomic sequences (a start codon to a stop codon in the genomic DNA) were aligned using ClustalX (Larkin et al., 2007). Phylogenetic trees of the aligned sequences were drawn using the neighbor-joining (NJ) method, including bootstrapping (Saitou and Nei, 1987) based on 1000 replicates using ClustalX or MEGA 5 (Tamura et al., 2011).

Quantitative Real-Time RT-PCR

Total RNAs were purified from each tissue using RNAqueous-Micro (Ambion) with Plant RNA Isolation Aid (Ambion). Each tissue was homogenized in lysis solution. Following total RNA purification, reverse transcription reactions were carried out using SuperScript III Reverse Transcriptase (Invitrogen). Quantitative real-time PCR was performed using the cDNA and Power SYBR Green PCR Master Mix (Applied Biosystems) on an Applied Biosystems StepOnePlus Real-Time PCR System. The PCR mixture consisted of 0.5 μM primers, appropriately diluted cDNA, and 1× master mix in a volume of 15 μl. The PCR program consisted of 95°C for 10 min, followed by 45 cycles at 95°C for 15 s and 60°C for 1 min. Subsequently, the melting curve was plotted to check the specificity of amplification according to the default setting. The C_T of each sample was determined according to the average of two or three technical replicates.

To quantify the absolute expression levels of the *CRP810* genes, including *CRP810_1* (*AtLURE1*) genes, and *MYB98*, the standard curve method was applied using template vectors of known copy number as standards. The vectors were constructed using a Zero Blunt TOPO PCR Cloning Kit (Invitrogen) to clone PCR products of the target sequences, which were amplified from pistil cDNA. To amplify each of the paralogous *CRP810_1*, *_2*, and *_3* genes, amplification refractory mutation system (ARMS) PCR analysis (Bai and Wong, 2004) was applied. For ARMS PCR analysis, primers with one or two mismatched nucleotides immediately upstream of the SNP site in the target sequence were designed. Specific amplification of a single gene was confirmed by real-time PCR using vectors of non-targeted paralogous genes as templates. The means and standard deviations of the absolute expression levels for each

gene were calculated from the values in three independent pistil cDNA samples and normalized to the *MYB98* absolute expression level.

To quantify the relative expression levels, the comparative C_T ($\Delta\Delta C_T$) method was applied as described below. First, for each sample, the ΔC_T of each gene compared to an internal control gene, *ACT2* (*At3g18780*), was determined using the formula ΔC_T = C_T (gene of interest) – C_T (*ACT2*). Next, for each tissue or genotype, the mean ΔC_T and standard error was calculated. Finally, the expression levels as the relative quantity (RQ) to a reference sample were calculated using the formula $RQ = 2^{-(\text{mean of } \Delta Ct \text{ [sample of interest]} - \text{mean of } \Delta Ct \text{ [reference sample]})}$.

Promoter GFP Analysis for *CRP810_1* genes

Sequences 1129, 665, 3304, 1789, and 1957 bp upstream of the transcription start site were used as promoter sequences of *CRP810_1.1*, *_1.2*, *_1.3*, *_1.4*, and *_1.5*, respectively. To prepare a subcloning vector containing the *GFP* sequence, *GFP* and the 5' linker sequence, amplified from pGWB4 (Nakagawa et al., 2007a) using the primers 5'linker_F+SpeI-SmaI (5'-gtaactagttctcccgggAAGGGTGGGCG-3') and GFP_R+SacI (5'-taggagctctactcgagattggtaccCTTGTACAGCTCGT-3'), were introduced into pT7Blue (Novagen) using *Spe*I and *Sac*I. Next, the promoter sequence and promoter sequences plus coding regions without the stop codon of each *CRP810_1* (*AtLURE1*) gene were amplified with iProof High-Fidelity DNA Polymerase (Bio-Rad) from genomic DNA. The amplified products were subcloned into the GFP vector using *Hin*dIII and *Sma*I. *GFP*-fused sequences were cut from the subcloned vectors and transferred to the pGWB500 series vector (Nakagawa et al., 2007b) with *Hin*dIII and *Sac*I, resulting in the binary vectors pGWB500-*pCRP810_1::GFP* series and

pGWB500-*pCRP810_1::CRP810_1-GFP* series. These constructs were transformed into wild-type *A. thaliana* plants (Col-0) using the floral dip method. Transformed plants were selected on medium containing 20 mg/l hygromycin B (Wako Pure Chemical Industries).

To observe GFP fluorescence in mature ovules, flowers of the transformed plants were emasculated before anthesis. For epifluorescence microscopy, an inverted microscope (IX71, Olympus) with a 3CCD camera (C7780-20, Hamamatsu Photonics) was used. For confocal laser scanning microscopy, an IX71 equipped with a disk-scan confocal system (CSU10, Yokogawa) and EM-CCD camera (Cascade II:512, Roper) was used.

Immunostaining

Recombinant CRP810_1.2 (AtLURE1.2) purified as described in the next section was prepared and used to immunize a rabbit. IgGs in the pre-immune serum and anti-CRP810_1.2 serum were purified by affinity chromatography (HiTrap Protein G HP, GE Healthcare). For immunostaining, the carpel walls were removed from the pistil, resulting in ovules on the septum. The ovules were then fixed using 4% paraformaldehyde in PBS for 40 min or a 9:1 mixture of ethanol and acetic acid overnight. After treatment with 0.2% Triton X-100 for 5 min and blocking with 3% bovine serum albumin (BSA) for 1 h at 37°C, the samples were treated with purified pre-immune and anti-CRP810_1.2 antibodies (1:1000 dilution) in 1% BSA for 1 h at 37°C. The samples were then treated with Alexa Fluor 488-conjugated anti-rabbit goat IgG (1:1000 dilution; Invitrogen) for 1 h at 37°C. The stained ovules were observed by epifluorescence microscope (BX51, Olympus) and confocal laser-scanning microscope

(LSM 780 NLO, Zeiss).

Immuno-Dot Blot Analysis

Ten microliters of purified recombinant His-tagged peptide was blotted onto a PVDF membrane (Immobilon-P, Millipore). The PVDF membrane was then treated with anti-CRP810_1.2 antibodies (primary antibody, 1:10,000 dilution) and peroxidase-conjugated anti-rabbit goat IgG (secondary antibody, 1:20,000 dilution; KPL). A chemiluminescent reagent (Immobilon Western Chemiluminescent HRP Substrate, Millipore; Light-Capture, ATTO) was used for signal detection.

Purification of Recombinant Proteins and *In vitro* Attraction Assay

The coding sequences of the predicted mature peptides of CRP810_1.1 to _1.5 (AtLURE1.1 to 1.5) and AlCRP810_1.3 (AlLURE1.3) were amplified from the cDNA of the pistil or genomic DNA and were cloned into pET-28a(+) (Novagen) using the *Bam*HI site to fuse a His tag to the N-terminus. The mutated CRP810_1.5-Y84C sequence was generated by PCR using the primer CRP810_1.5 MP_F+BamHI and mismatched primer (5'-TTATTTAATATCACTAATACTGcAACGAC-3'), and a second round of PCR using the same primer pair as for CRP810_1.5. Note that although the full sequence of AlLURE1.3 contains a premature stop codon in the signal peptide, the mature AlLURE1.3 peptide shows just two amino acid differences compared to its closest paralog, AlLURE1.9, and was capable of attracting *A. lyrata* pollen tubes. These expression vectors were transformed into *E. coli* strain BL21-CodonPlus (Stratagene). The His-tagged peptides were expressed at 37°C for 5 h and purified by metal affinity chromatography with HisTrap FF (for CRP810_1.2, _1.3, _1.4, and AlCRP810_1.3; GE

Healthcare) or TALON Metal Affinity Resins (for CRP810_1.1, _1.5, and CRP810_1.5-Y84C; Clontech). TfLURE1 and -2 were prepared as described previously (Okuda et al., 2009). The subsequent procedures, namely, refolding of the peptides, preparation of the gelatin beads, and criteria for judgment of the attracted pollen tubes, generally followed the procedure described previously for TfLUREs (Okuda et al., 2009). The peptides were dialyzed (Spectra/Por3 MWCO:3500; Spectrum Laboratories) and refolded using a solution containing glutathione (reduced and oxidized forms; Wako Pure Chemical Industries) and L-arginine ethyl ester dihydrochloride (Sigma) for 4 days at 4°C. For the *in vitro* attraction assay using gelatin beads, 1 µl of purified peptide in buffer (50 mM Tris-HCl, pH 7.0) was mixed with 2 µl of 10% (w/v) gelatin (Nacalai Tesque) solution and 1 µl of 1 mM Alexa Fluor 488 or 568 conjugated with 10-kDa dextran (Invitrogen). Gelatin beads were formed by adding ~200 µl of hydrated silicone oil, vortexing, and cooling on ice. The gelatin beads were manipulated using the point of a glass needle and placed in front of the tip of a pollen tube under an inverted microscope (IX71, Olympus). In the assay, pollen tubes growing toward the beads with a >30º change were designated as “attracted” pollen tubes.

For the *in vitro* attraction assay, pollen tube growth medium (Palanivelu and Preuss, 2006; Hamamura et al., 2011) was used. A total of 120–150 µl of medium was poured into the well, which was made from silicone rubber with a 10 mm × 36 mm rectangular hole on a cover glass. A pistil emasculated 1 day before was hand-pollinated and cut off at the junction between the style and ovary using a 27-gauge needle. Next, the cut stigma with the style was placed on the medium; the cut edge of the style was at a right angle to the medium. The ovules were also placed on the side of the cut edge from which pollen tubes emerged through the style. After setting the style and ovules,

another cover glass was covered with silicone rubber to keep the medium from drying out during incubation. The style and ovules on the medium were incubated at 22°C in the dark until the pollen tube attraction assay was performed.

Generation of RNAi Constructs

The *CRP810_1.2* (*AtLURE1.2*) nucleotide sequence was used as a representative trigger for the inhibition of *CRP810_1* genes by RNAi since it shares >96% identity with *CRP810_1.3*, *1.4*, and *1.5*, and 89% identity with *CRP810_1.1*. Furthermore, it contains a common sequence of up to 33 bp with *CRP810_1.1* to *1.5*. Since RNAi can be mediated by RNAs 21 and 22 bp in length (Elbashir et al., 2001), the RNAi construct against *CRP810_1.2* was expected to target all *CRP810_1* genes. The RNAi construct was designed to express double-stranded RNA (dsRNA) under control of the synergid-specific *MYB98* promoter (Figure 15A). To generate inverted repeat sequences of *CRP810_1.2* coding sequence for the RNAi construct, nucleotides 72–1067 of the *GUS* coding sequence as a linker for the dsRNA, which was amplified with GoTaq DNA polymerase (Promega) using the primers GUSlinker_F (5'-TCGCGAAAACTGTGGAATTG-3') and GUSlinker_R (5'-CCGACAGCAGCAGTTTCATC-3'), was first cloned into pT7Blue T-vector (Novagen), resulting in the *GUS-linker* sequence. *CRP810_1.2* was also amplified using the primers *CRP810_1.2*_F+BamHI-SpeI (5'-cgcggatccactagtATGAAGTTGCCTATT-3') and *CRP810_1.2*_R+XbaI-EcoRI (5'-ccggaattctctagaTTATTTAATATCACT-3'). The amplified product was ligated into a flanking region of the *GUS-linker* sequence using *Spe*I and *Xba*I, and then ligated into another flanking region using *Bam*HI and *Eco*RI, resulting in *CRP810_1-RNAi*. The

MYB98 promoter, which specifically drives the RNAi sequence in synergid cells, was amplified using the primers pMYB98_TOPO_F (5'-caccGGTGAAGAGAGAGAGAGAGATTG-3') and pMYB98_R+EcoRI-SphI (5'-gcatgcgaattcTGTTTTGGAAAGGAG-3'), and introduced into pENTR/D-TOPO (Invitrogen). The *CRP810_1-RNAi* sequence and *GUS-linker* sequence were connected downstream of the *MYB98* promoter using *Eco*RI and *Sph*I. The *pMYB98:: CRP810_1-RNAi* and *pMYB98::GUS-linker* were transferred to the binary vector pGWB1 (Nakagawa et al., 2007a) using the LR recombination reaction (Invitrogen), resulting in the binary vectors pGWB1-*CRP810_1-RNAi* (RNAi) and pGWB1-*GUS-linker* (vector control). These constructs were transformed into wild-type *A. thaliana* plants by the floral dip method. Transformed plants were selected with 50 mg/l hygromycin B (Wako Pure Chemical Industries).

Analysis of Pollen Tube Guidance of the RNAi Plants in the Pistil and on Medium

For the analysis of pollen tube guidance in the pistil, the carpel walls were removed from the pistil about 1 day after flowering using a 27-gauge needle, and the resulting ovules and septum were stained with 0.1% aniline blue in 0.1 M K_3PO_4 without fixation. To evaluate abnormal pollen tube guidance around the micropyle, the number of ovules was counted only when the pollen tube(s) was observable from the funiculus to the ovule in the prepared slide. Otherwise, the ovule was designated ND. Because a pollen tube was observed at almost all funiculi in the RNAi pistil and wild type, this criterion for the count appeared to have no bias. Defects in micropylar pollen tube guidance were classified into two groups. A class I abnormality was defined as one or more "wandering" pollen tubes with ultimate entry of the tube into the micropyle. A

class II abnormality was defined as no pollen tubes entering the micropyle after growing up to the funiculus. “Wandering” was defined as a pollen tube that took a 180º turn back on the funiculus or grew on the surface of the ovule.

For competition analysis of pollen tube guidance on medium, two ovules (e.g., a wild-type ovule and an RNAi ovule) were arranged with their micropylar openings close together under a stereomicroscope. After incubation at 22°C in the dark, the pollen tube first reaching the space between the two ovules was carefully observed. Next, the pollen tube was observed until either ovule attracted it to the micropyle. If neither ovule attracted it, that trial was designated as not determined (ND).

Sequence Determination of *AtLURE1.1* to *1.6* in Various Accessions

In 12 accessions of *A. thaliana* (Cvi-0, Est-1, Mr-0, Tsu-1, Nok-3, Fei-0, Ts-1, Pro-0, Kondara, Ms-0, Bur-0, and Ws-2), the genomic sequences of *AtLURE1.1* to *1.6* were investigated by PCR and direct sequencing using the Sanger method. These 12 accessions were picked out according to the genetic relationships among 95 accessions (Aranzana et al., 2005). They were likely to be distributed throughout the genetic relationships.

The coding regions of the genomic sequences were determined. First, PCR to amplify the coding region was performed using genomic DNA from each accession. The primers were designed using SNPs from the *AtLURE1.1* to *1.6* sequences in Col-0. Second, nested PCR was performed for *AtLURE1.1* to *1.6*. Primary PCR primers were designed for the sequences of a flanking gene or intergenic region. Secondary PCR primers were designed to amplify all of the *AtLURE1* genes in Col-0. The products were subsequently sequenced. If multiple peaks were detected, the sequence could not be

determined. Sequencing after cloning was avoided because the nucleotides, especially in the heteroduplex DNA, may have been modified by *E. coli*.

Pollen Tube Attraction by *Torenia fournieri* Ovules Expressing *AtLURE1.2*

To generate the construct for *T. fournieri* expressing *AtLURE1.2* (Figure 25A), the *AtLURE1.2* genomic sequence (including the 3′ untranslated region) and the *GFP* sequence were connected to the downstream region of the *TfLURE2* promoter (Figure 24B), as identified by thermal asymmetric interlaced (TAIL)-PCR. The two sequences were ligated and then introduced into the binary vector pPZP211 (Hajdukiewicz et al., 1994). The construct was transformed into selfed generations of *T. fournieri* cv. 'blue and white.' Transformed T_1 heterozygous plants were used for the interspecific pollen tube attraction assay. In the assay, *A. thaliana* pollen tubes grown through a cut style were incubated for 4–5 h on growth medium for *T. fournieri* (Okuda et al., 2009) using the well described in the *in vitro* attraction assay of *Arabidopsis*, and then hydrated silicone oil was poured into the well. Ovules from transformed *T. fournieri* were dissected in the hydrated silicone oil and manipulated using a glass needle under an inverted microscope (IX71, Olympus). For confocal imaging, an LSM 780 NLO (Zeiss) system was used.

Accession Numbers

The accession numbers of the *CRP810* genes are as follows: *CRP810_1.1* (At5g43285), *_1.2* (At5g43510), *_1.3* (At5g43513), *_1.4* (At5g43518), *_1.5* (At5g43525), *_1.6* (At5g43516, a pseudogene), *CRP810_2.1* (*At5g48515*), *_2.2* (*At5g48595*), *_2.3* (*At5g48605*), *_3.1* (*At4g08869*), *_3.2* (*At4g08875*), *_4* (*At5g50423*), *_5* (*At5g18403*), *_6*

(*At5g18407*), _7 (*At5g60805*), and _8 (*At4g08485*).

Primer Sequences

The sequences of the additional primers used in this study are available at http://www.plosbiology.org/article/fetchSingleRepresentation.action?uri=info:doi/10.1371/journal.pbio.1001449.s014

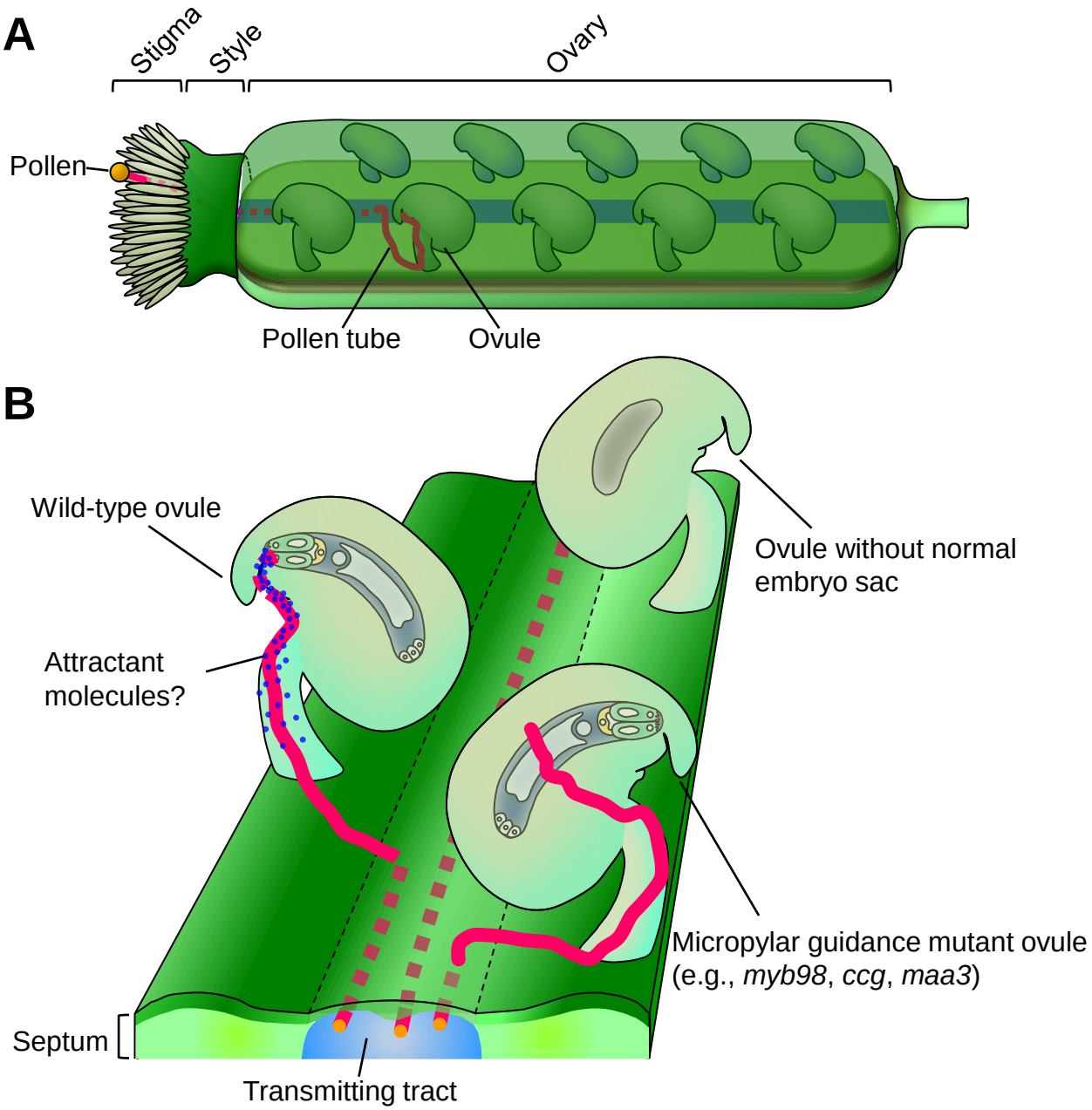

Figure 1. Schematic representations of pollen tube guidance in the pistil of *Arabidopsis thaliana*

(A) Guidance from the stigma to the ovule. A pollen tube (red solid and dashed line) germinated from a pollen grain penetrates the stigma cell and the style, and enters the transmitting tract (shown as blue region) within the ovary. The pollen tube emerges from the transmitting tract and grows to the ovule.

(B) Close-up from the transmitting tract to the embryo sac. Ovules are aligned on the septum (parietal placentas). Pollen tubes (shown as red dashed lines) grow straight into the transmitting tract. A pollen tube emerges on the surface of the septum, targets a wild-type ovule, and consequently reaches the synergid cell without deviation, probably related to a predicted attractant molecule(s). Another pollen tube also targets a micropylar guidance mutant ovule, but does not enter the micropyle and wanders on the surface of the ovule despite arriving at the funiculus. No pollen tube grows to an ovule without a normal embryo sac.

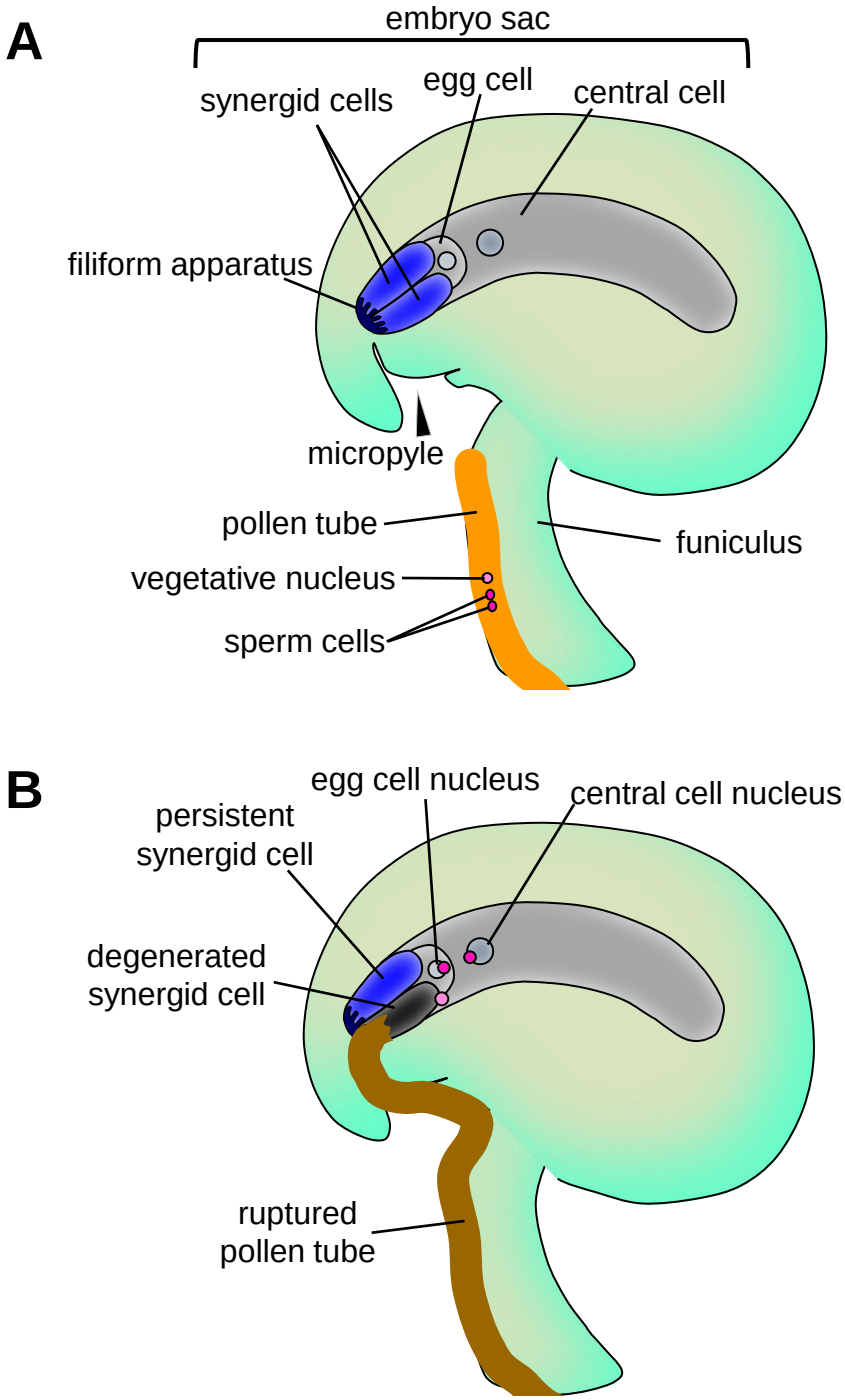

Figure 2. Schematic representations of pollen tube attraction toward the embryo sac and reception in the synergid cell of *A. thaliana*

(A) Pollen tube attraction from the funiculus to the embryo sac through the micropyle. The pollen tube on the funiculus is attracted by putative attractant(s) secreted from the two synergid cells.

(B) Pollen tube reception and rupture to release the two sperm cells to the egg and central cells. The pollen tube reaching the embryo sac is received by one of the two synergid cells. After the reception, degeneration of the synergid cell and rupture of the pollen tube occur to release pollen tube contents including the two sperm cells. One of the sperm cells fertilizes with the egg cell and the other one with the central cell.

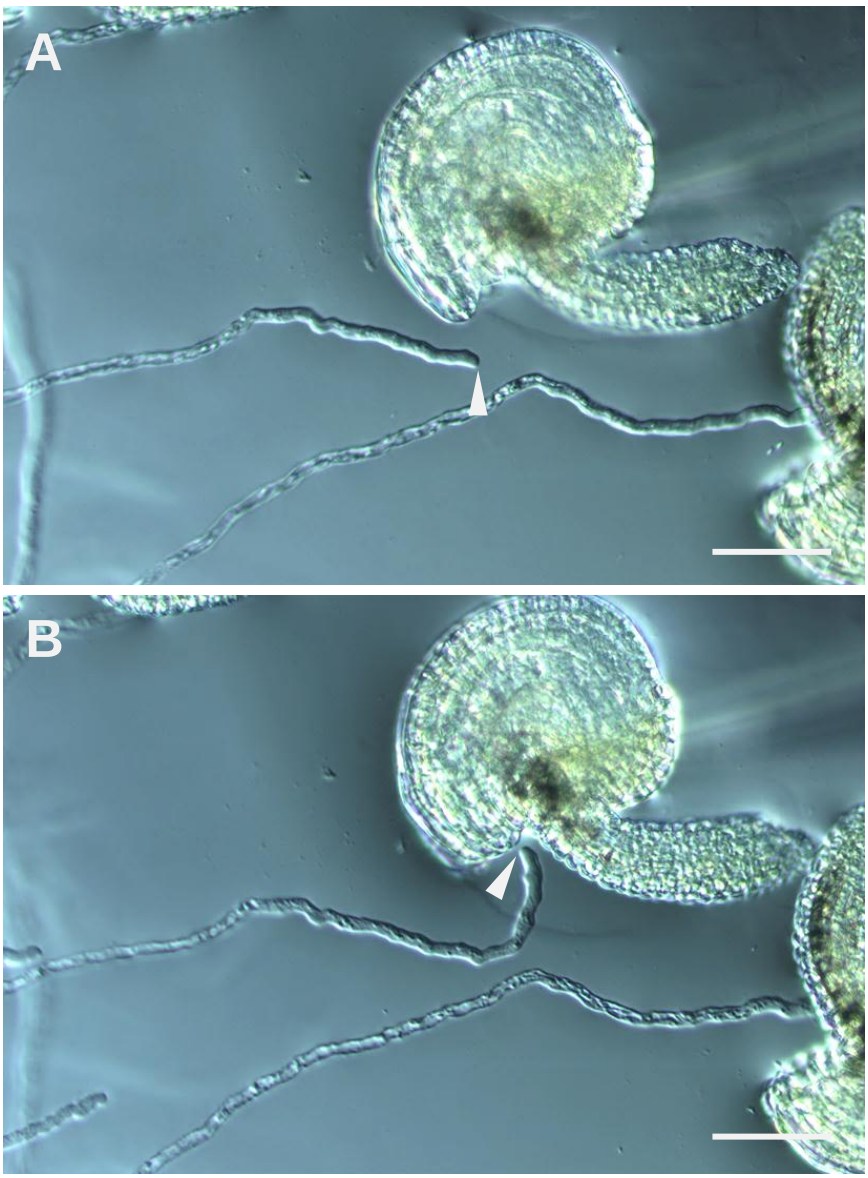

Figure 3. Pollen tube attraction to the micropyle of the *A. thaliana* ovule in an *in vitro* system.
(A) An isolated ovule was manipulated with a glass needle and was placed near the tip of a pollen tube, with micropylar end close to it. (B) Approximately 20 minutes after manipulation, the pollen tube turned toward the micropyle, indicating that some attractant signals are diffused from the micropyle of the ovule. Scale bars, 50 μm. Arrowheads indicate the position of the tip of the pollen tube.

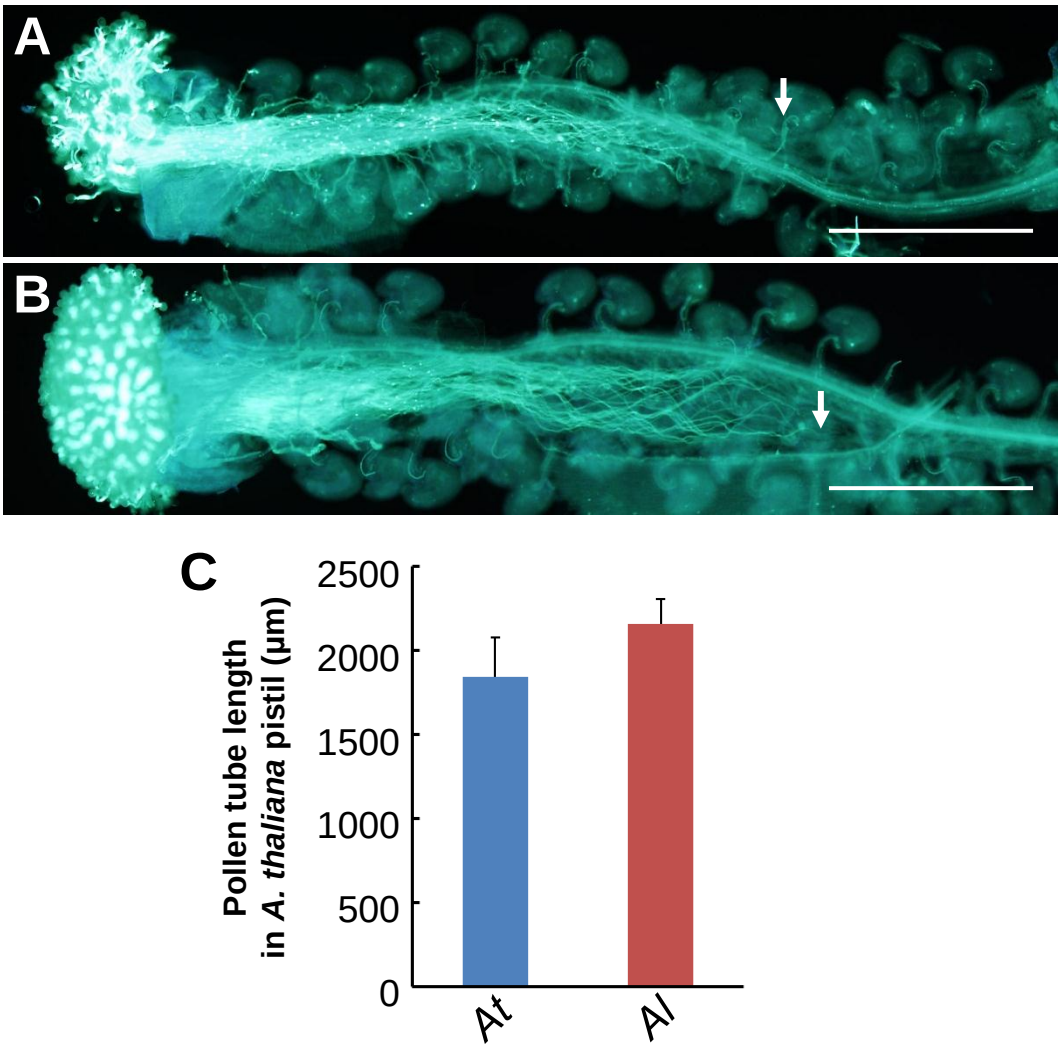

Figure 4. Pollen tube growth of *A. thaliana* and *A. lyrata* in *A. thaliana* pistils.
(A and B) Pollen tube growth inside the *A. thaliana* pistils. Pollen tubes of *A. thaliana* (A) and *A. lyrata* (B) were stained with aniline blue solution 6 hours after pollination. Bundle of pollen tubes between the upper and lower ovules are thought to be pollen tubes that grow in transmitting tract from stigma side (left) to basal side (right). Arrows indicate the positions of the tip of the longest pollen tubes. Scale bars, 500 µm.
(C) The length of the longest pollen tube inside the *A. thaliana* pistils 6 hours after pollination. The length was measured from the stigma end to the tip of the longest pollen tube. The data are the means and standard deviations per silique for *A. thaliana* (*At*, blue bar) and *A. lyrata* (*Al*, red bar) pollen tubes.

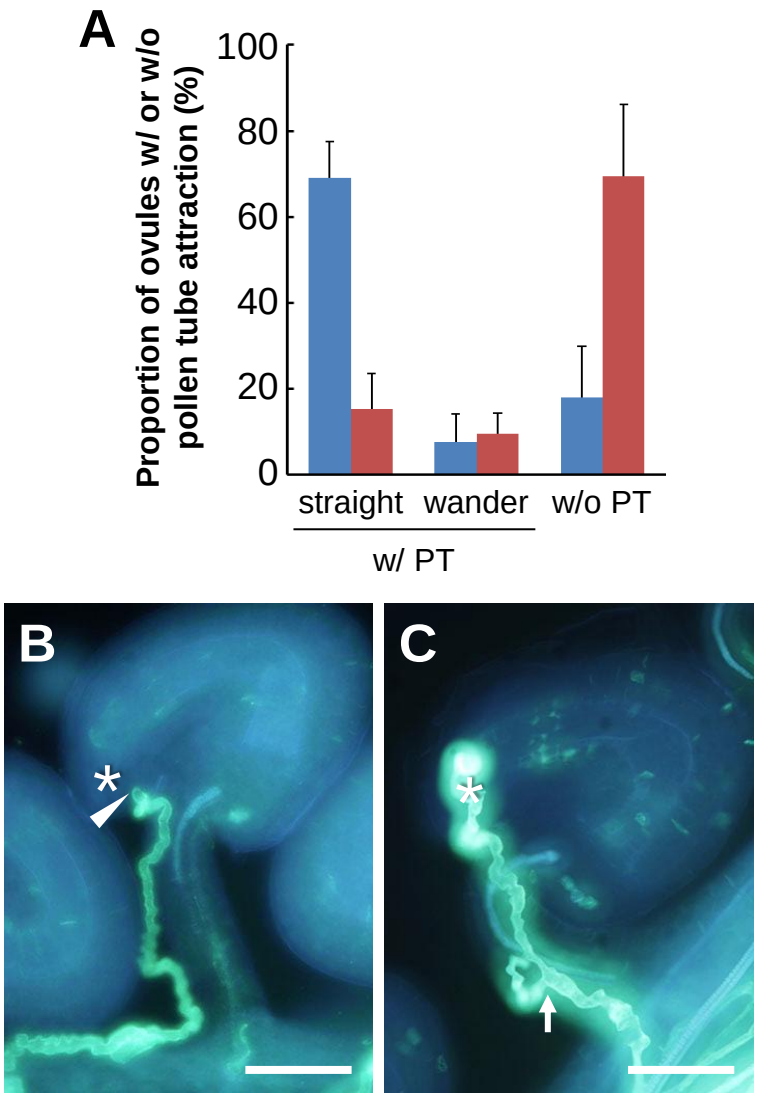

Figure 5. Interspecific incompatibility in pollen tube attraction toward ovules in *A. thaliana* pistils.

(A) The proportion of *A. thaliana* ovules associated with or without *A. thaliana* (blue bars) or *A. lyrata* (red bars) pollen tubes in the *A. thaliana* pistils 12 hours after pollination. Ovules that attract pollen tubes toward their micropyle (w/ PT) are classified into two groups by pollen tube growth on the funiculus: straight growth toward the micropyle (straight) and wandering growth with 180º turning back (wander). The data are the means and standard deviations per silique.

(B and C) Abnormal growths of *A. lyrata* pollen tubes on the *A. thaliana* funiculus. These pollen tubes were classified into "straight" in (A), but showed the abnormal growths despite attraction toward the micropyle (asterisks). (B) An arrowhead indicates the tip of a pollen tube that arrested its growth around the micropyle. (C) An arrow indicates branching of a pollen tube on the funiculus. Scale bars, 50 µm.

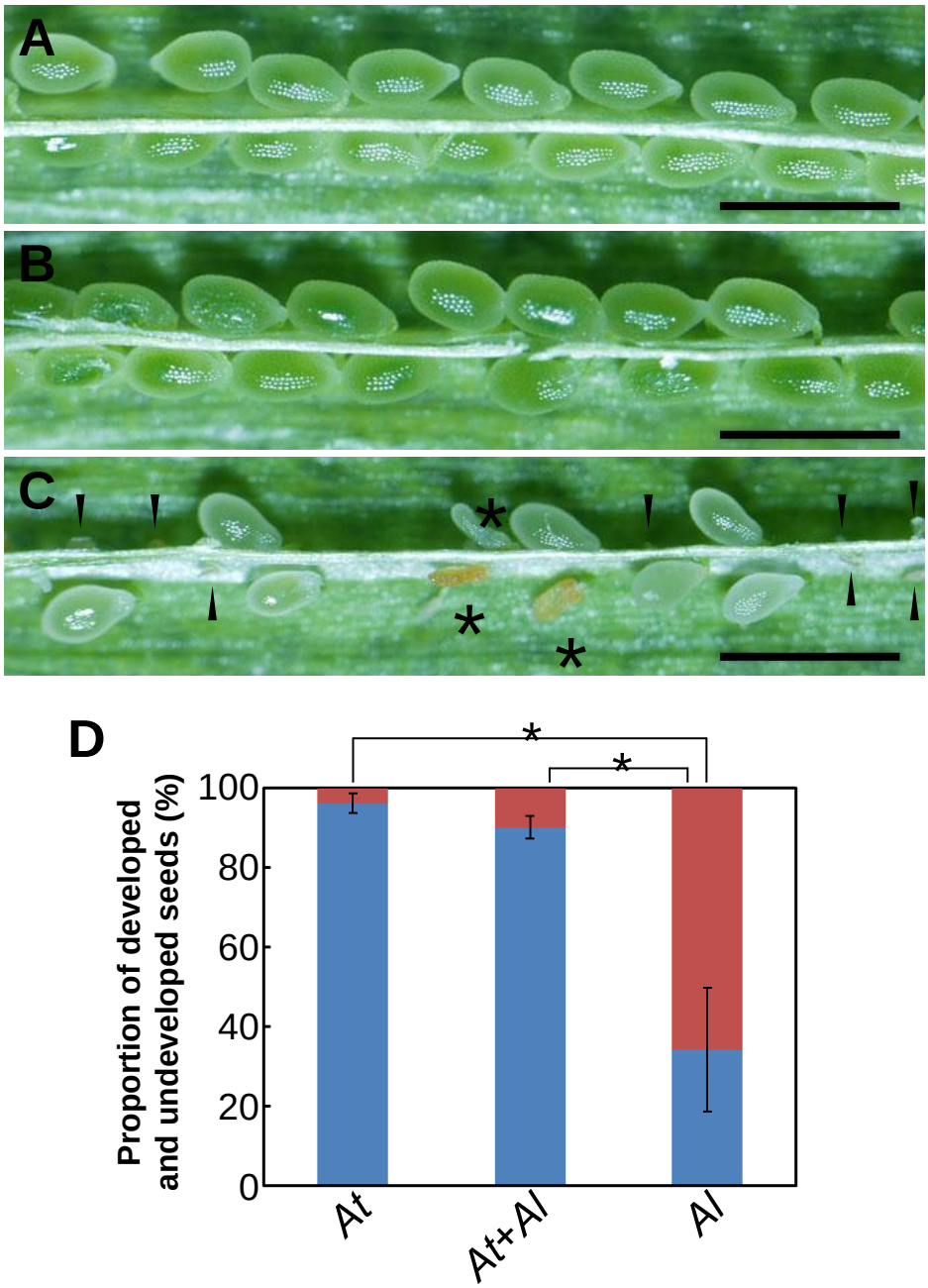

Figure 6. Self-, cross-, and double-pollination to *A. thaliana* pistils.
(A-C) Developed and undeveloped seeds inside siliques 7 days after pollination. The siliques had almost full seed set by pollination with pollen from *A. thaliana* (A) and *A. thaliana* and *A. lyrata* simultaneously (B) or decreased seed set by pollination with pollen from *A. lyrata* (C). Arrowheads indicate undeveloped ovules. Asterisks mark aborted seeds probably due to conflicts between female factors from *A. thaliana* and male factors from *A. lyrata*. Note that developing seeds observed in (C) are smaller than that in (A) and (B). Scale bars, 1 mm.
(D) The proportion of developed and undeveloped seeds by pollination with pollen from *A. thaliana* (*At*) and *A. thaliana* and *A. lyrata* simultaneously (*At+Al*), and *A. lyrata* (*Al*). Blue and red regions indicate the proportion of developed and undeveloped seeds, respectively. The error bars represent standard deviations of proportions per silique. Asterisks indicate significant differences (Student's *t*-test; $P < 0.01$).

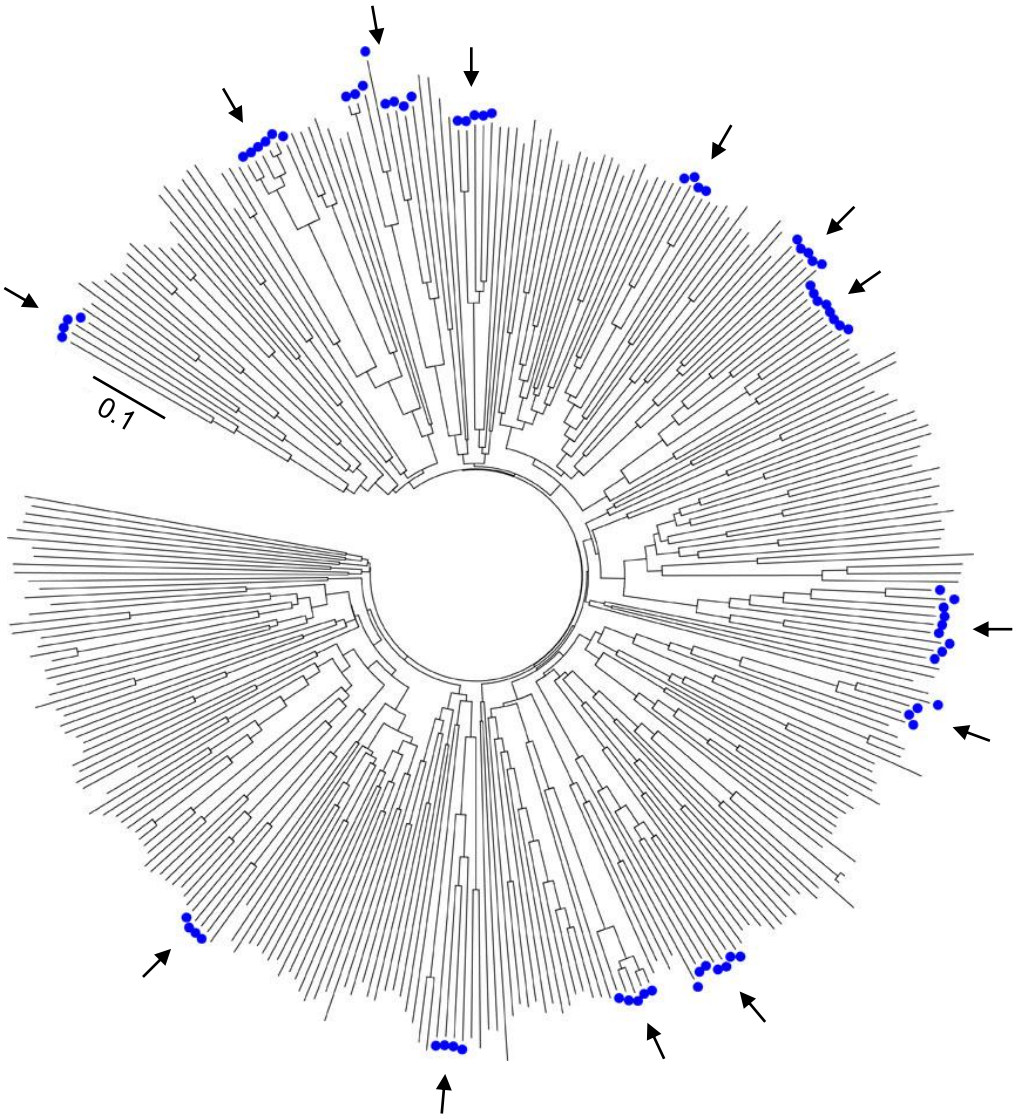

Figure 7. A phylogenetic tree of 317 DEFL peptides of *A. thaliana*.
The phylogenetic tree was constructed using putative full-length amino acid sequences of 317 DEFL peptides of *A. thaliana* (Silverstein, et al., 2005) by the neighbor-joining method. Blue filled circles mark paralogous DEFL peptides consisting of four or more sequences supported by high bootstrap values (≥ 90%). Arrows indicate 13 groups of the paralogous DEFL peptides. The scale shows the number of substitutions per site.

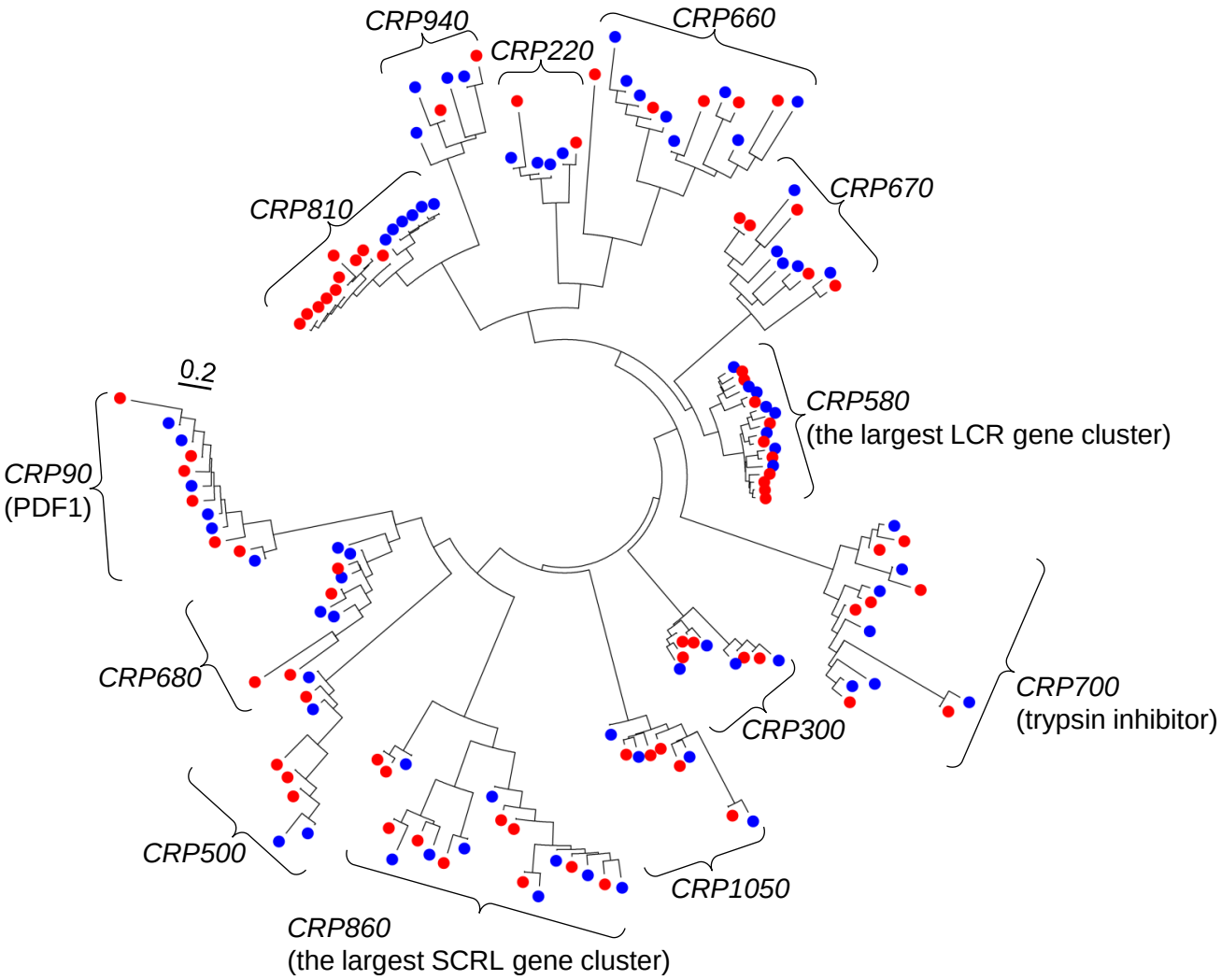

Figure 8. A phylogenetic tree of paralogous *DEFL* genes of *A. thaliana* and a close relative *A. lyrata*.

The tree includes 13 subtrees, which belong to 13 *CRP* subgroups. Each subtree contains four or more paralogous *DEFL* genes of *A. thaliana* (blue filled circle) and their orthologs from *A. lyrata* (red filled circle). The scale shows the number of substitutions per site. The *CRP90* subtree contains *AtPDF1* genes (Thomma et al., 2002). The *CRP700* subtree contains *A. thaliana* trypsin inhibitor (*ATTI*) genes (Clauss and Mitchell-Olds, 2004). The *CRP580* and *CRP860* subtrees contain genes that form the largest gene cluster of *LCR* (low molecular weight, cysteine-rich) and *SCRL* (*SCR*-like), respectively (Vanoosthuyse et al., 2001). The *CRP810* subtree branched into *A. thaliana* and *A. lyrata* gene clusters.

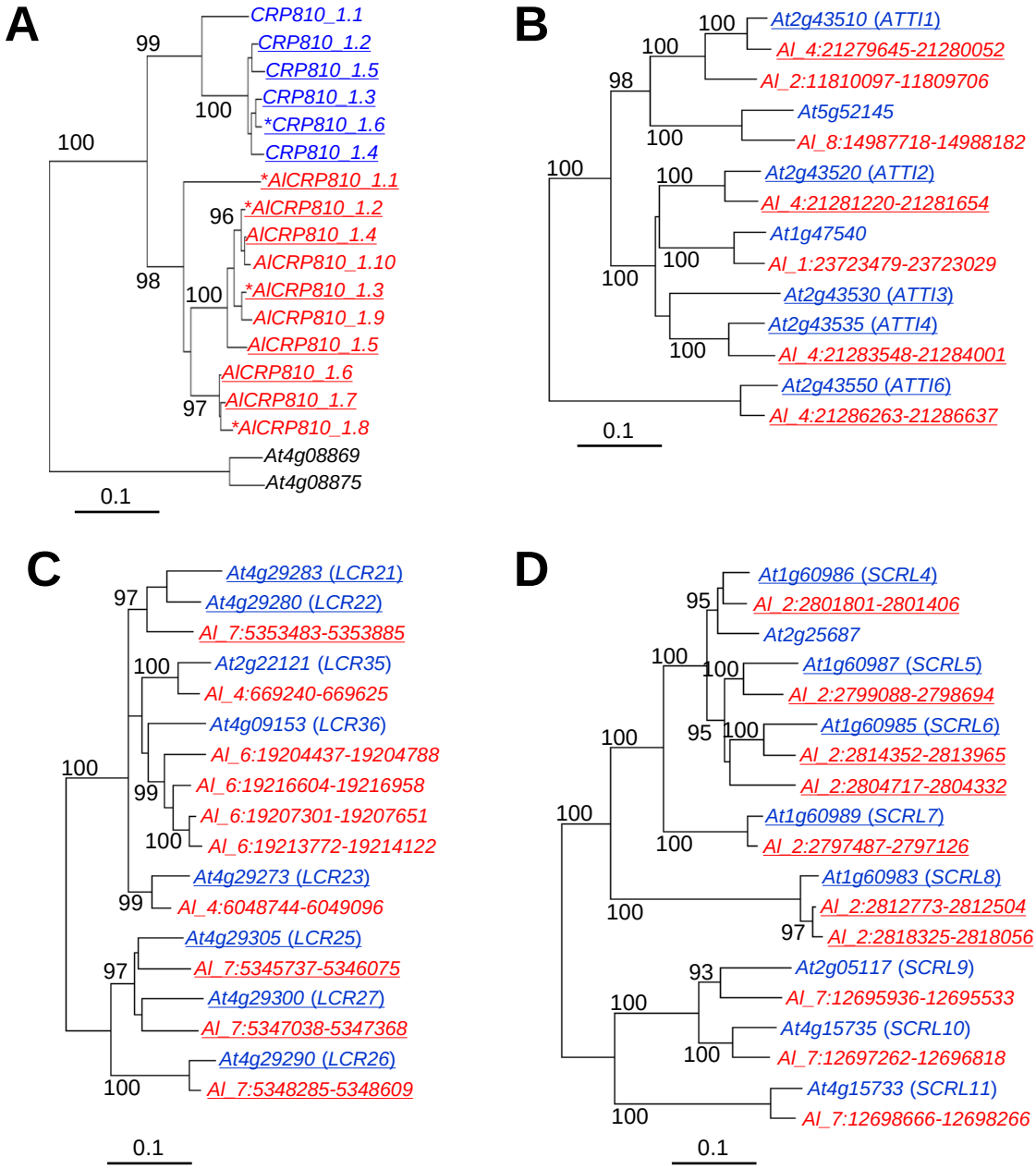

Figure 9. Phylogenetic trees of paralogous *DEFL* genes clustered in the *A. thaliana* genome and their orthologous genes in *A. lyrata*.

Phylogenetic trees of the *CRP810_1* genes (A), *CRP700* genes (*A. thaliana* trypsin inhibitor, *ATTI*) (B), *CRP580* genes (low molecular weight, cysteine-rich, *LCR*) (C), and *CRP860* genes (*SCR*-like, *SCRL*) (D), and their orthologous genes in *A. lyrata*, based on the coding region of their genomic sequences. The tree of the *CRP810_1* genes includes *At4g08869* and *At4g08875* (the closest related genes to *CRP810_1* genes) as the outgroup. The trees of *CRP700*, *CRP580*, and *CRP860* are representative clusters that contain tandemly-arrayed genes in the genome. The genes with asterisks are probably nonfunctional. Only bootstrap values ≥ 90 are indicated. The scale shows the number of substitutions per site. *A. thaliana* genes are shown in blue while *A. lyrata* genes are shown in red. The underlined genes are tandemly arrayed genes in the genome and syntenic genes shown in Figure 10.

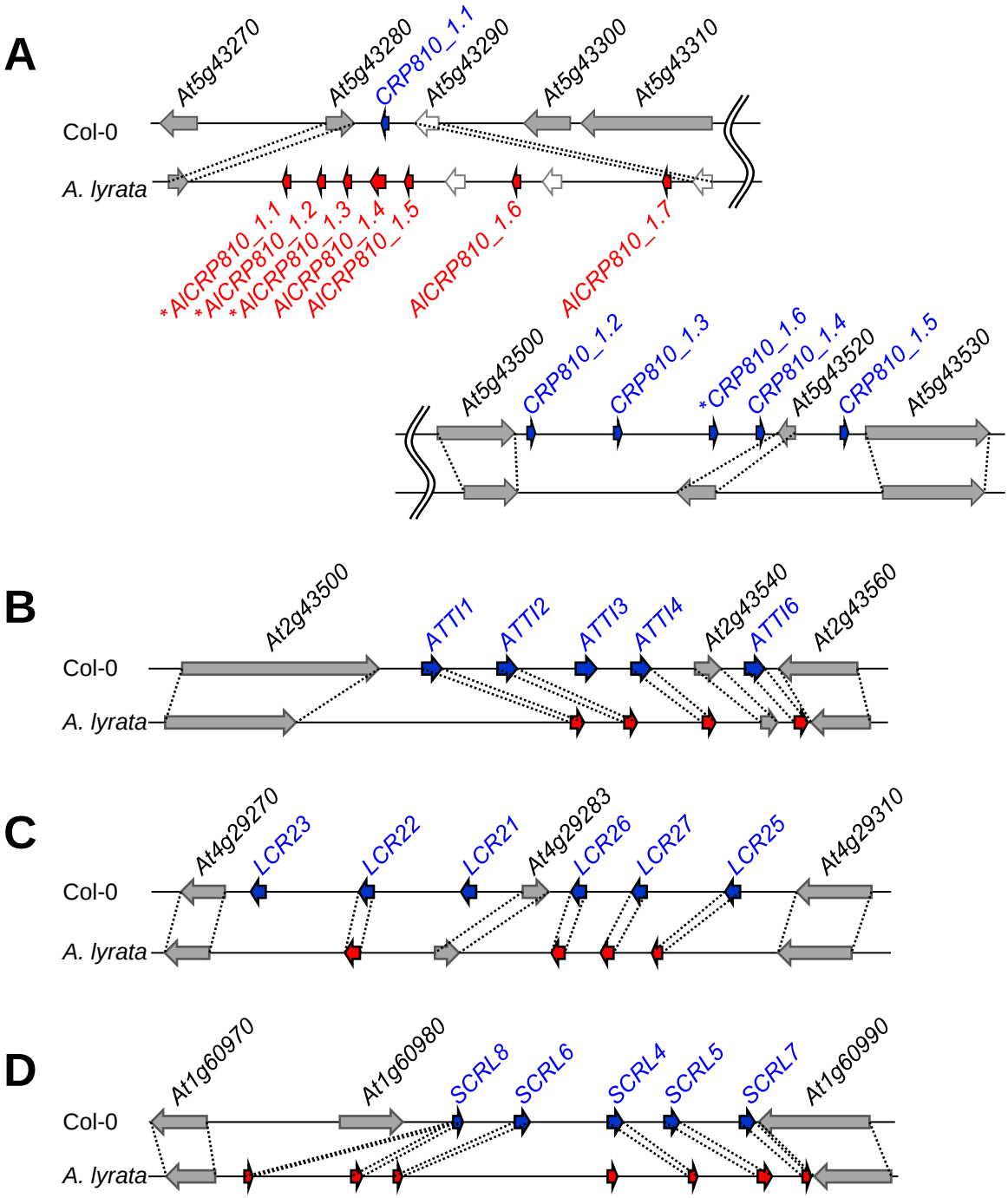

Figure 10. Synteny analysis of paralogous *DEFL* genes clustered in the *A. thaliana* genome and their orthologous genes in *A. lyrata*.
Schematic representations of syntenic regions containing *CRP810_1* genes (A), *ATTI* genes (B), *LCR* genes (C), and *SCRL* genes (D) in the *A. thaliana* (Col-0) and *A. lyrata* genomes. Blue, red, and gray arrows represent the loci of the *A. thaliana* (Col-0) genes, their syntenic genes in *A. lyrata*, and unrelated genes, respectively. Dashed lines indicate syntenic genes between *A. thaliana* and *A. lyrata*. The genes with asterisks are probably nonfunctional.

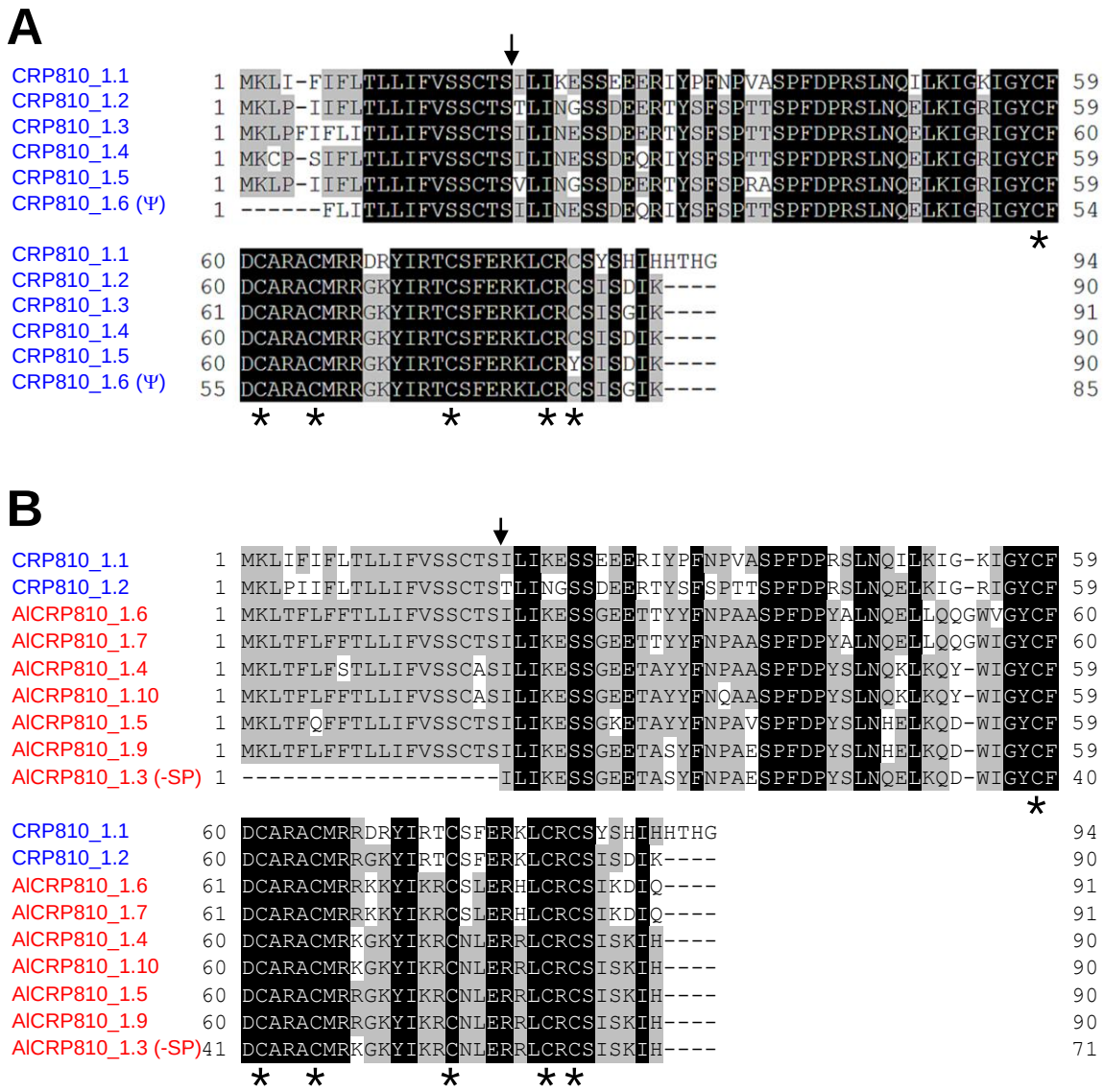

Figure 11. Multiple alignments of CRP810_1 peptides of *A. thaliana* and comparison with AlCRP810_1 peptides of *A. lyrata*.

Multiple alignments of the full-length amino acid sequences of CRP810_1.1 to _1.5 and CRP810_1.6 (Ψ) (A), and CRP810_1.1, _1.2 peptides, their orthologs in *A. lyrata* (AlCRP810_1), and an assumptive sequence of mature peptide of AlCRP810_1.3 following the putative cleavage site (B). Black and gray backgrounds indicate amino acids conserved among six and three or more sequences (A) and nine and five or more sequences (B), respectively. The arrow indicates the position of the predicted cleavage sites. Asterisks mark conserved cysteine residues.

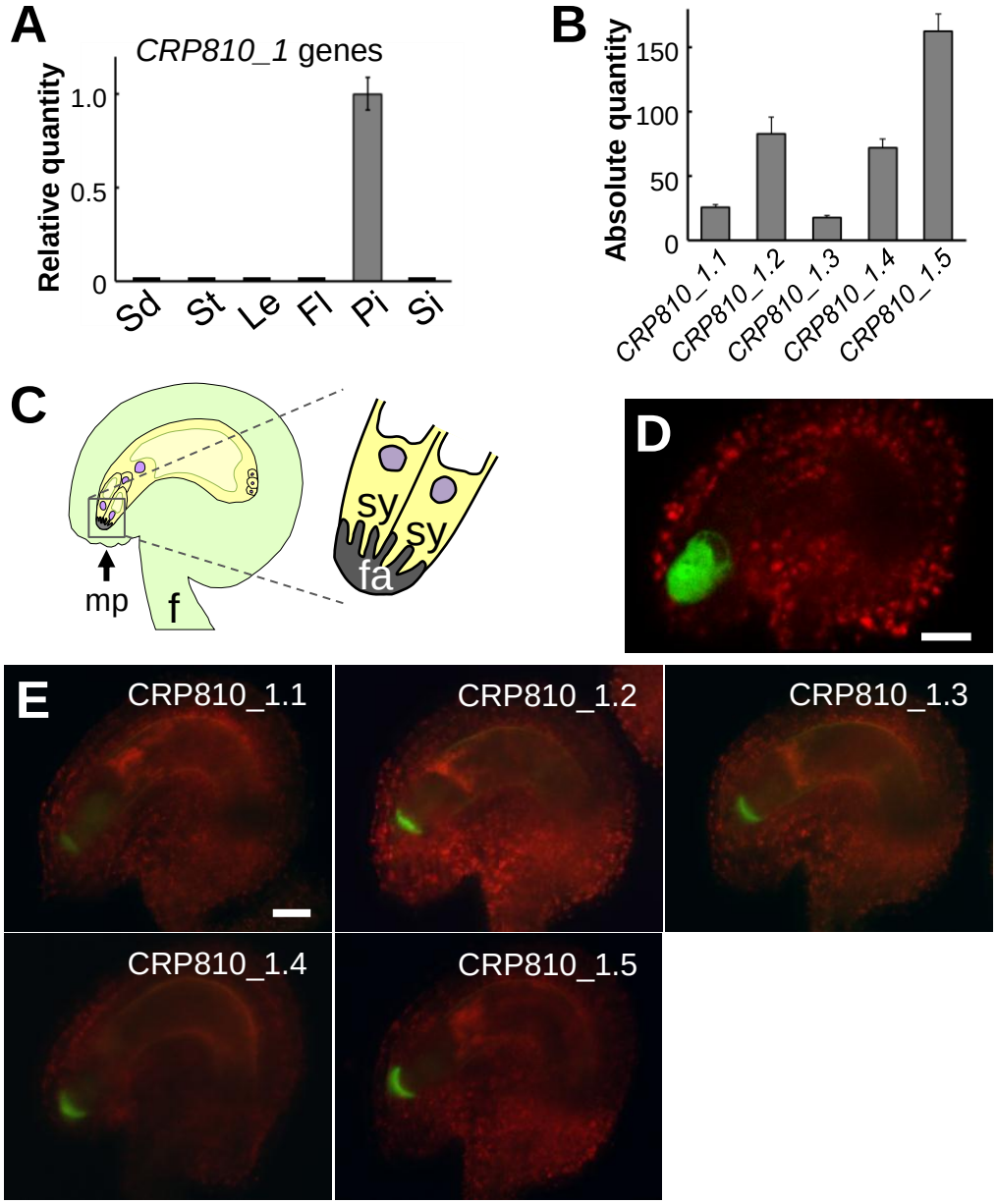

Figure 12. Expression pattern and localization of CRP810_1 peptides.
(A) Real-time qRT-PCR analysis of *CRP810_1* genes (*CRP810_1.1* to *_1.6*) in seedlings 10 days after germination (Sd), stems (St), leaves (Le), open flowers without the pistil (Fl), pistils (Pi), and siliques 2 days after pollination (Si). Relative quantities are expression levels relative to that in the pistil. Each expression level was normalized to that of *ACT2*. The data are the means and standard errors of three independent samples.
(B) Absolute gene expression levels of *CRP810_1* genes. Absolute quantity represents the copy number of cDNA per that of *MYB98* cDNA. The means and standard deviations of three independent experiments are shown.
(C) Schematic representation of the ovule (left) and part of the synergid cell (sy) (right) in *A. thaliana*. The filiform apparatus (fa) is formed by the thickened cell walls of the synergid cells. f, funiculus; mp, micropyle.
(D) Confocal laser scanning microscopic (CLSM) image of a *pCRP810_1.2::GFP* ovule. Scale bar, 20 µm.
(E) Fluorescence microscopic images of *pCRP810_1::CRP810_1-GFP* ovules. Scale bar, 20 µm.

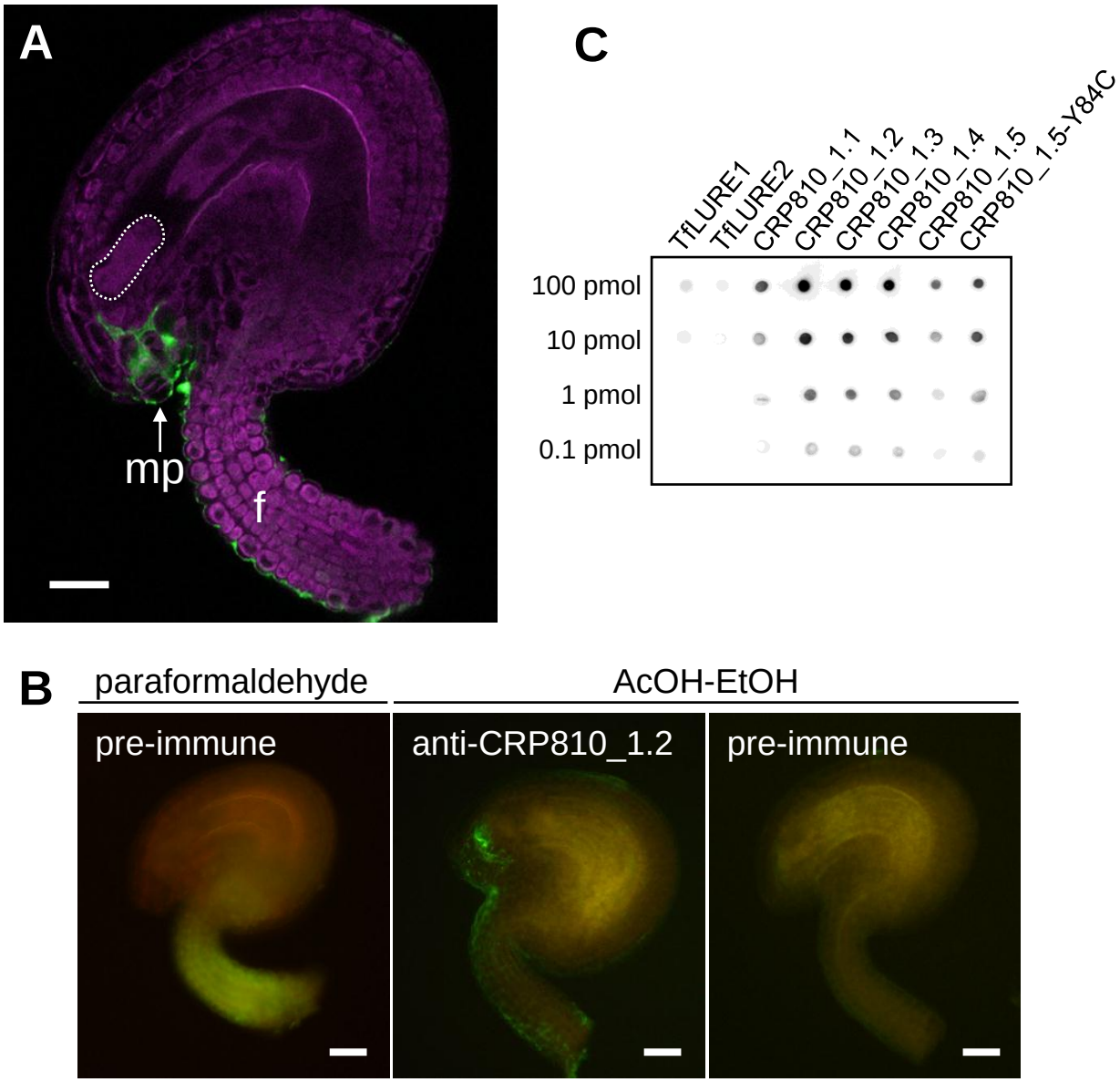

Figure 13. Localization of endogenous secreted CRP810_1 peptides .

(A) A CLSM image of an ovule after immunostaining with anti-CRP810_1.2 antibodies. Green Alexa Fluor fluorescence (for CRP810_1 peptides) was observed at the micropyle and funicular surface. Magenta indicates autofluorescence of the ovule. The synergid cell is delineated by the dashed line. Scale bar, 20 μm.

(B) Fluorescence microscopic images of immunostained ovules using anti-CRP810_1.2 antibodies and pre-immune IgG as a negative control. In the immunostained ovule fixed in a 9:1 mixture of ethanol:acetic acid (AcOH–EtOH), Green Alexa Fluor fluorescence was observed in a similar way to the ovule fixed in paraformaldehyde (A). Pre-immune IgG was not bound to the micropylar opening of the ovule when the ovule was fixed in AcOH–EtOH or paraformaldehyde. Scale bar, 50 μm.

(C) Immuno-dot blot analysis confirming the recognition capability of the anti-CRP810_1.2 antibody. The total amount of blotted peptide is shown on the left. All His-tagged CRP810_1 peptides were detected in a concentration-dependent manner, while His-tagged TfLURE1 and 2 as controls were barely detected. Among the CRP810_1 peptides, the signals for CRP810_1.1, which showed lower identity to CRP810_1.2, and CRP810_1.5, which lacked a single conserved cysteine, are comparatively weak.

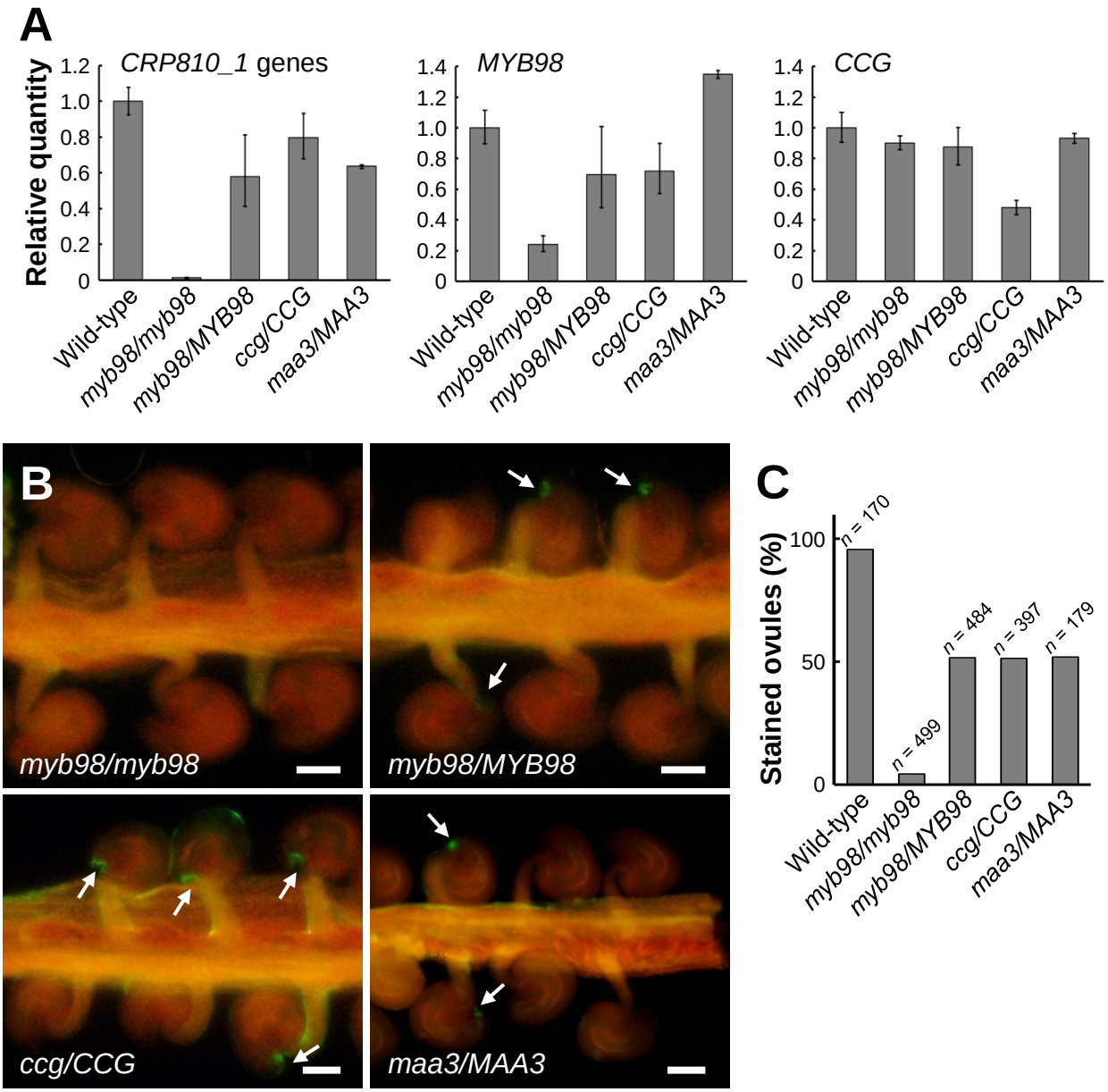

Figure 14. Expression of *CRP810_1* genes and secretion of CRP810_1 peptides in the female gametophytic mutants.

(A) qRT-PCR analysis of the female gametophytic mutants, *myb98*/*myb98*, *myb98*/*MYB98*, *ccg*/*CCG*, and *maa3*/*MAA3*. The expression levels of the *AtLURE1* genes, *MYB98*, and *CCG* are represented as relative quantities to wild type. Each expression level was normalized to that of *ACT2*. The data are the means and standard errors of three independent experiments. *MYB98* mRNA was detected even in *myb98*/*myb98*, consistent with data showing that the *myb98*/*myb98* mutant expresses truncated *MYB98* mRNA (Kasahara et al., unpublished data).

(B) Immunostaining with anti-CRP810_1.2 antibodies for the mutants. Representative fluorescence microscopic images of ovules on the septum are shown. Arrows indicate fluorescence around the micropylar end of the ovules. Scale bars, 50 μm.

(C) The rate of immunostained ovules to the total number (*n*) of ovules in the wild type and mutants.

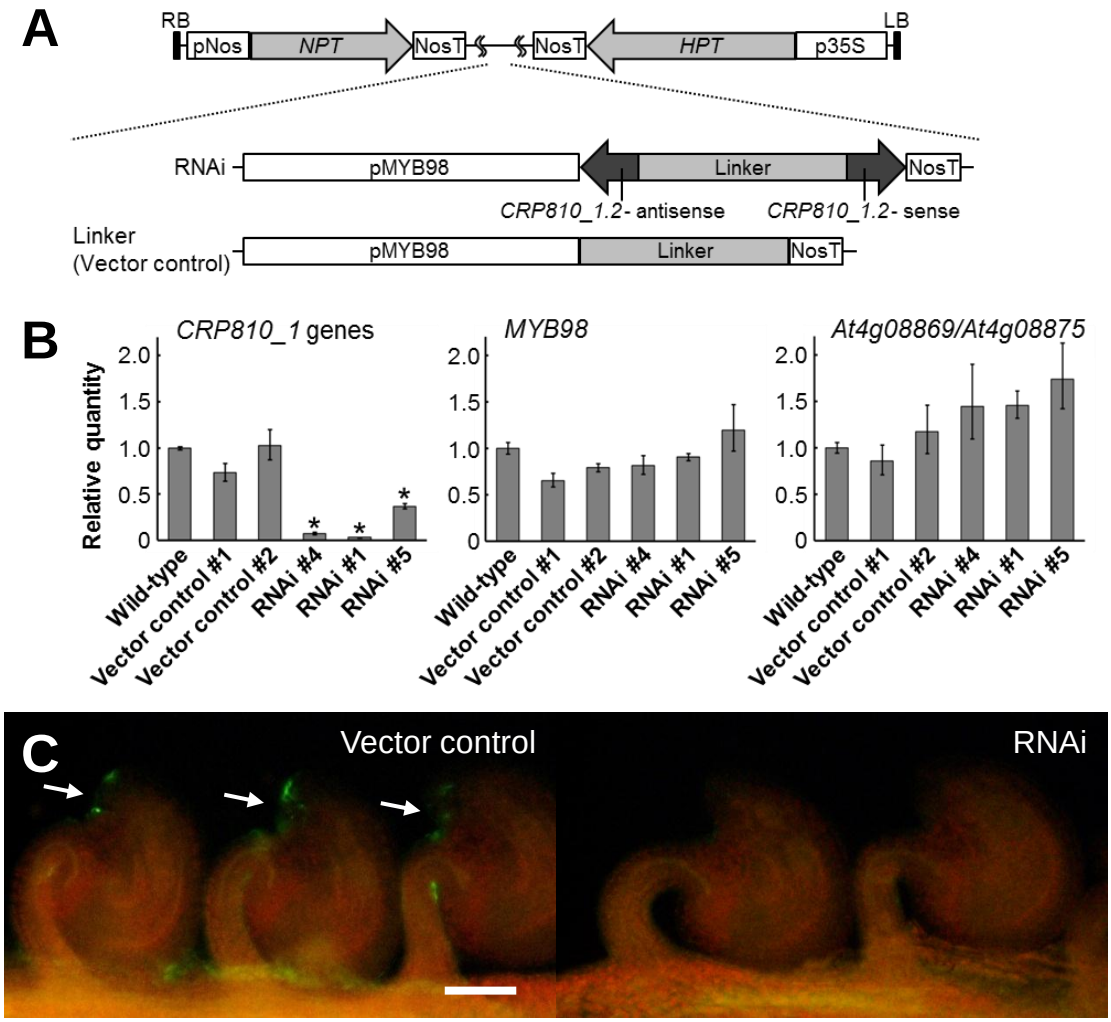

Figure 15. Simultaneous knockdown of *CRP810_1* genes by RNAi.
(A) Schematic representation of the RNAi constructs. The graphics represent the T-DNA region between the right (RB) and left (LB) borders (upper), the structures of *CRP810_1*-RNAi (RNAi, middle), and the linker (vector control, lower), respectively. The *MYB98* promoter (pMYB98) was used to drive the RNAi sequence in the synergid cells. *NPT*, neomycin phosphotransferase; *HPT*, hygromycin phosphotransferase; pNos, *nopaline synthase* promoter; NosT, *nopaline synthase* terminator; p35S, cauliflower mosaic virus (CaMV) *35S* promoter.
(B) Real-time qRT-PCR analysis of *CRP810_1*, *MYB98*, and *At4g08869/At4g08875* in the pistils of the RNAi and vector control lines. Synergid-specific *MYB98* and the closest *CRP810* genes (*At4g08869* and *At4g08875*) were used to confirm the specific downregulation of the *CRP810_1* genes. The relative quantities are the expression levels relative to that in the wild type. Two independent vector control lines and three independent RNAi lines were thought to be homozygous T_3 lines. Each expression level was normalized to that of *ACT2*. The data are the means and standard errors of three sibling plants. Asterisks indicate significant differences compared with the wild type according to Dunnett's test ($P < 0.05$) by ANOVA.
(C) Representative fluorescence microscopic image of immunostained ovules on the septum with anti-CRP810_1.2 antibodies for the vector control and RNAi line. Arrows indicate fluorescence around the micropylar end of the ovules. Scale bar, 50 μm.

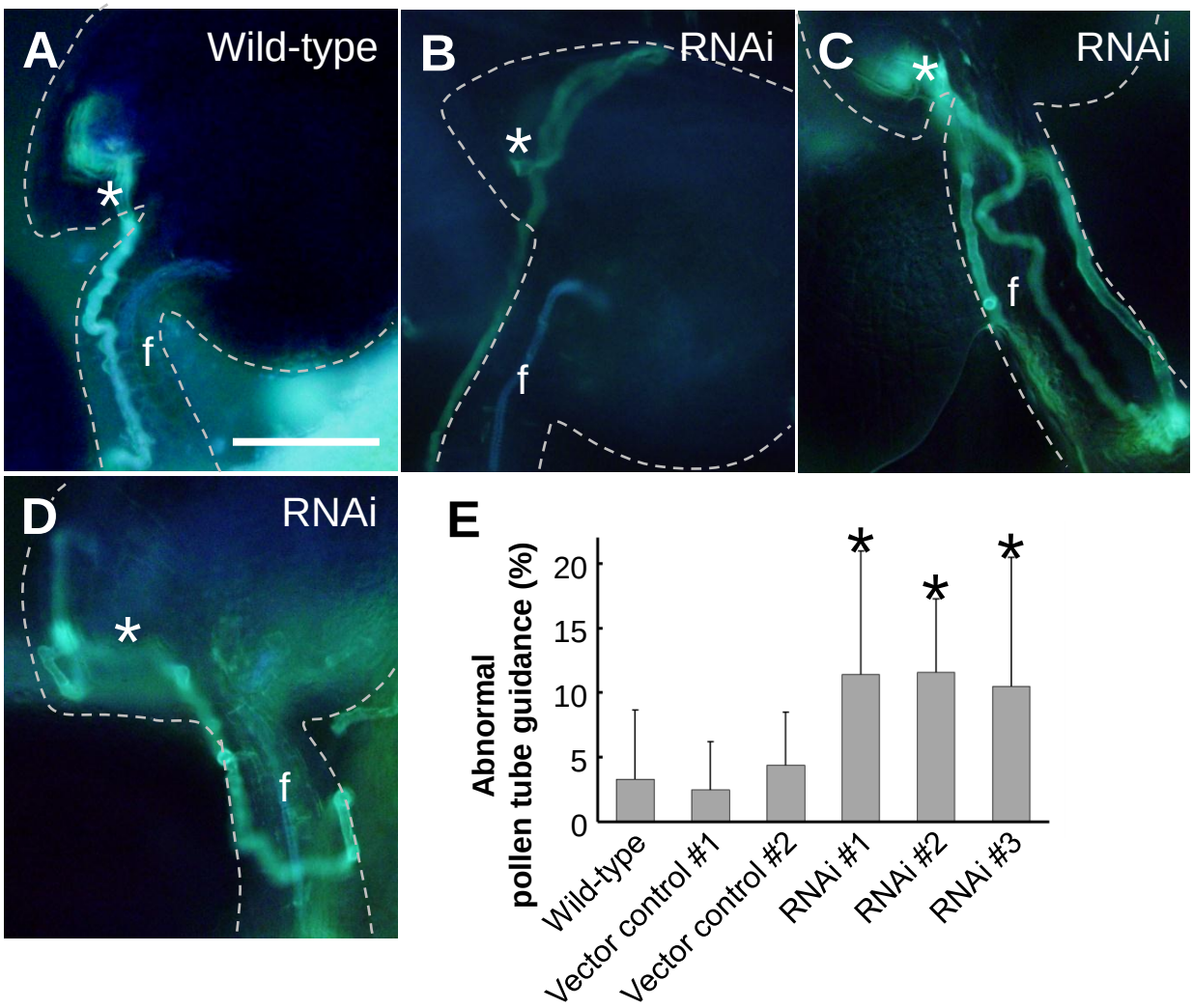

Figure 16. Knockdown analyses of the defects in micropylar guidance *in vivo*.
(A-D) Aniline blue staining for pollen tubes inside the pistil. Asterisks indicate the micropylar opening. The ovule is delineated by the dashed line. f, funiculus. (A) The pollen tube was attracted normally to the wild-type ovule. (B) The pollen tube went past the micropylar opening and then turned back and grew into the micropyle. (C) The pollen tube growing on the funiculus (left side) went back down (right side) near the micropylar opening and then grew on the funiculus again (center) and reached the micropyle. (D) The wandering pollen tube failed to grow into the micropyle. Scale bar, 50 µm for (A-D).
(E) Summary of abnormal pollen tube guidance around the micropylar opening in wild-type and transgenic ovules. Sums of class I and class II abnormalities in pollen tube guidance are shown. The data are averages and standard deviations of the frequencies per pistil. The total numbers of counted ovules are 339, 230, 183, 389, 135, and 173 for wild-type, vector control #1, #2, RNAi #1, #2, and #3 ovules, respectively. The frequencies of RNAi lines (#1-3) are significantly different from the wild type (asterisks, $P < 0.01$).

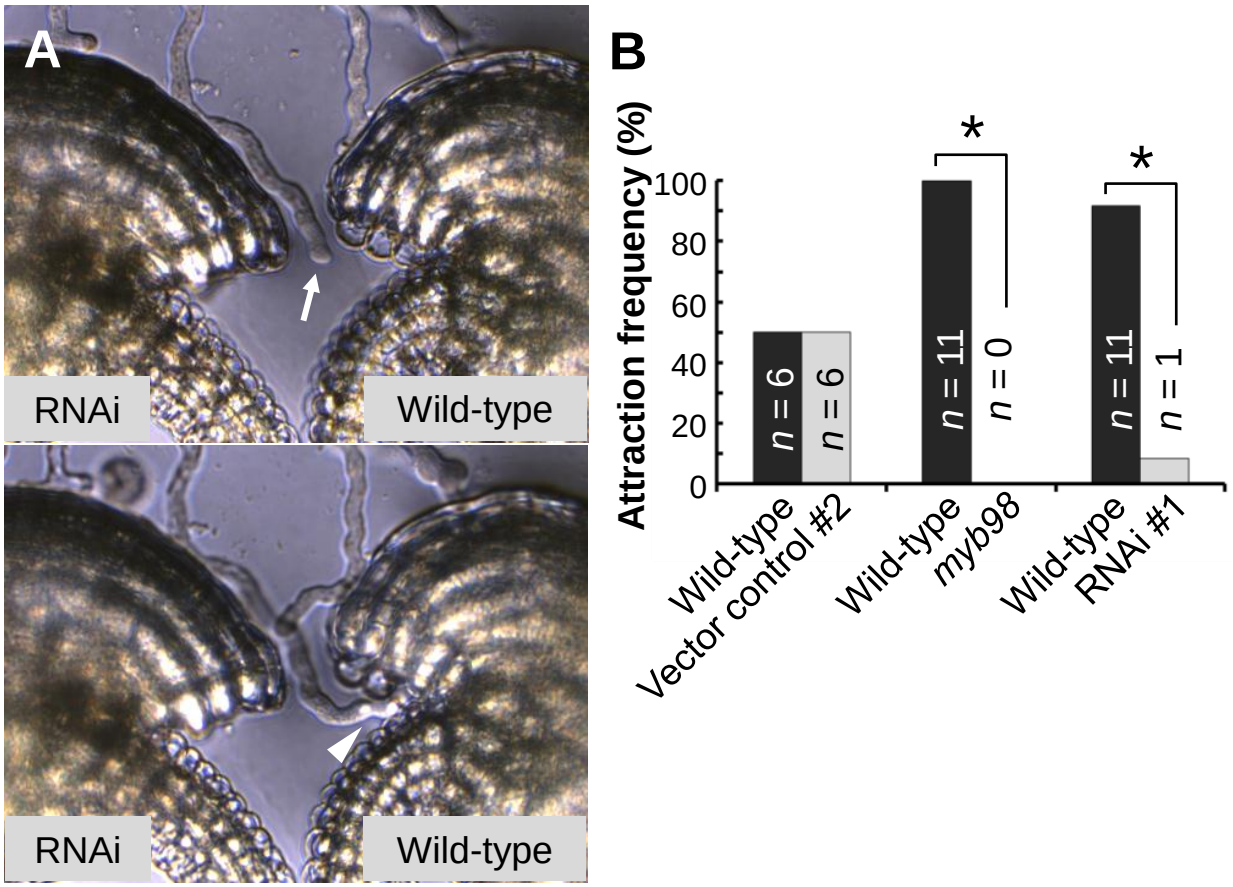

Figure 17. *In vitro* comparative pollen tube attraction assay using the RNAi ovule.
(A) An arrow indicates the tip of the pollen tube that was initially between the wild-type and RNAi ovules (upper panel). The pollen tube was preferentially attracted to the wild-type ovule (lower panel). An arrowhead indicates the pollen tube entering the wild-type micropyle.
(B) Summary of attraction frequencies in this assay. The attraction frequencies for the wild-type ovule (black boxes) or competing ovules (gray boxes) are represented collaterally. The numbers (*n*) are the total number of pollen tubes competitively attracted to the ovules. Asterisks indicate significant differences from a 1:1 ratio in the binomial test ($P < 0.01$).

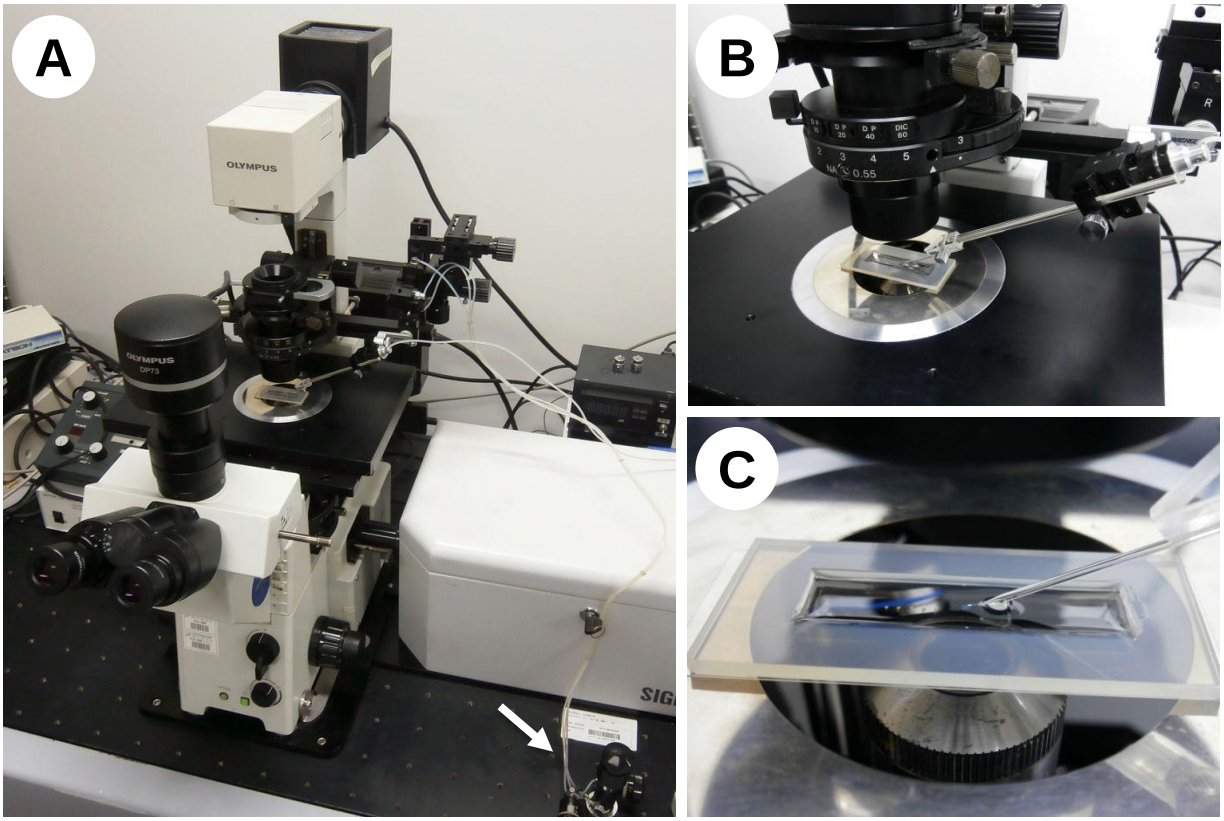

Figure 18. Microscope system used for *in vitro* pollen tube attraction assay of *Arabidopsis*.
(A) An inverted microscope (IX71, Olympus) equipped with a micromanipulator (Narishige). Oil hydraulic micromanipulator (arrow) was used for fine manipulation.
(B) Close-up of the microscope stage with a well for pollen tubes and glass needle attached to the manipulater.
(C) Close-up of the well on the microscope stage. The well is made from silicone rubber with a rectangular hole on a cover glass. Hydrated silicone oil is poured into the well to avoid the medium and pollen tubes from drying out during the assay.

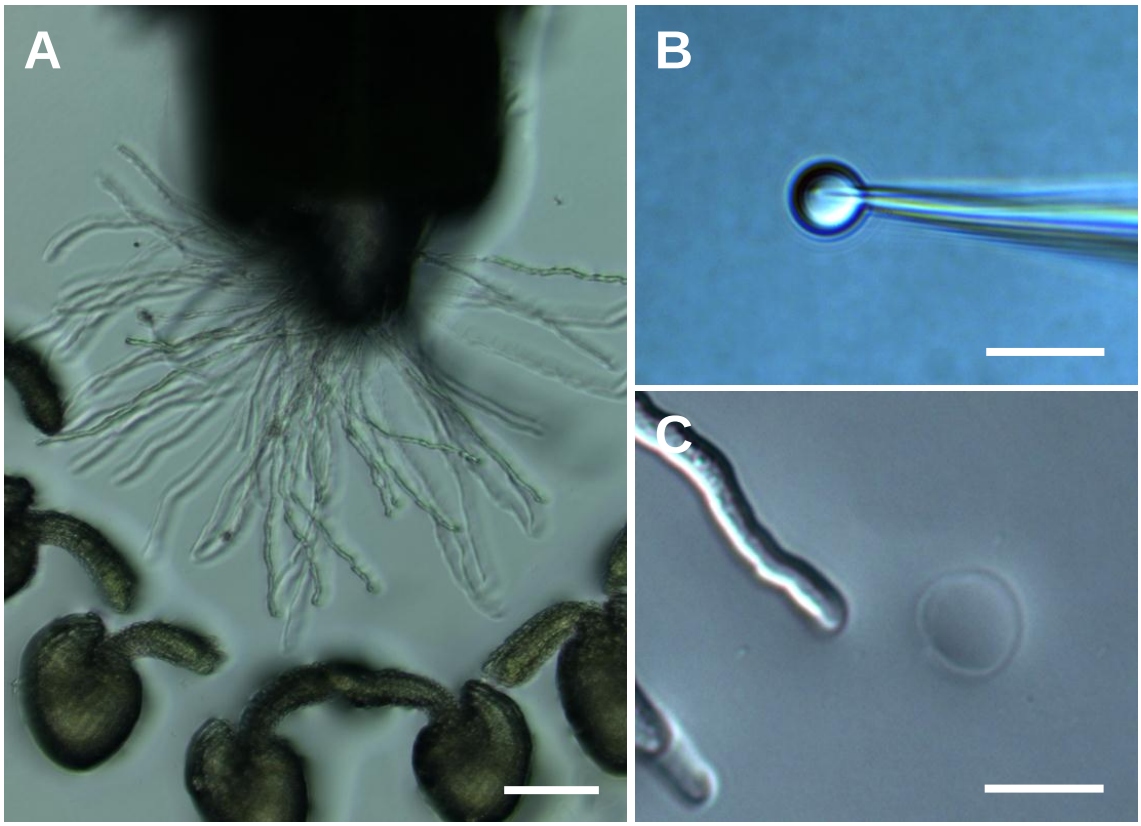

Figure 19. *In vitro* pollen tube attraction assay of *Arabidopsis*.
(A) *In vitro* pollen tube growth. Pollen tubes through the cut style were grown on medium using an *in vitro* system. Ovules were co-cultured because unknown protein(s) derived from the ovules could promote pollen tube growth and/or attraction. Around 5 h after the start of incubation, the pollen tube attraction assays were started. The picture shows pollen tubes emerging from the cut style and ovules 6 h after the start of incubation. Scale bar, 100 μm.
(B) A gelatin bead manipulated with a glass needle. The gelatin bead was attached to the tip of the glass needle and placed on the medium through micromanipulation. Scale bar, 20 μm.
(C) A gelatin bead placed in front of the tip of a pollen tube. The gelatin bead was slowly dissolved in the medium to spread the proteins embedded in it. Scale bar, 20 μm.

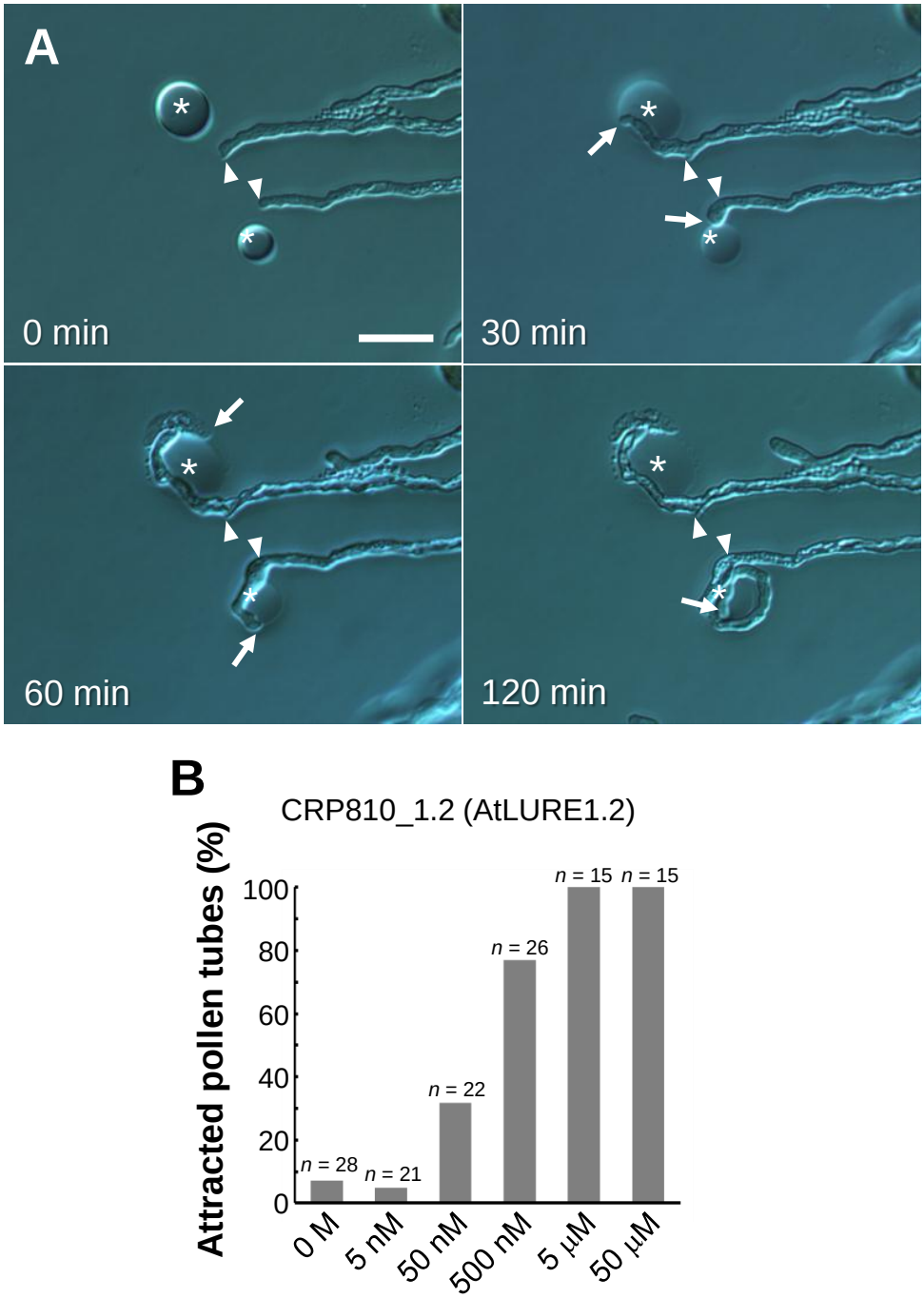

Figure 20. *In vitro* pollen tube attraction assay using recombinant CRP810_1.2.
(A) Pollen tube attraction toward gelatin beads containing 50 µM histidine-tagged CRP810_1.2. Arrowheads mark the position of the pollen tube tips when the gelatin beads (asterisk) were placed (0 min). Arrows indicate the tips of pollen tubes growing toward the beads 30 and 60 min after placement. At 60 min, the upper pollen tube was spontaneously disrupted and the lower pollen tube was trapped at the bead. Scale bar, 20 µm.
(B) Concentration-dependent pollen tube attraction activity of CRP810_1.2 (AtLURE1.2). The data are the frequencies for the total number of pollen tubes (*n*) in at least three assays. Pollen tubes growing toward beads with a >30º change were designated as attracted pollen tubes.

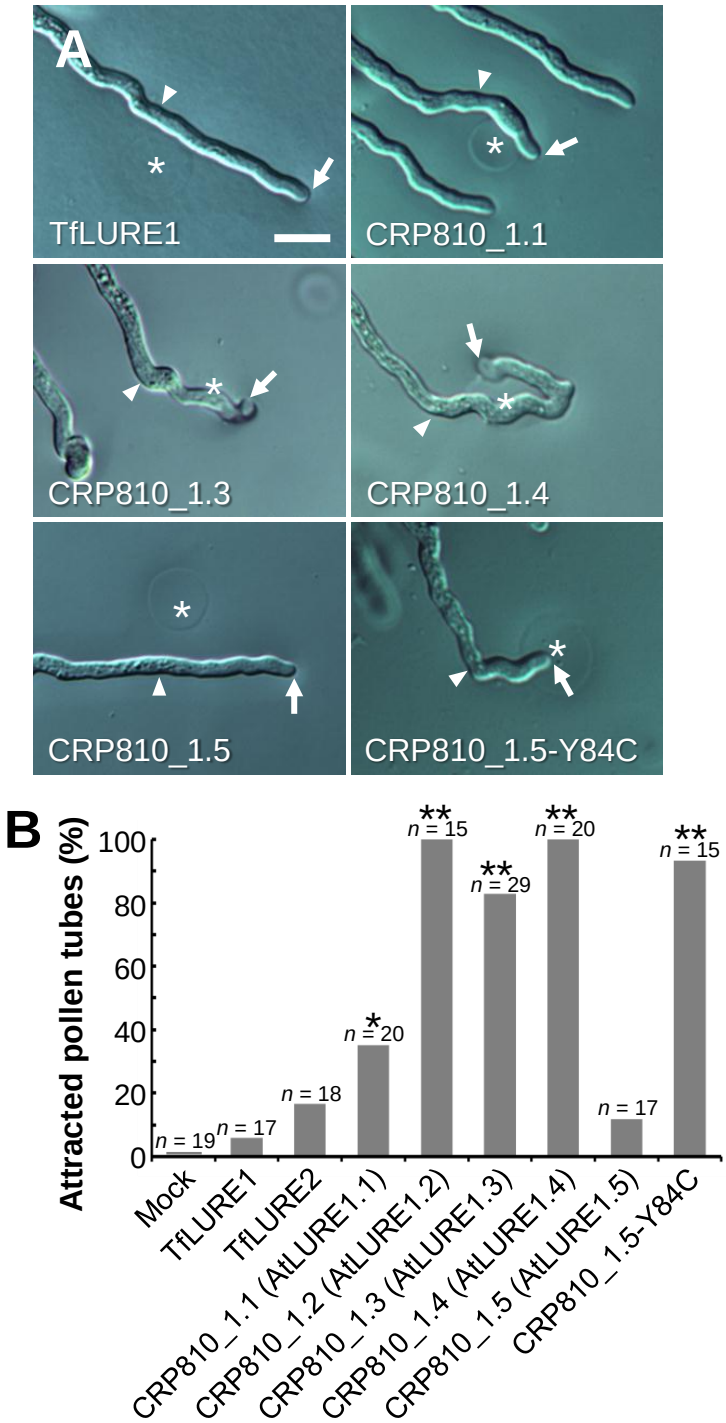

Figure 21. *In vitro* pollen tube attraction assay using recombinant proteins of paralogous CRP810_1 and TfLUREs.

(A) Representative samples of attracted or non-attracted pollen tubes to recombinant TfLURE1 and CRP810_1. Arrowheads mark the position of the pollen tube tip when the gelatin beads (asterisk) were placed. Arrows indicate the tips of the pollen tubes. Scale bar, 20 μm.

(B) Summary of the rates of attraction of the pollen tubes to each recombinant protein. The data are the frequencies for the total number of pollen tubes (*n*) in at least three assays per protein. An asterisk and double asterisks indicate significant differences compared with buffer alone (0 M) (Figure 20) using Fisher's exact test (**P* < 0.03; ***P* < 0.01).

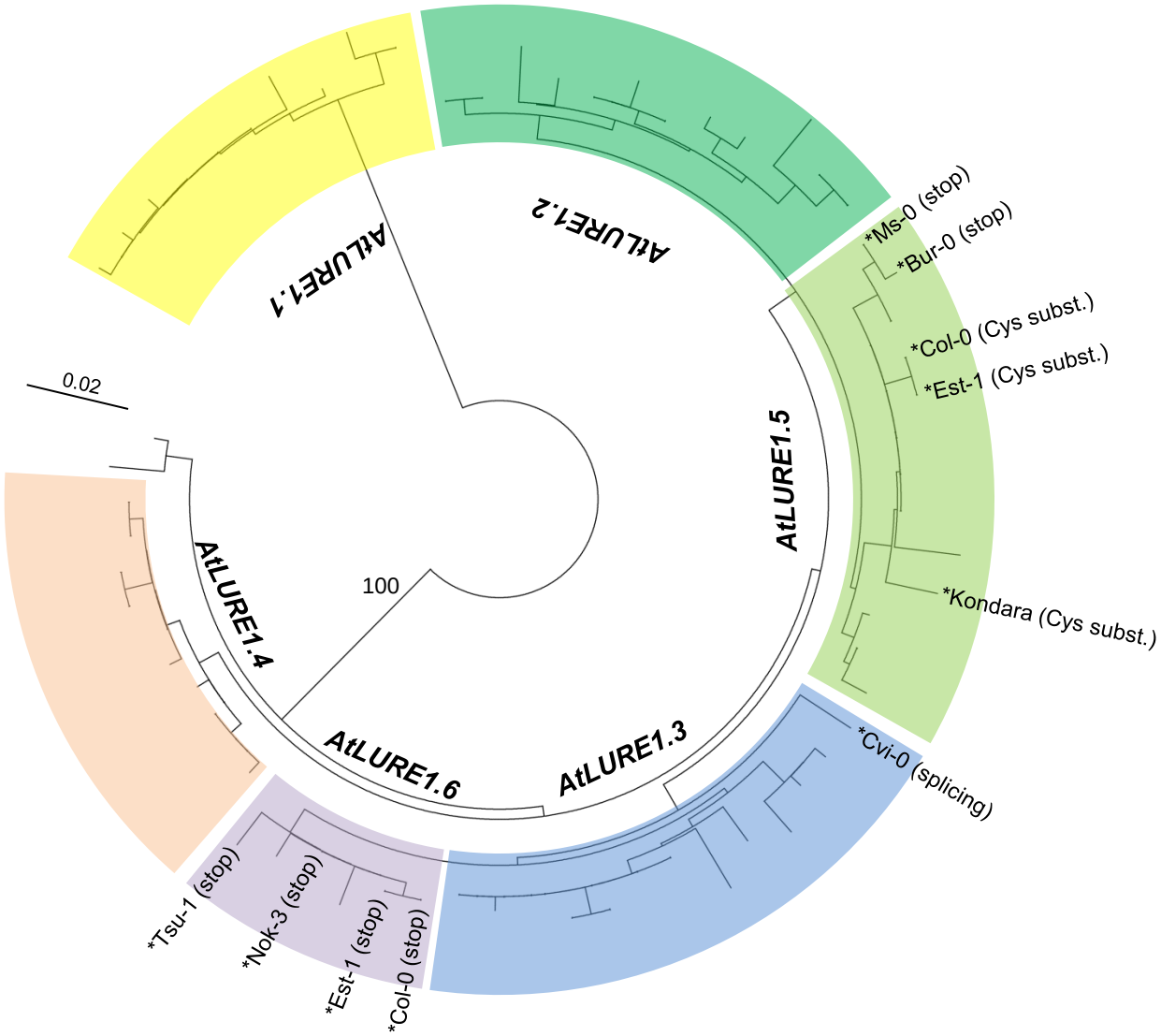

Figure 22. Sequence variation of *AtLURE1* (*CRP810_1*) genes in various accessions of *A. thaliana*.

A phylogenetic tree of six *AtLURE1* (*AtLURE1.1* to *1.6*) from the Col-0 accession and 60 sequences from 12 other *A. thaliana* accessions based on the coding region of their genomic sequences. Each background color indicates subtrees containing *AtLURE1.1* to *1.6*. The scale shows the number of substitutions per site. The genes with asterisks are probably nonfunctional. The sequences are available at http://www.plosbiology.org/article/fetchSingleRepresentation.action?uri=info:doi/10.1371/journal.pbio.1001449.s011.

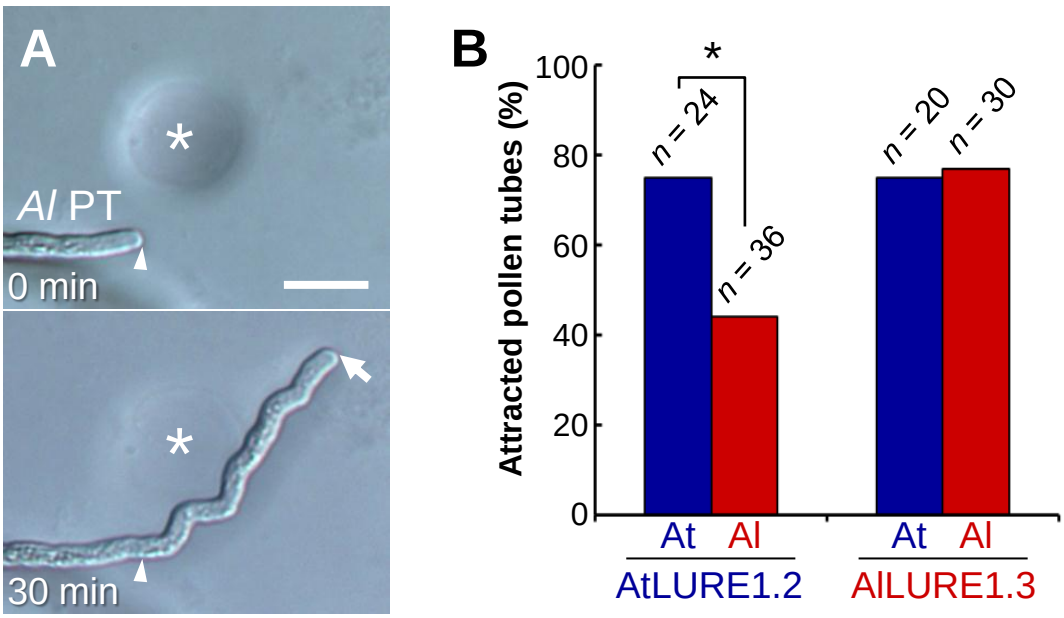

Figure 23. Pollen tube attraction of *A. lyrata* and species preferentiality of AtLURE1 and AlLURE1 peptides.

(A) A representative example of an attracted pollen tube of *A. lyrata* (*Al* PT) to recombinant AlCRP810_1.3 (AlLURE1.3). Arrowheads mark the position of the pollen tube tip when a gelatin bead (asterisk) was placed. An arrow indicates the tip of the pollen tube. Scale bar, 20 µm.

(B) Attraction activity of AtLURE1.2 (5 µM) and AlLURE1.3 (50 µM) to *A. thaliana* and *A. lyrata* pollen tubes. The data represent the frequencies of the total number of attracted pollen tubes (*n*) in at least three assays. An asterisk indicates a significant difference according to Fisher's exact test (**P* = 0.033). Note that the effective rate for each recombinant peptide is unknown because of differing efficiencies in peptide refolding.

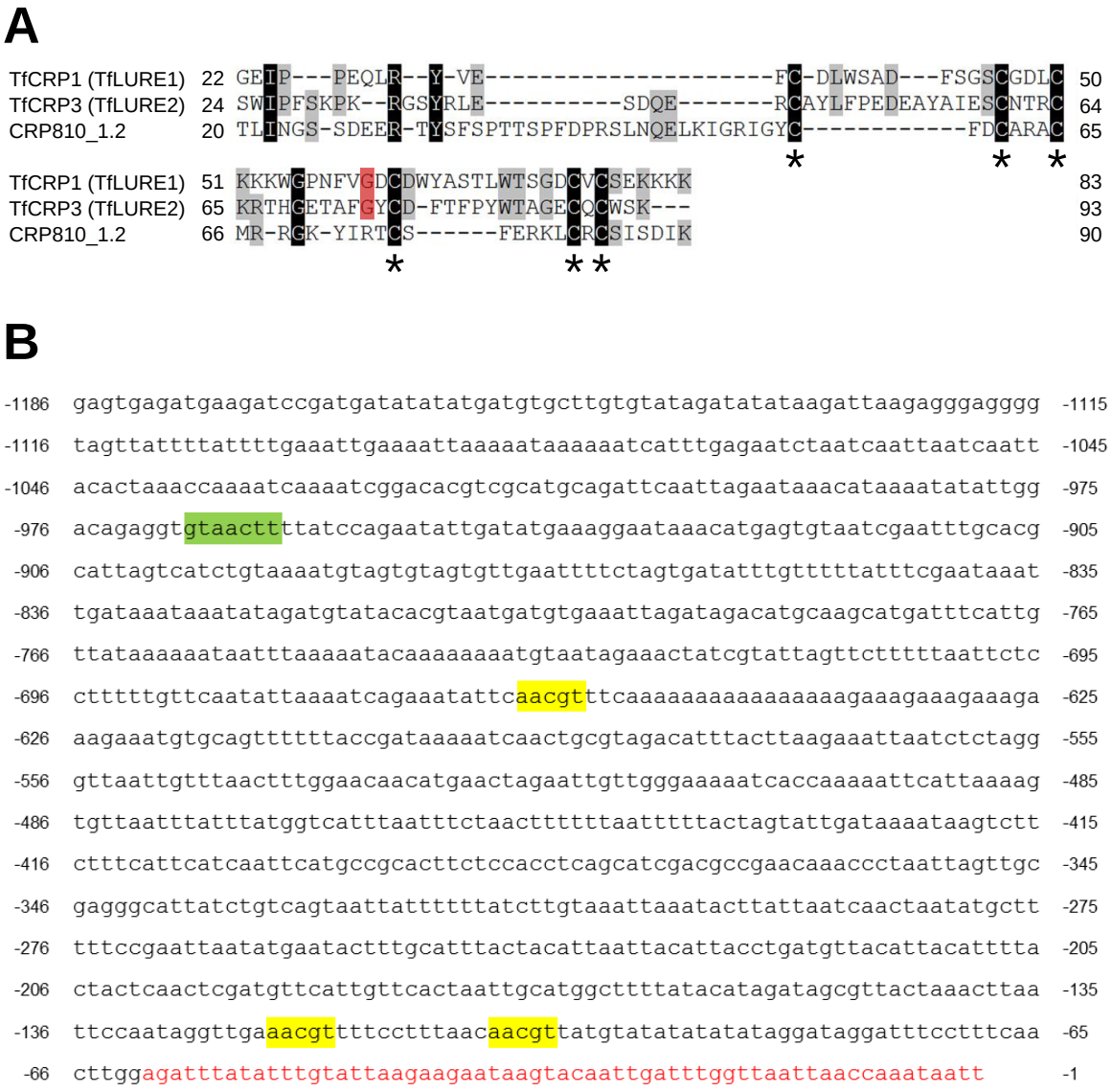

Figure 24. Sequence comparison of TfLUREs and CRP810_1.2 peptides and the promoter sequence of *TfLURE2*.

(A) Putative mature peptides of TfCRP1 (TfLURE1) and TfCRP3 (TfLURE2), pollen tube attractants of *Torenia fournieri*, and CRP810_1.2 (AtLURE1.2) as a representative CRP810_1 peptide are shown. Asterisks mark conserved cysteine residues. A red highlight indicates glycine residues for the gamma-core motif conserved in TfLUREs but not in AtLURE1.

(B) Upstream sequence of a translation start site of *TfLURE2*. A green highlight and yellow highlights indicate *cis*-element GTAACNT, which is suggested to be MYB98-binding sequence, and *cis*-element AACGT, which is necessary and sufficient for *AtLURE1.2* (DD2) expression in the synergid cell of *A. thaliana*, respectively (Punwani et al., 2008). Red letters mark 5' untranslated region of *TfLURE2*.

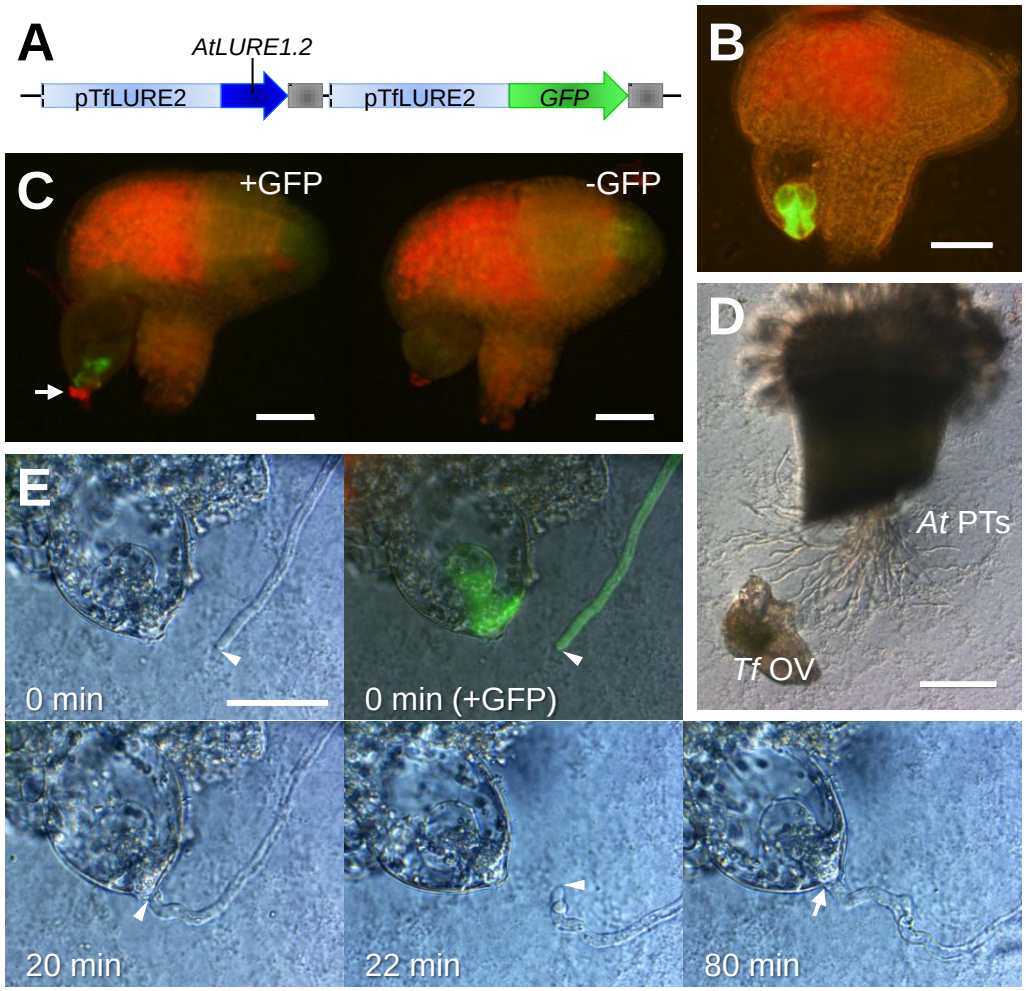

Figure 25. Interspecific pollen tube attraction assay using transgenic *T. fournieri* ovules and *A. thaliana* pollen tubes.

(A) Schematic representation of the sequences introduced into *T. fournieri*. The *TfLURE2* promoter (pTfLURE2) was used to express both *AtLURE1.2* (from the translation initiation codon to the putative 3′ untranslated region) and *GFP* genes in synergid cells. Gray boxes indicate *nopaline synthase* terminators.

(B) GFP expression in two synergid cells of the transgenic *T. fournieri* ovule. Scale bar, 50 µm.

(C) Immunostaining of transgenic *T. fournieri* ovules with anti-AtLURE1.2 (CRP810_1.2) antibodies. Red Alexa Fluor fluorescence for AtLURE1.2 (arrow) was observed at the micropylar surface of the embryo sac of the ovule labeled with GFP (left panel). In the ovule without GFP labeling (right panel), a weaker pseudo-signal was observed. Scale bars, 50 µm.

(D) An overview of the pollen tube attraction assay. Pollen tubes of *A. thaliana* (*At* PTs) are observed emerging from a cut style and growing across the medium. A manipulated *T. fournieri* ovule (*Tf* OV) was placed near the out-growing pollen tubes. Scale bar, 200 µm.

(E) Pollen tube attraction toward the synergid cell of a transgenic *T. fournieri* ovule. Arrowheads indicate the position of the tip of the *A. thaliana* pollen tube. At 0 min, an ovule was placed in front of the tip of the pollen tube using a glass needle. The pollen tube was labeled by pollen-expressed *pLAT52::GFP*. The pollen tube was attracted to the ovule (20 min). After shifting the position of the transgenic ovule (22 min), the pollen tube redirected itself once again toward the micropyle (80 min). The arrow indicates the ovular micropyle penetrated by the attracted pollen tube. Scale bar, 50 µm.

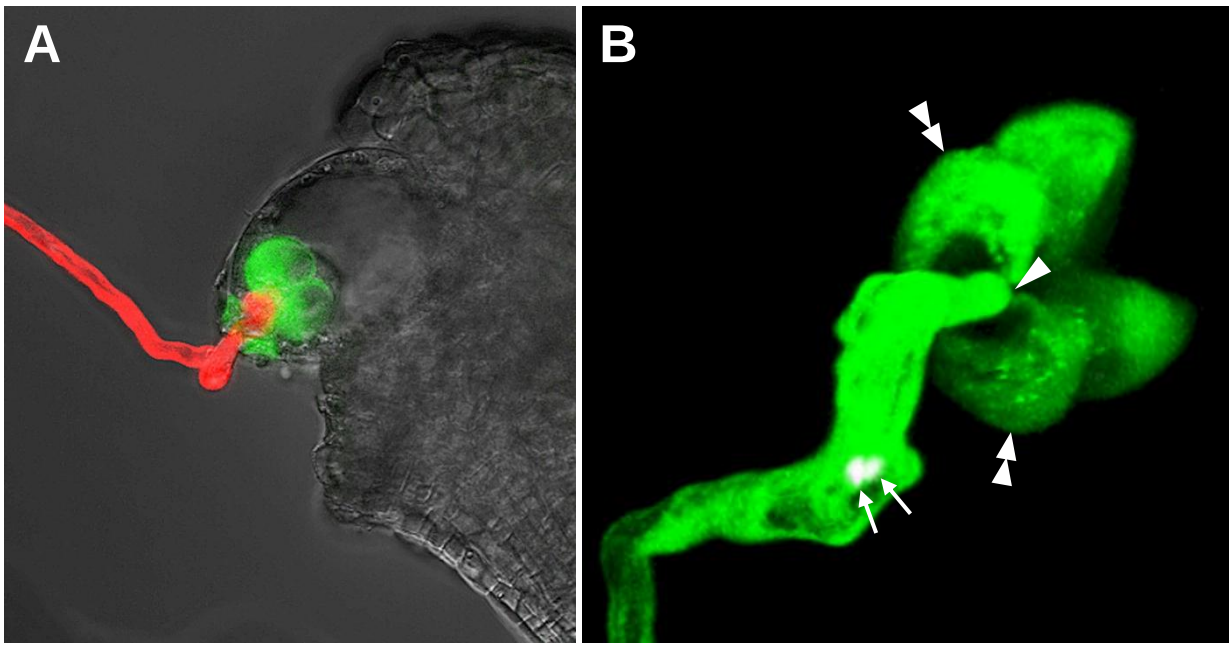

Figure 26. Penetration of *A. thaliana* pollen tubes into transgenic *T. fournieri* ovules after interspecific pollen tube attraction.
(A) A CLSM image of the transgenic *T. fournieri* ovule, demonstrating that the tip of the *A. thaliana* pollen tube (*pLAT52::TagRFP*) has fully penetrated the transgenic embryo sac.
(B) A projection of a three-dimensional reconstruction from CLSM images of cytosolic GFP-expressing synergid cells in the transgenic *T. fournieri* ovule and an attracted *A. thaliana* pollen tube (*pLAT52::GFP*×*pHTR10::HTR10:mRFP*). The arrowhead, double arrowheads, and arrow indicate the tip of the pollen tube, two synergid cells, and sperm nuclei (marked by *pHTR10::HTR10:mRFP*), respectively. The projection is an oblique perspective viewed from the micropylar end of the embryo sac. The pollen tube entered the embryo sac at the filiform apparatus, which is surrounded by two synergid cells and an egg cell (left third part lacking GFP staining, adjacent to the two synergid cells). Note that discharge of sperm cells did not occur.

A

-864 tcttcccgattcccacatgacggcgccatttggtgatggtagaaatcaccaattacgtttttgtagggga -795

-794 tcgtgggagaaaatggcgattagacgacgatgaagtagtattgattgagtgagtgattggttttgaattc -725

-724 tcgtccccccttcctttgtgggtgctcaaaggttttatactgaaaaaagttatcgaagggcagattcgtc -655

-654 attttccattgataatacagtggggaacatatgcagtgaagcaggctctttgggccttgtcccaatagct -585

-584 ttattttctaatagctttatttctttaatgggccttgcattattgatgcatgacttattaggccggccca -515

-514 gtttagatttgaatacaaaaaatgaggtcgataatgctacccacatcacattatcgtttgatttgttttc -445

-444 tggtattcgaaccgcaaaataatacaatttccatccataactgatattattttagttgttacgtgtagtg -375

-374 tggacccccctcgattccttttcatatgtcgctttgtacatccaatacaatcttaaatgcttaatttccac -305

-304 atatttagcctttgtggagtcaaagtgaaattgatgttcatgattaagcaaggttagtttcgtcaaatgt -235

-234 ttcaaagtttgatttggccgaggggggatcacacgagagttaatgtgatatttattaacaaccaataaaaa -165

-164 tgagatcaattaatcgaacccaatttaatgtaacttaaatattgttcttatttttatgcgtttcactaag -95

-94 tggctggtgtataaaatccaacattcacatatctaagccgtgaactcaaaaaattcattaggttttaaca -25

-24 ttttaaaaaaaaaaataaattaaa -1

B

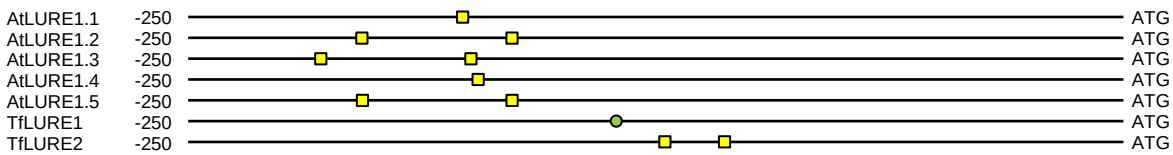

Figure 27. Promoter sequence of *TfLURE1* and depiction of promoters of *AtLURE1* and *TfLUREs* showing positions of conserved elements.

(A) Upstream sequence of a translation start site of *TfLURE1*. A green highlight indicates *cis*-element GTAACNT. Red letters mark 5' untranslated region of *TfLURE1*.

(B) Depiction of upstream sequences of translation start sites of *AtLURE1* genes and *TfLURE1*, *-2* genes. Yellow filled squares and green filled circle indicate the position of the *cis*-elements GTAACNT and AACGT, respectively, in the forward orientation. The *TfLURE2* promoter has the AACGT element conserved in all of *AtLURE1* promoters whereas the *TfLURE1* promoter has the GTAACNT element which is suggested to be MYB98-binding sequence (Punwani et al., 2008).

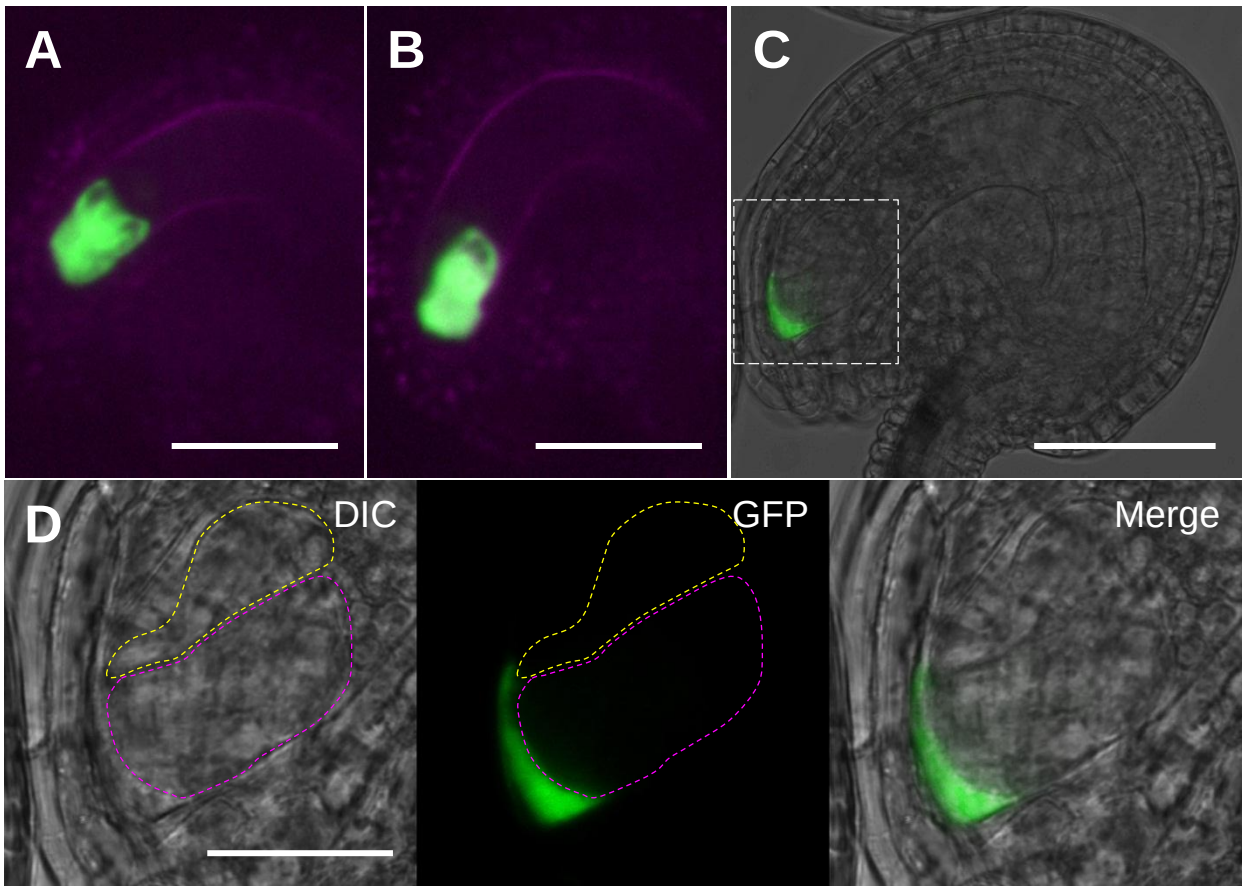

Figure 28. GFP expression driven by promoters of TfLUREs in *A. thaliana* synergid cells.

(A and B) CLSM images of *pTfLURE1::GFP* ovule (A) and *pTfLURE2::GFP* ovule (B). Magenta color indicates autofluorescence of the ovule. GFP fluorescence was specifically observed in the synergid cells of the ovule. Two synergid cells (A) and one of two synergid cells (B) are found in these single plane images. Scale bars, 50 µm.

(C) A single plane image of *pTfLURE2::TfLURE2-GFP* ovule by LSM 780 NLO. GFP signal was merged with a differential interference contrast (DIC) image. TfLURE2-GFP was observed at the micropylar end of the embryo sac. Scale bars, 50 µm.

(D) Zoomed images of region of a white dashed square in (C). Outlines of the egg and synergid cells are delineated as observed in the DIC image by the yellow and pink dashed lines, respectively. TfLURE2-GFP signal was localized at the outside of the synergid cell membrane. Scale bar, 20 µm.

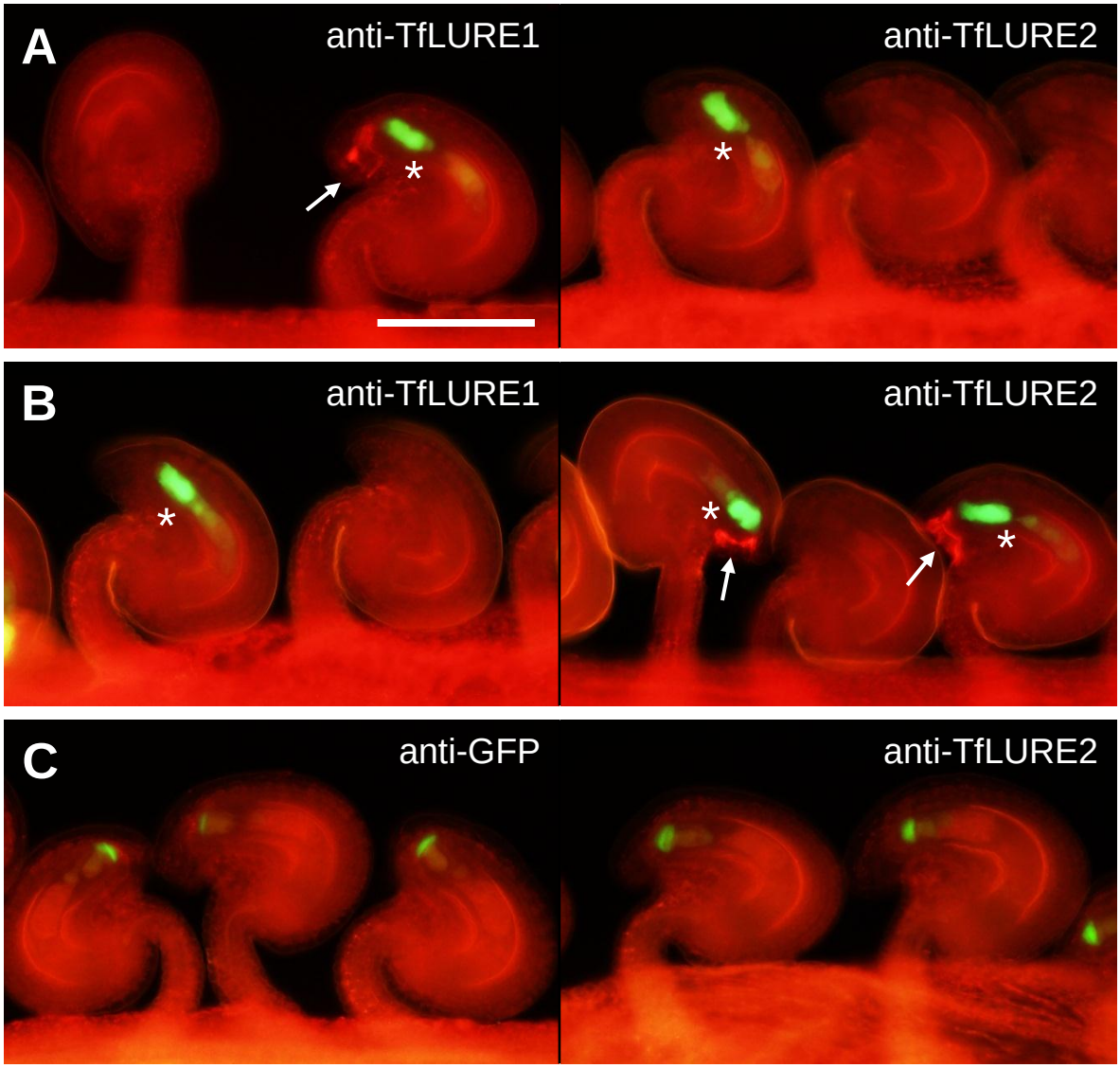

Figure 29. Secretion of TfLURE peptides from the synergid cell of transgenic *A. thaliana*.

(A and B) Immunostaining of ovules of *pMYB98::GFP/pTfLURE1::TfLURE1* and *pMYB98::GFP/pTfLURE2::TfLURE2* heterozygous plants with anti-TfLURE1 (left) or anti-TfLURE2 (right) antibodies. Asterisks mark GFP signals in the synergid cell, indicating embryo sac possessing the transgene. Arrows indicate red Alexa Fluor fluorescence for each of TfLURE peptides around the micropyle of the GFP-positive ovules immunostained by anti-TfLURE1 (A) or anti-TfLURE2 (B). Scale bar, 100 μm for (A-C).

(C) Immunostaining of *pTfLURE2::TfLURE2-GFP* ovules with anti-GFP (left) or anti-TfLURE2 (right) antibodies. Secreted TfLURE2-GFP signal was scarcely detected around the micropyle by these antibodies. Note that proteins in the filiform apparatus of the synergid cell are unable to be recognized by antibodies probably due to the immunostaining procedure without cell-wall degradation.

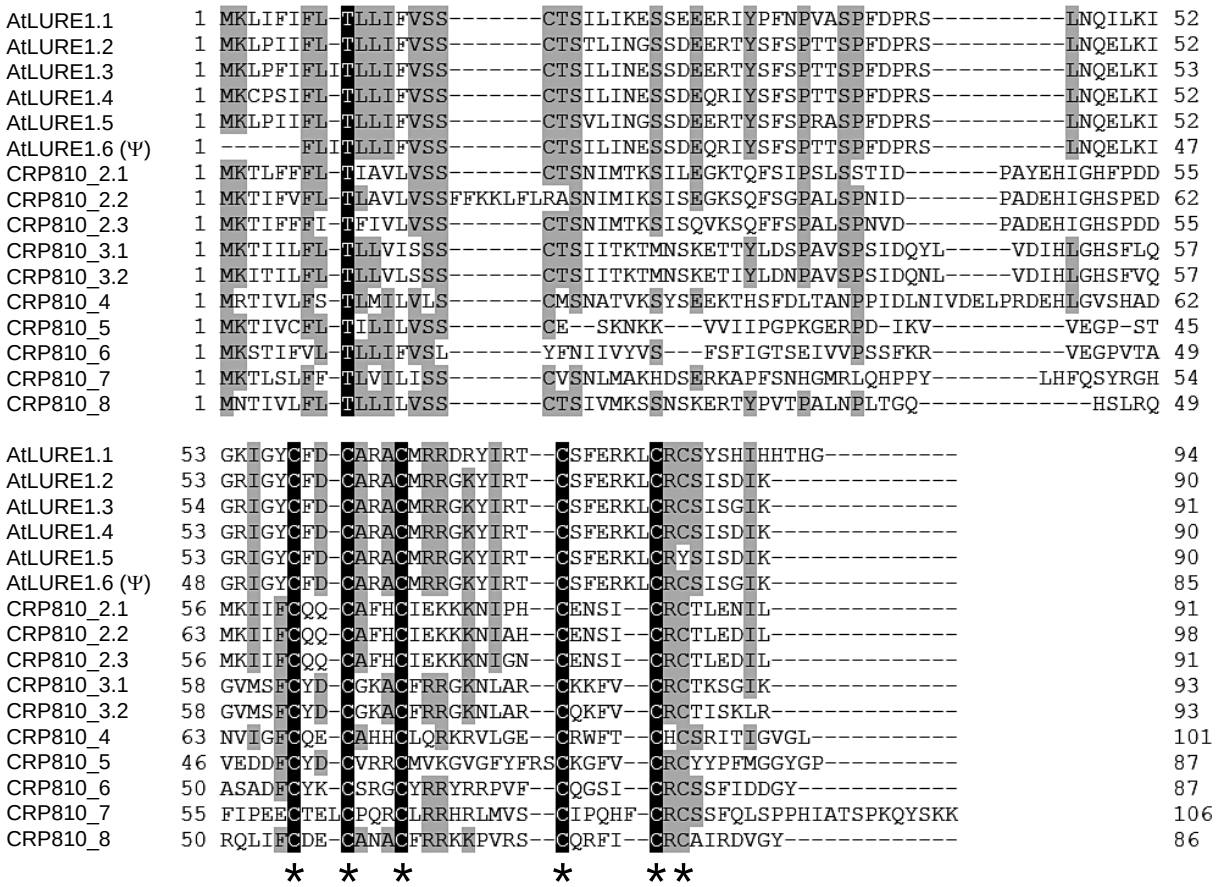

Figure 30. A multiple alignment of CRP810 peptides.
A multiple alignment of the full-length amino acid sequences of 16 CRP810 peptides in *A. thaliana*. Black and gray backgrounds indicate amino acids conserved among 16 and 8 or more sequences, respectively. Asterisks mark conserved cysteine residues.

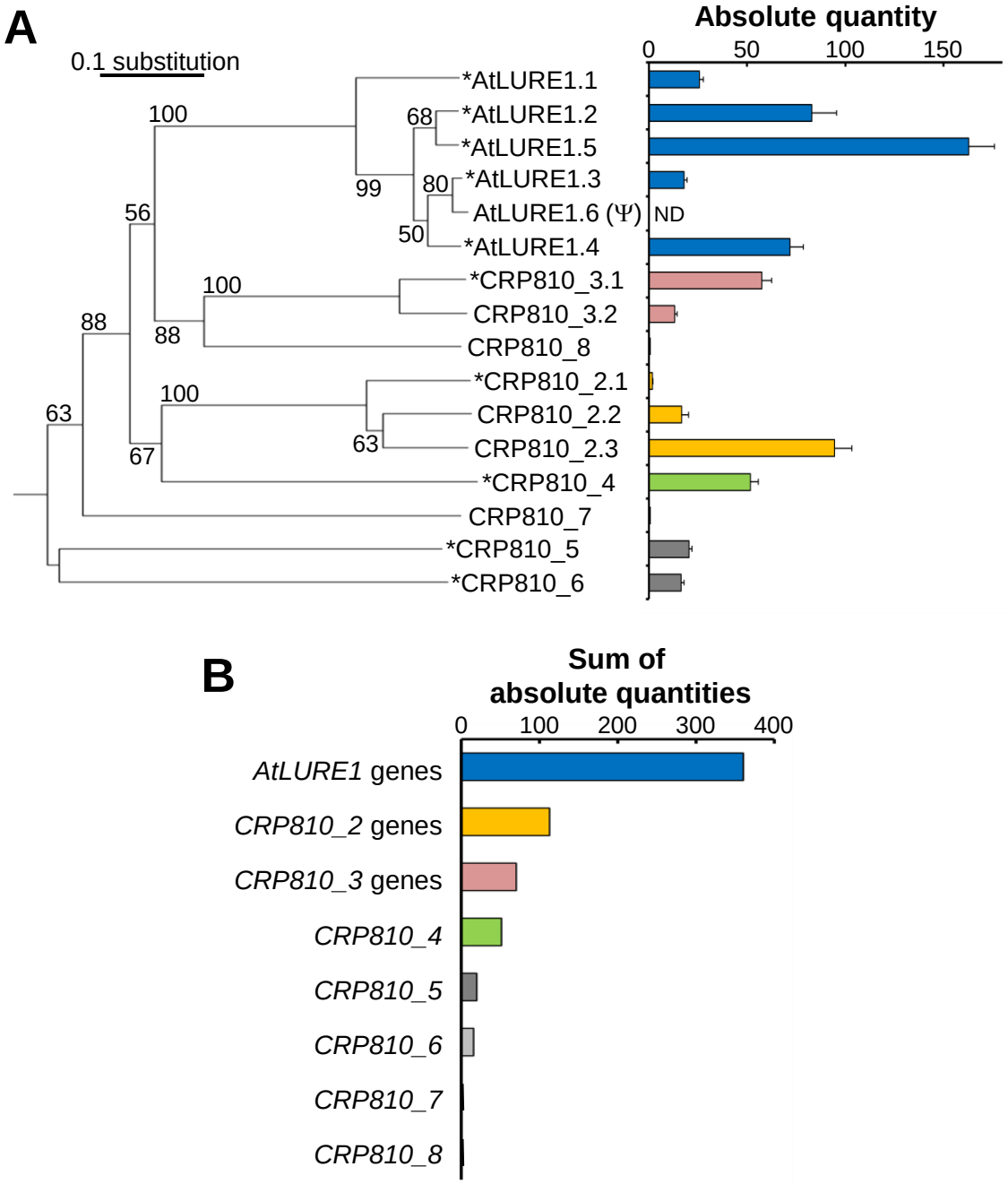

Figure 31. Expression analysis of *CRP810* genes in *A. thaliana* pistil.
(A) A phylogenetic relationship (left) and absolute gene expression levels in the pistil (right) of the *CRP810* genes. Asterisks mark genes downregulated in *myb98* according to a genome-wide analysis (Jones-Rhoades et al., 2007). The bootstrap values more than 50 for the NJ method are indicated as percentages. The scale shows the number of amino acid substitutions per site. Absolute quantity represents the copy number of cDNA per that of *MYB98* cDNA. The means and standard deviations of 3 independent experiments are shown.
(B) Absolute gene expression levels for paralogous gene groups. For *AtLURE1* (*CRP810_1*), *CRP810_2*, and *_3*, the values are the sum of the absolute quantities for each paralogous gene. The *CRP810* genes were numbered from *CRP810_1* (*AtLURE1*) to *_8* according to the level of expression in each group.

Table 1. Sequences of paralogous *DEFL* genes in *A. thaliana* and their orthologs in *A. lyrata*

Homology Group[a]	Multiply duplicated *CRP810_1* genes of *A. thaliana*	Orthologous gene of *A. lyrata*			
		Location	Synteny consevation[b]	Amino acid sequence identity[c]	Notes
CRP810	*At5g43285* (*CRP810_1.1*)	scaffold_8: 4561525-4561886	Yes	-	*AlCRP810_1.1* Disruption of start codon by single base substitution
		scaffold_8: 4559431-4559791	Yes	-	*AlCRP810_1.2* Stop mutation by single base substitution
		scaffold_8: 4557801-4558162	Yes	-	*AlCRP810_1.3* Stop mutation by one base deletion
		scaffold_8: 4556184-4556544	Yes	66 / 90 (73%)	*AlCRP810_1.4*
		scaffold_8: 4554538-4554918	Yes	65 / 90 (72%)	*AlCRP810_1.5*
		scaffold_8: 4547970-4548319	Yes	64 / 90 (71%)	*AlCRP810_1.6*
		scaffold_8: 4538868-4539229	Yes	65 / 90 (72%)	*AlCRP810_1.7*
		scaffold_97: 545-906 (complementary)	Yes	-	*AlCRP810_1.8* Stop mutation by single base substitution
		scaffold_1021: 829-1191 (complementary)	Yes	65 / 90 (72%)	*AlCRP810_1.9*
		scaffold_1021: 2448-2808 (complementary)	Yes	65 / 90 (72%)	*AlCRP810_1.10*
	At5g43510 (*CRP810_1.2*)	-	No	61 / 89 (68%) ~ 64 / 90 (71%)	-
	At5g43513 (*CRP810_1.3*)	-	No	64 / 89 (71%) ~ 66 / 89 (74%)	-
	At5g43518 (*CRP810_1.4*)	-	No	61 / 89 (68%) ~ 61 / 83 (73%)	-
	At5g43525 (*CRP810_1.5*)	-	No	61 / 89 (68%) ~ 64 / 90 (71%)	-
	At5g43516 (*CRP810_1.6*, Ψ)	-	No	-	-

[a] Homology group identifiers have been assigned in Silverstein et al., 2005.

[b] Yes, *A. thaliana* and *A. lyrata* genes showed a conserved synteny.

[c] The identity of aligned full-length amino acid sequences was determined by homology analysis in GENETYX.

The full data set for the other multiply duplicated DEFL genes and their orthologs in *A. lyrata* is available at http://www.plosbiology.org/article/fetchSingleRepresentation.action?uri=info:doi/10.1371/journal.pbio.1001449.s010.

Table 2. Pairwise comparisons between five *AtLURE1* genes and six *AlLURE1* genes

Full sequence (length = 90)						
	AlLURE1.4	*AlLURE1.5*	*AlLURE1.6*	*AlLURE1.7*	*AlLURE1.9*	*AlLURE1.10*
AtLURE1.1	0.8633 (0.1917 0.2221)	1.0656 (0.2007 0.1883)	0.9996 (0.2127 0.2128)	0.9660 (0.2063 0.2135)	0.9458 (0.2005 0.2120)	0.9164 (0.1944 0.2121)
AtLURE1.2	0.6451 (0.2090 0.3240)	0.8090 (0.2025 0.2503)	0.5802 (0.2032 0.3502)	0.5599 (0.1968 0.3516)	0.7344 (0.2023 0.2755)	0.6750 (0.2117 0.3136)
AtLURE1.3	0.5946 (0.2001 0.3366)	0.7420 (0.1938 0.2611)	0.5545 (0.1965 0.3543)	0.5347 (0.1902 0.3557)	0.6747 (0.1936 0.2869)	0.6220 (0.2028 0.3260)
AtLURE1.4	0.6711 (0.2207 0.3289)	0.8435 (0.2142 0.2540)	0.6041 (0.2148 0.3557)	0.5836 (0.2084 0.3571)	0.7655 (0.2140 0.2796)	0.7018 (0.2234 0.3184)
AtLURE1.5	0.6627 (0.2152 0.3247)	0.8318 (0.2087 0.2509)	0.5963 (0.2093 0.3510)	0.5758 (0.2029 0.3523)	0.7550 (0.2085 0.2761)	0.6932 (0.2178 0.3143)
Putative mature peptide (length = 71)						
	AlLURE1.4	*AlLURE1.5*	*AlLURE1.6*	*AlLURE1.7*	*AlLURE1.9*	*AlLURE1.10*
AtLURE1.1	0.8179 (0.2131 0.2605)	1.0152 (0.2295 0.2261)	0.9661 (0.2529 0.2618)	0.9290 (0.2444 0.2631)	0.9093 (0.2369 0.2605)	0.8388 (0.2205 0.2628)
AtLURE1.2	0.6134 (0.2270 0.3700)	0.7975 (0.2236 0.2803)	0.5484 (0.2321 0.4231)	0.5260 (0.2238 0.4254)	0.7290 (0.2310 0.3169)	0.6280 (0.2345 0.3735)
AtLURE1.3	0.5791 (0.2238 0.3864)	0.7494 (0.2204 0.2940)	0.5413 (0.2315 0.4277)	0.5191 (0.2232 0.4300)	0.6867 (0.2278 0.3317)	0.5929 (0.2313 0.3901)
AtLURE1.4	0.5979 (0.2259 0.3778)	0.7785 (0.2225 0.2858)	0.5341 (0.2309 0.4324)	0.5122 (0.2227 0.4347)	0.7112 (0.2299 0.3232)	0.6120 (0.2334 0.3814)
AtLURE1.5	0.6329 (0.2349 0.3712)	0.8233 (0.2315 0.2811)	0.5655 (0.2400 0.4245)	0.5427 (0.2316 0.4267)	0.7520 (0.2389 0.3178)	0.6474 (0.2425 0.3746)
First cysteine to last cysteine (length = 27)						
	AlLURE1.4	*AlLURE1.5*	*AlLURE1.6*	*AlLURE1.7*	*AlLURE1.9*	*AlLURE1.10*
AtLURE1.1	0.7588 (0.2007 0.2645)	0.5261 (0.1826 0.3470)	0.4214 (0.1601 0.3799)	0.4214 (0.1601 0.3799)	0.5261 (0.1826 0.3470)	0.7588 (0.2007 0.2645)
AtLURE1.2	0.6422 (0.1632 0.2542)	0.6644 (0.1361 0.2049)	0.3895 (0.1552 0.3986)	0.3895 (0.1552 0.3986)	0.6644 (0.1361 0.2049)	0.6422 (0.1632 0.2542)
AtLURE1.3	0.6422 (0.1632 0.2542)	0.6644 (0.1361 0.2049)	0.3895 (0.1552 0.3986)	0.3895 (0.1552 0.3986)	0.6644 (0.1361 0.2049)	0.6422 (0.1632 0.2542)
AtLURE1.4	0.6422 (0.1632 0.2542)	0.6644 (0.1361 0.2049)	0.3895 (0.1552 0.3986)	0.3895 (0.1552 0.3986)	0.6644 (0.1361 0.2049)	0.6422 (0.1632 0.2542)
AtLURE1.5	0.7211 (0.1828 0.2535)	0.7590 (0.1551 0.2044)	0.4388 (0.1744 0.3975)	0.4388 (0.1744 0.3975)	0.7590 (0.1551 0.2044)	0.7211 (0.1828 0.2535)

Values indicate dN/dS (dN, dS) for pairwise comparisons between five *AtLURE1* genes and six *AlLURE1* genes. The values were estimated using the method of Nei and Gojobori (1986) implemented in the yn00 program of the PAML version 4.5 (Yang, 2007).

Table 3. Pairwise comparisons between *AtLURE1.1* and the other paralogous *AtLURE1* genes (*1.2-1.5*)

Full sequence (length = 90)				
	AtLURE1.2	*AtLURE1.3*	*AtLURE1.4*	*AtLURE1.5*
AtLURE1.1	0.6963 (0.1180 0.1695)	0.5532 (0.1067 0.1928)	0.6846 (0.1176 0.1717)	0.6947 (0.1179 0.1698)
Putative mature peptide (length = 71)				
	AtLURE1.2	*AtLURE1.3*	*AtLURE1.4*	*AtLURE1.5*
AtLURE1.1	0.6413 (0.1297 0.2023)	0.5230 (0.1224 0.2340)	0.5592 (0.1152 0.2060)	0.6392 (0.1296 0.2028)
First cysteine to last cysteine (length = 27)				
	AtLURE1.2	*AtLURE1.3*	*AtLURE1.4*	*AtLURE1.5*
AtLURE1.1	0.1468 (0.0315 0.2143)	0.1468 (0.0315 0.2143)	0.1468 (0.0315 0.2143)	0.2233 (0.0477 0.2138)

Values indicate dN/dS (dN, dS) for pairwise comparisons between *AtLURE1.1* and the other paralogous *AtLURE1* genes (*1.2 -1.5*). The values were estimated using the method of Nei and Gojobori (1986) implemented in the yn00 program of the PAML version 4.5 (Yang, 2007).

Table 4. McDonald-Kreitman tables for *AtLURE1* genes

Gene	Polymorphic sites		Fixed differences[a]		Neutrality index (pN/pS)/(dN/dS)	McDonald-Kreitman test[b]
	Synonymous (pS)	Nonsynonymous (pN)	Synonymous (dS)	Nonsynonymous (dN)		
AtLURE1.1	3	6	12	33	0.727	$P = 0.696$
AtLURE1.2	6	9	16	33	0.727	$P = 0.757$
AtLURE1.3	6	11	14	29	0.885	$P = 1.000$
AtLURE1.4	0	5	17	32	NA	$P = 0.167$
AtLURE1.5	1	14	17	31	7.677	$P = 0.047$
AtLURE1.6	2	5	17	30	1.417	$P = 1.000$

[a] Compared with *AlLURE1.5* as a representative from *AlLURE1* genes.

[b] Fisher's exact test.

Conclusion and Perspectives

In this study, I identified pollen tube attractants, the AtLURE1 peptides, secreted from the synergid cell in the model plant *A. thaliana*. I also succeeded in breaking down the reproductive isolation barriers in pollen tube attraction and penetration of the embryo sac by introducing the single *AtLURE1* gene into *T. fournieri*. My results suggest that the LURE-type DEFL peptides, specifically expressed in the synergid cell, function universally as species-specific pollen tube attractants in flowering plants, especially dicotyledonous plants, to form reproductive barriers. The identification of the AtLURE1 peptides has an impact on the research field of plant reproduction, including female gametophyte development, polarized growth mechanisms of the pollen tube, and species-specific evolution of reproductive factors. For example, I showed that secretion of the AtLURE1 peptides by the synergid cells is impaired in the ovules of *ccg* and *maa3* mutants (Figure 14), suggesting that the central cell and RNA metabolism are important for full function of the synergid cell. Further studies in connection with AtLURE1 peptides are required to accelerate our understanding of gene regulatory networks in terms of mechanisms for generating attractants, as well as molecular mechanisms of pollen tube growth and guidance.

One of the most fascinating study areas in plant reproduction is elucidating how the direction of tip growth of the pollen tube is controlled (Takeuchi and Higashiyama, 2011). Identifying the receptor(s) for LURE peptides is important in understanding the mechanism of pollen tube attraction. AtLURE1 peptides have species-specific activity (Figure 23), and additional peptides belonging to the CRP810 subgroup are likely to be expressed in the synergid cell of *A. thaliana* (Figure 30). It can be assumed that the corresponding partner receptors are also encoded by genes from a

multigene family and show rapid molecular evolution allowing interactions with attractant molecules on the surface of the pollen tube. But what is the LURE receptor? To my knowledge, no receptor directly mediating a change in the direction of pollen tube growth has been reported in flowering plants. However, several pollen tube molecules involved in pollen tube growth and guidance have recently been reported. It should be noted that receptor-like kinases (RLKs) and ligand-gated ion channels expressed in the pollen and pollen tube are involved in the binding of CRPs, including DEFL peptides. In *Brassica* spp., defensin-like SCR/SP11, the male determinant of self-incompatibility, binds to *S*-receptor kinase (SRK), belonging to the RLK family, in the stigma to control pollen tube germination (Kachroo et al., 2001; Takayama et al., 2001). In tomato, pollen-specific CRP LAT52, which is involved in pollen tube germination and growth, interacts with LePRK2, a RLK with leucine-rich repeat motifs, for autocrine regulation (Tang et al., 2002). On the other hand, defensin-like ZmES4, which is expressed predominantly in synergid cells, interacts with the K^+ channel to rupture the pollen tube (Amien et al., 2010). From these findings, it appears that AtLURE1 may interact with RLKs expressed in the pollen tube or with molecules controlling ion flux (Wheeler et al., 2010; Takeuchi and Higashiyama, 2011). Focusing on these molecules, I am now attempting to identify molecule(s) involved in the reception of AtLURE1 peptides in the pollen tube of *A. thaliana*. T-DNA insertional loss-of-function mutants for these genes, including *RLK*s, are available in *A. thaliana* and will be used to assess whether pollen tubes of the mutants for these genes can respond to AtLURE1 peptides. The identification of AtLURE1 peptides in this study should help in identifying the receptor(s) of pollen tube attractants.

In addition to the receptor molecules for attractants, the way in which polarized pollen tube growth is regulated inside the growing pollen tube should be investigated. It has been known that ion dynamics are related to pollen tube growth (Konrad et al., 2011). In particular, the tip-focused Ca^{2+} gradient is important for pollen tube growth. However, the mechanism of the relationship between a cytosolic Ca^{2+} concentration gradient and the change in growth direction of the pollen tube is largely unknown. Recently, it has been reported that the cytosolic Ca^{2+} concentration in the tip of the pollen tube increases near wild-type ovules, but not *myb98* ovules, indicating an association between an extraneous attraction signal and cytosolic Ca^{2+} signaling for changing the direction of pollen tube tip-growth (Iwano et al., 2012). I can now use the AtLURE1 peptide in the pollen tube attraction assay developed in this study (Figures 18-21) and reveal the relationship between an increase in cytosolic Ca^{2+} concentration and the change in growth direction in more detail. At the same time, factor(s) directly involved in Ca^{2+} uptake should be identified. I am focusing on cyclic nucleotide-gated channels (CNGCs) and glutamate receptors (GLRs) expressed in the pollen tube, some of which have been reported to be essential for normal pollen tube growth and to be involved in Ca^{2+} uptake (Frietsch et al., 2007; Michard et al., 2011). The identification of essential factors controlling pollen tube growth and guidance, including the receptor for LURE peptides and the Ca^{2+} channels, will shed light on universal mechanisms for chemotactic signaling in various organisms as well as mechanisms of speciation and plant reproduction.

References

Aida R, Shibata M (1995) *Agrobacterium*-mediated transformation of Torenia (*Torenia fournieri*). Breed Sci 45: 71-74.

Alandete-Saez M, Ron M, McCormick S (2008) GEX3, expressed in the male gametophyte and in the egg cell of *Arabidopsis thaliana*, is essential for micropylar pollen tube guidance and plays a role during early embryogenesis. Mol Plant 1: 586-598.

Alonso JM, Stepanova AN, Leisse TJ, Kim CJ, Chen H, et al. (2003) Genome-wide insertional mutagenesis of *Arabidopsis thaliana*. Science 301: 653-657.

Amien S, Kliwer I, Márton ML, Debener T, Geiger D, et al. (2010) Defensin-like ZmES4 mediates pollen tube burst in maize via opening of the potassium channel KZM1. PLoS Biol 8: e1000388.

APG III (2009) An update of the Angiosperm Phylogeny Group classification for the orders and families of flowering plants: APG III. Bot J Linn Soc 161: 105–121.

Arabidopsis Genome Initiative (2000) Analysis of the genome sequence of the flowering plant *Arabidopsis thaliana*. Nature 408: 796-815.

Aranzana MJ, Kim S, Zhao K, Bakker E, Horton M, et al. (2005) Genome-wide association mapping in *Arabidopsis* identifies previously known flowering time and pathogen resistance genes. PLoS Genet 1: 531-539.

Bai RK, Wong LJC (2004) Detection and quantification of heteroplasmic mutant mitochondrial DNA by real-time amplification refractory mutation system quantitative PCR analysis: a single-step approach. Clin Chem 50: 996-1001.

Berger F, Hamamura Y, Ingouff M, Higashiyama T (2008) Double fertilization -

caught in the act. Trends Plant Sci 13: 437-443.

Bikard D, Patel D, Le Metté C, Giorgi V, Camilleri C, et al. (2009) Divergent evolution of duplicate genes leads to genetic incompatibilities within *A. thaliana*. Science 323: 623-626.

Boavida LC, Vieira AM, Becker JD, Feijó JA (2005) Gametophyte interaction and sexual reproduction: how plants make a zygote. Int J Dev Biol 49: 615-632.

Cao J, Schneeberger K, Ossowski S, Günther T, Bender S, et al. (2012) Whole-genome sequencing of multiple *Arabidopsis thaliana* populations. Nat Genet 43: 956-963.

Clough SJ, Bent AF (1998) Floral dip: A simplified method for Agrobacterium-mediated transformation of *Arabidopsis thaliana*. Plant J 16: 735-743.

Chen YH, Li HJ, Shi DQ, Yuan L, Liu J, et al. (2007) The central cell plays a critical role in pollen tube guidance in *Arabidopsis*. Plant Cell 19: 3563-3577.

Cheung AY, Wang H, Wu HM (1995) A floral transmitting tissue-specific glycoprotein attracts pollen tubes and stimulates their growth. Cell 82: 383-393.

Clark NL, Findlay GD, Yi X, MacCoss MJ, Swanson WJ (2007a) Duplication and selection on abalone sperm lysin in an allopatric population. Mol Biol Evol 24: 2081-2090.

Clark RM, Schweikert G, Toomajian C, Ossowski S, Zeller G, et al. (2007b) Common sequence polymorphisms shaping genetic diversity in *Arabidopsis thaliana*. Science 317: 338-342.

Clauss MJ, Mitchell-Olds T (2004) Functional divergence in tandemly duplicated *Arabidopsis thaliana* trypsin inhibitor genes. Genetics 166: 1419-1436.

Coyne JA, Orr HA (2004) Speciation. Sunderland, MA: Sinauer Associates Inc.

Crawford BC, Ditta G, Yanofsky MF (2007) The NTT gene is required for transmitting-tract development in carpels of *Arabidopsis thaliana*. Curr Biol 17: 1101-1108.

Dresselhaus T, Márton ML (2009) Micropylar pollen tube guidance and burst: adapted from defense mechanisms? Curr Opin Plant Biol 12: 773-780.

Elbashir SM, Lendeckel W, Tuschl T (2001) RNA interference is mediated by 21- and 22-nucleotide RNAs. Genes Dev 15: 188-200.

Escobar-Restrepo JM, Huck N, Kessler S, Gagliardini V, Gheyselinck J, et al. (2007) The FERONIA receptor-like kinase mediates male–female interactions during pollen tube reception. Science 317: 656–660.

Frietsch S, Wang YF, Sladek C, Poulsen LR, Romanowsky SM, et al. (2007) A cyclic nucleotide-gated channel is essential for polarized tip growth of pollen. Proc Natl Acad Sci U S A 104: 14531-14536.

Ganz T (2003) Defensins: antimicrobial peptides of innate immunity. Nat Rev Immunol 3: 710-720.

Ge L, Gou X, Yuan T, Strout GW, Nakashima J, et al. (2011) Migration of sperm cells during pollen tube elongation in Arabidopsis thaliana: behavior during transport, maturation and upon dissociation of male germ unit associations. Planta 233: 325-332.

Gray-Mitsumune M, Matton DP (2006) The *EGG APPARATUS 1* gene from maize is a member of a large gene family found in both monocots and dicots. Planta 223: 618-625.

Gross-Hardt R, Kägi C, Baumann N, Moore JM, Baskar R, et al. (2007) *LACHESIS*

restricts gametic cell fate in the female gametophyte of *Arabidopsis*. PLoS Biol 5: e47.

Hajdukiewicz P, Svab Z, Maliga P (1994) The small, versatile *pPZP* family of *Agrobacterium* binary vectors for plant transformation. Plant Mol Biol 25: 989-994.

Haldane JBS (1949) Disease and evolution. Suppl Ric Sci 19: 68-76.

Hamamura Y, Saito C, Awai C, Kurihara D, Miyawaki A, et al. (2011) Live-cell imaging reveals the dynamics of two sperm cells during double fertilization in *Arabidopsis thaliana.* Curr Biol 21: 497-502.

Higashiyama T (2002) The synergid cell: attractor and acceptor of the pollen tube for double fertilization. J Plant Res 115: 149-160.

Higashiyama T (2010) Peptide signaling in pollen-pistil interactions. Plant Cell Physiol 51: 177-189.

Higashiyama T, Hamamura Y (2008) Gametophytic pollen tube guidance. Sex Plant Reprod 21: 17-26.

Higashiyama T, Inatsugi R, Sakamoto S, Sasaki N, Mori T, et al. (2006) Species preferentiality of the pollen tube attractant derived from the synergid cell of *Torenia fournieri*. Plant Physiol 142: 481-491.

Higashiyama T, Kuroiwa H, Kuroiwa T (2003) Pollen-tube guidance: beacons from the female gametophyte. Curr Opin Plant Biol 6: 36-41.

Higashiyama T, Yabe S, Sasaki N, Nishimura Y, Miyagishima S, et al. (2001) Pollen tube attraction by the synergid cell. Science 293: 1480-1483.

Hu TT, Pattyn P, Bakker EG., Cao J, Cheng JF, et al. (2011) The *Arabidopsis lyrata* genome sequence and the basis of rapid genome size change. Nat Genet 43:

476-481.

Huang CK, Huang LF, Huang JJ, Wu SJ, Yeh CH, et al. (2010). A DEAD-box protein, AtRH36, is essential for female gametophyte development and is involved in rRNA biogenesis in Arabidopsis. Plant Cell Physiol 51: 694-706.

Hulskamp M, Schneitz K, Pruitt RE (1995) Genetic evidence for a long-range activity that directs pollen tube guidance in Arabidopsis. Plant cell 7: 57-64.

Iwano M, Ngo QA, Entani T, Shiba H, Nagai T, et al. (2012) Cytoplasmic Ca^{2+} changes dynamically during the interaction of the pollen tube with synergid cells. Development 139: 4202-4209.

Jiggins FM, Kim KW (2005) The evolution of antifungal peptides in Drosophila. Genetics 171: 1847-1859.

Johnson MA., Preuss D (2002) Plotting a course: multiple signals guide pollen tubes to their targets. Dev Cell 2: 273-281.

Jones-Rhoades MW, Borevitz JO, Preuss D (2007) Genome-wide expression profiling of the *Arabidopsis* female gametophyte identifies families of small, secreted proteins. PLoS Genet 3: 1848-1861.

Kägi C, Baumann N, Nielsen N, Stierhof YD, Gross-Hardt R (2010) The gametic central cell of *Arabidopsis* determines the lifespan of adjacent accessory cells. Proc Natl Acad Sci U S A 107: 22350-22355.

Kachroo A, Schopfer CR, Nasrallah ME, Nasrallah JB (2001) Allele-specific receptor-ligand interactions in *Brassica* self-incompatibility. Science 293: 1824-1826.

Kanaoka MM, Kawano N, Matsubara Y, Susaki D, Okuda S, et al. (2011) Identification and characterization of TcCRP1, a pollen tube attractant from

Torenia concolor. Ann Bot 108: 739-747.

Kasahara RD, Portereiko MF, Sandaklie-Nikolova L, Rabiger DS, Drews GN (2005) *MYB98* is required for pollen tube guidance and synergid cell differentiation in *Arabidopsis*. Plant Cell 17: 2981-2992.

Kim S, Mollet JC, Dong J, Zhang K, Park SY, Lord EM (2003) Chemocyanin, a small basic protein from the lily stigma, induces pollen tube chemotropism. Proc Natl Acad Sci USA 100:16125-16130.

Koch MA, Haubold B, Mitchell-Olds T (2000) Comparative evolutionary analysis of chalcone synthase and alcohol dehydrogenase loci in *Arabidopsis*, *Arabis*, and related genera (Brassicaceae). Mol Biol Evol 17: 1483-1498.

Konrad KR, Wudick MM, Feijó JA (2011) Calcium regulation of tip growth: new genes for old mechanisms. Curr Opin Plant Biol 14: 721-730.

Larkin MA, Blackshields G, Brown NP, Chenna R, McGettigan PA, et al. (2007) Clustal W and Clustal X version 2.0. Bioinformatics 23: 2947-2948.

Lazzaro BP (2008) Natural selection on the *Drosophila* antimicrobial immune system. Curr Opin Microbiol 11: 284-289.

Leister D (2004). Tandem and segmental gene duplication and recombination in the evolution of plant disease resistance gene. Trends Genet 20: 116-122.

Li N, Yuan L, Liu N, Shi D, Li X, et al. (2009) *SLOW WALKER2*, a NOC1/MAK21 homologue, is essential for coordinated cell cycle progression during female gametophyte development in Arabidopsis. Plant Physiol 151: 1486-1497.

Márton ML, Cordts S, Broadhvest J, Dresselhaus T (2005) Micropylar pollen tube guidance by egg apparatus 1 of maize. Science 307: 573-576.

Márton ML, Fastner A, Uebler S, Dresselhaus T (2012) Overcoming hybridization

barriers by the secretion of the maize pollen tube attractant ZmEA1 from *Arabidopsis* ovules. Curr Biol DOI 10.1016/j.cub.2012.04.061

McDonald JH, Kreitman M (1991) Adaptive protein evolution at the *Adh* locus in *Drosophila*. Nature 351: 652-654.

Michard E, Lima PT, Borges F, Silva AC, Portes MT, et al. (2011) Glutamate receptor-like genes form Ca^{2+} channels in pollen tubes and are regulated by pistil D-serine. Science 332: 434-437.

Mizuta Y, Harushima Y, Kurata N (2010) Rice pollen hybrid incompatibility caused by reciprocal gene loss of duplicated genes. Proc Natl Acad Sci U S A 107: 20417-20422.

Moll C, von Lyncker L, Zimmermann S, Kägi C, Baumann N, et al. (2008) *CLO*/*GFA1* and *ATO* are novel regulators of gametic cell fate in plants. Plant J 56: 913-921.

Nakagawa T, Kurose T, Hino T, Tanaka K, Kawamukai M, et al. (2007a) Development of series of Gateway Binary Vectors, pGWBs, for realizing efficient construction of fusion genes for plant transformation. J Biosci Bioeng 104: 34-41.

Nakagawa T, Suzuki T, Murata S, Nakamura S, Hino T, et al. (2007b) Improved Gateway Binary Vectors: high-performance vectors for creation of fusion constructs in transgenic analysis of plants. Biosci Biotechnol Biochem 71: 2095-2100.

Nei M, Gojobori T (1986) Simple methods for estimating the numbers of synonymous and nonsynonymous nucleotide substitutions. Mol Biol Evol 3: 418-426.

Nei M, Rooney AP (2005) Concerted and birth-and-death evolution of multigene

families. Annu Rev Genet 39: 121-152.

Nielsen R, Bustamante C, Clark AG, Glanowski S, Sackton TB, et al. (2005) A scan for positively selected genes in the genomes of humans and chimpanzees. PLoS Biol 6: e170.

Ohnishi T, Takanashi H, Mogi M, Takahashi H, Kikuchi S, et al. (2011) Distinct gene expression profiles in egg and synergid cells of rice as revealed by cell type-specific microarrays. Plant Physiol 155: 881-891.

Ohno S (1970) Evolution by Gene Duplication. Berlin: Springer-Verlag.

Okuda S, Tsutsui H, Shiina K, Sprunck S, Takeuchi H, et al. (2009) Defensin-like polypeptide LUREs are pollen tube attractants secreted from synergid cells. Nature 458: 357-361.

Pagnussat GC, Yu HJ, Sundaresan V (2007) Cell-fate switch of synergid to egg cell in *Arabidopsis eostre* mutant embryo sacs arises from misexpression of the BEL1-like homeodomain gene *BLH1*. Plant Cell 19: 3578-3592.

Palanivelu R, Brass L, Edlund AF, Preuss D (2003) Pollen tube growth and guidance is regulated by POP2, an *Arabidopsis* gene that controls GABA levels. Cell 114: 47-59.

Palanivelu R, Preuss D (2006) Distinct short-range ovule signals attract or repel *Arabidopsis thaliana* pollen tubes *in vitro*. BMC Plant Biol 6: 7.

Patil AA, Cai Y, Sang Y, Blecha F, Zhang G (2005) Cross-species analysis of the mammalian beta-defensin gene family: presence of syntenic gene clusters and preferential expression in the male reproductive tract. Physiol Genomics 23: 5-17.

Punwani JA, Rabiger DS, Drews GN (2007) MYB98 positively regulates a battery of

synergid-expressed genes encoding filiform apparatus-localized proteins. Plant Cell 19: 2557-2568.

Punwani JA, Rabiger DS, Lloyd A, Drews GN (2008) The *MYB98* subcircuit of the synergid gene regulatory network includes genes directly and indirectly regulated by MYB98. Plant J 55: 406-414.

Rast JP, Smith LC, Loza-Coll M, Hibino T, Litman GW (2006) Genomic insights into the immune system of the sea urchin. Science 314: 952-956.

Ray S, Park SS, Ray A (1997) Pollen tube guidance by the female gametophyte. Development 124: 2489-2498.

Rieseberg LH, Willis JH (2007) Plant speciation. Science 317: 910-914.

Sackton TB, Lazzaro BP, Schlenke TA, Evans JD, Hultmark D, et al. (2007) Dynamic evolution of the innate immune system in *Drosophila*. Nat Genet 39: 1461-1468.

Saitou N, Nei M (1987) The neighbor-joining method: a new method for reconstructing phylogenetic trees. Mol Biol Evol 4: 406-425.

Schopfer CR, Nasrallah ME, Nasrallah JB (1999) The male determinant of self-incompatibility in *Brassica*. Science 286: 1697-1700.

Shi DQ, Liu J, Xiang YH, Ye D, Sundaresan V, et al. (2005) *SLOW WALKER1*, essential for gametogenesis in Arabidopsis, encodes a WD40 protein involved in 18S ribosomal RNA biogenesis. Plant Cell 17: 2340-2354.

Shimizu KK (2002) Ecology meets molecular genetics in *Arabidopsis*. Popul Ecol 44: 221-233.

Shimizu KK, Ito T, Ishiguro S, Okada K (2008) *MAA3* (*MAGATAMA3*) helicase gene is required for female gametophyte development and pollen tube guidance in

Arabidopsis thaliana. Plant Cell Physiol 49: 1478-1483.

Shimizu KK, Okada K (2000) Attractive and repulsive interactions between female gametophytes in *Arabidopsis* pollen tube guidance. Development 127: 4511-4518.

Silverstein KA, Graham MA, Paape TD, VandenBosch KA (2005) Genome organization of more than 300 defensin-like genes in *Arabidopsis*. Plant Physiol 138: 600-610.

Silverstein KA, Moskal Jr. WA, Wu HC, Underwood BA, Graham MA, et al. (2007) Small cysteine-rich peptides resembling antimicrobial peptides have been under-predicted in plants. Plant J 51: 262-280.

Stewman SF, Jones-Rhoades M, Bhimalapuram P, Tchernookov M, Preuss D, et al. (2010) Mechanistic insights from a quantitative analysis of pollen tube guidance. BMC Plant Biol 10: 32.

Swanson WJ, Vacquier VD (2002) The rapid evolution of reproductive proteins. Nat Rev Genet 3: 137-144.

Takayama S, Shiba H, Iwano M, Shimosato H, Che FS, et al. (2000) The pollen determinant of self-incompatibility in *Brassica campestris*. Proc Natl Acad Sci U S A. 97: 1920-1925.

Takayama S, Shimosato H, Shiba H, Funato M, Che FS, et al. (2001) Direct ligand-receptor complex interaction controls *Brassica* self-incompatibility. Nature 413: 534-538.

Takeuchi H, Higashiyama T (2011) Attraction of tip-growing pollen tubes by the female gametophyte. Curr Opin Plant Biol 14: 614-621.

Tamura K, Peterson D, Peterson N, Stecher G, Nei M, et al. (2011) MEGA5:

Molecular Evolutionary Genetics Analysis using Maximum Likelihood, Evolutionary Distance, and Maximum Parsimony Methods. Mol Biol Evol 28: 2731-2739.

Tang W, Ezcurra I, Muschietti J, McCormick S (2002) A cysteine-rich extracellular protein, LAT52, interacts with the extracellular domain of the pollen receptor kinase LePRK2. Plant Cell 14: 2277-2287.

Thomma BP, Cammue BP, Thevissen K (2002) Plant defensins. Planta 216: 193-202.

Van der Pluijm JE (1964) An electron microscopic investigation of the filiform apparatus in the embryo sac of *Torenia fournieri*. In: Linskens HF (ed) Pollen physiology and fertilization. North-Holland Publ Co, Amsterdam, pp. 8-16.

Vanoosthuyse V, Miege C, Dumas C, Cock JM (2001) Two large *Arabidopsis thaliana* gene families are homologous to the *Brassica* gene superfamily that encodes pollen coat proteins and the male component of the self-incompatibility response. Plant Mol Biol 46: 17-34.

Wang H, Boavida LC, Ron M, McCormick S (2008) Truncation of a protein disulfide isomerase, PDIL2-1, delays embryo sac maturation and disrupts pollen tube guidance in *Arabidopsis thaliana*. Plant Cell 20: 3300-3311.

Wheeler MJ, Vatovec S, Franklin-Tong VE (2010) The pollen S-determinant in *Papaver*: comparisons with known plant receptors and protein ligand partners. J Exp Bot 61: 2015-2025.

Wu HM, Wang H, Cheung AY (1995) A pollen tube growth stimulatory glycoprotein is deglycosylated by pollen tubes and displays a glycosylation gradient in the flower. Cell 82: 395-403.

Yamagata Y, Yamamoto E, Aya K, Win KT, Doi K, et al. (2010) Mitochondrial gene

in the nuclear genome induces reproductive barrier in rice. Proc Natl Acad Sci U S A 107: 1494-1499.

Yang Z (2007) PAML 4: phylogenetic analysis by maximum likelihood. Mol Biol Evol 24: 1586-1591.

Yoshida K, Saitoh H, Fujisawa S, Kanzaki H, Matsumura H, et al. (2009) Association genetics reveals three novel avirulence genes from the rice blast fungal pathogen *Magnaporthe oryzae*. Plant Cell 21: 1573-1591.

Acknowledgements

I wish to express deep gratitude to my supervisor, Professor Tetsuya Higashiyama, for his kind instruction and inspiring advices throughout this study in our laboratory (Group of Plant Reproductive Systems, Division of Biological Science, Graduate School of Science, Nagoya University). I thank Associate Professor Narie Sasaki for her kind instruction and suggestions especially about molecular biological approaches. I also thank Assistant Professor Masahiro M. Kanaoka for his useful advices especially about botanical experiments. I appreciate Dr. Frédéric Berger (Temasek Lifesciences Laboratory, Singapore) for helpful discussion and critical comments on this study; Dr. Kentaro K. Shimizu (University of Zurich, Switzerland) for discussions, critical reading of a published manuscript, and the *maa3/MAA3* mutant seeds; Dr. Akira Kawabe (Kyoto Sangyo University) for the *A. lyrata* plants and seeds; Dr. Kentaro Yoshida (Sainsbury Laboratory, Norwich, UK) for kind advices about molecular evolutionary analysis; Dr. Sumie Ishiguro (Graduate School of Bioagricultural Sciences, Nagoya University) for providing genomic DNAs and seeds of various accessions; and Dr. Kurataka Otsuka for custom array analysis. I am deeply grateful to Dr. Ryushiro D. Kasahara for his appropriate suggestions about botanical experiments. I extend grateful thanks to Dr. Yuki Hamamura for her encouragement and support throughout this study, especially microscope study. I am grateful to Dr. Kie Itoh for her great advices about molecular biological approaches in the beginning of my research career. I thank present and former senior colleagues in our laboratory, Dr. Minako Ueda (NAIST), Dr. Daisuke Kurihara, Dr. Ryoko Yui, Dr. Hiroyuki Kakui, Dr. Daisuke Maruyama, Dr. Hideki Takanashi, Dr. Yoko Mizuta, and Dr. Takamasa Suzuki, for their supports and discussions. I also thank present and former junior fellows in our laboratory, Mr. Hiroki Tsutsui, Mr. Nao

Kawano, Mr. Takashi Sakakibara, Ms. Kyoko Deguchi, Mr. Hiroaki Goto, Ms. Moe Nishimaki, Ms. Taeko Sasaki, Ms Tomoko Tsuruta, Mr. Motoki Kuzuya, Mr. Keita Goou, Ms. Yuri Aoki, Ms. Kaho Yamada, Mr. Jun-ich Taniguchi, Mr. Takao Yamamoto, and many others for their supports and kindness. I am particularly grateful to my fellows at this laboratory, Ms. Akane Mizukami, Mr. Satohiro Okuda, Mr. Daichi Susaki, and Ms. Keiko Shiina, for their constant support, kindness, and encouragement. Lastly, I wish to thank all my friends for their kindness, my family for their help, and Ms. Shiori Nagahara for the greatest support.

副論文

A species-specific cluster of defensin-like genes encodes diffusible pollen tube attractants in *Arabidopsis*

種特異的なディフェンシン様遺伝子群は

シロイヌナズナにおける拡散性の花粉管誘引物質をコードする

Hidenori Takeuchi and Tetsuya Higashiyama

PLoS Biology, **10**, e1001449 (2012)

参考論文 1

Defensin-like polypeptide LUREs are pollen tube attractants secreted from synergid cells

助細胞から分泌される花粉管誘引物質は

ディフェンシン様のポリペプチド **LURE** である

Satohiro Okuda, Hiroki Tsutsui, Keiko Shiina, Stefanie Sprunck,
Hidenori Takeuchi, Ryoko Yui, Ryushiro D. Kasahara, Yuki Hamamura,
Akane Mizukami, Daichi Susaki, Nao Kawano, Takashi Sakakibara,
Shoko Namiki, Kie Itoh, Kurataka Otsuka, Motomichi Matsuzaki,
Hisayoshi Nozaki, Tsuneyoshi Kuroiwa, Akihiko Nakano,
Masahiro M. Kanaoka, Thomas Dresselhaus, Narie Sasaki
and Tetsuya Higashiyama

Nature, **458**, 357-361 (2009)

参考論文 2

Attraction of tip-growing pollen tubes by the female gametophyte

雌性配偶体による先端成長する花粉管の誘引

Hidenori Takeuchi and Tetsuya Higashiyama

Current Opinion in Plant Biology, **14**, 1–8 (2011)